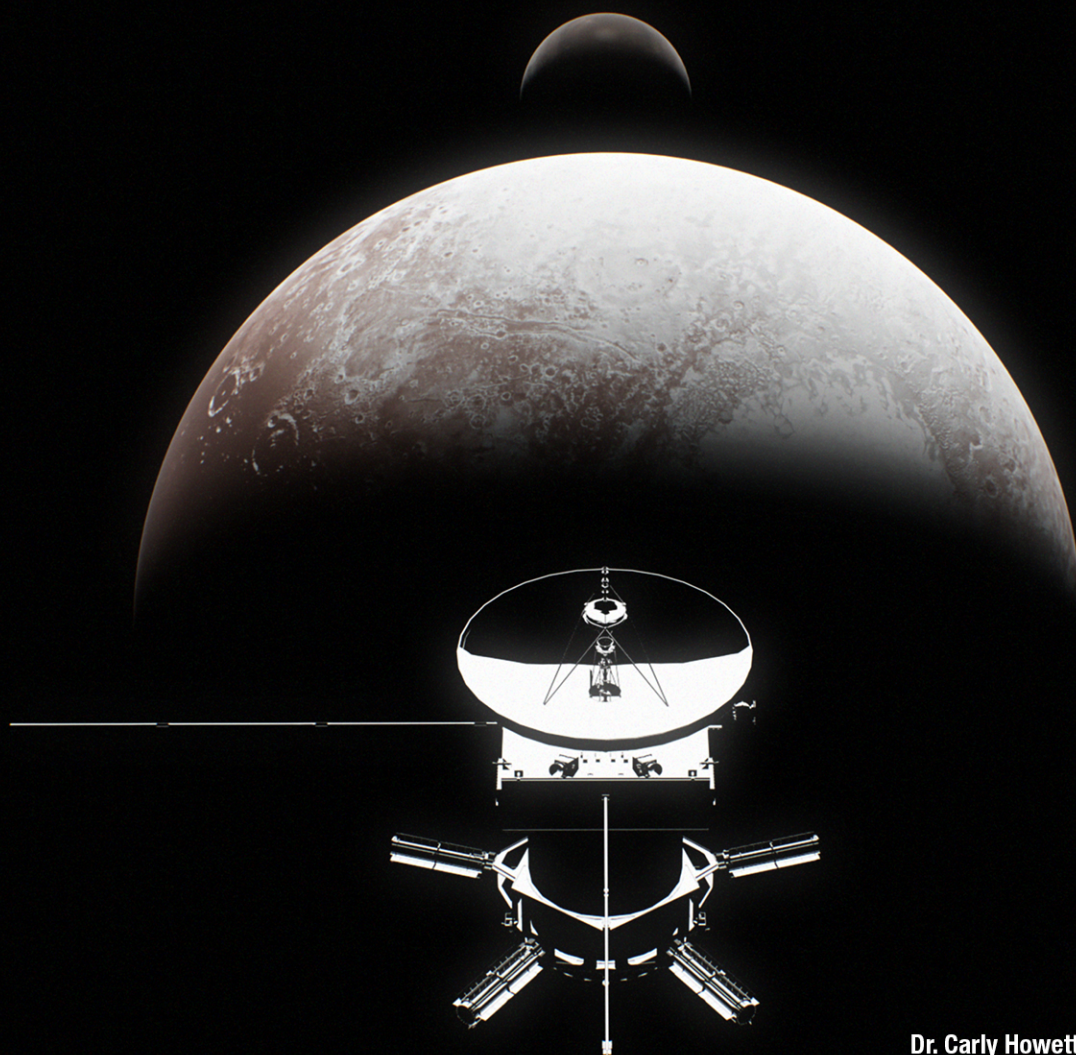




PLANETARY MISSION CONCEPT STUDY

PERSEPHONE:

A Pluto-System Orbiter & Kuiper Belt Explorer



Dr. Carly Howett, Principal Investigator
howett@boulder.swri.edu

Dr. Stuart Robbins, Deputy Principal Investigator
stuart@boulder.swri.edu

Mr. Karl Fielhauer, Study Lead
karl.fielhauer@jhuapl.edu

Mr. Clint Apland, Study Co-Lead
clint.apland@jhuapl.edu

Study Participants

Role	Name	Organization
Principal Investigator	Dr. Carly Howett	SwRI
Deputy Principal Investigator	Dr. Stuart Robbins	SwRI
APL Study Lead	Mr. Karl Fielhauer	APL
Science Team		
Particle and Fields	Dr. Heather Elliot (Lead)	SwRI
	Dr. Robert J. Wilson	CU
Satellite Science	Dr. Simon Porter (Lead)	SwRI
	Dr. Carolyn Ernst	APL
Composition	Dr. Silvia Protopapa (Lead)	SwRI
	Dr. Amanda Hendrix	PSI
Geology	Dr. Kelsi Singer (Lead)	SwRI
	Dr. Jani Radebaugh	BYU
Interior	Dr. Francis Nimmo (Lead)	UC Santa Cruz
	Dr. John Spencer	SwRI
	Dr. William McKinnon	Wash. U.
KBO Exploration	Dr. Anne Verbiscer (Lead)	U. of Virginia
	Dr. Alan Stern	SwRI
	Dr. Bryan Holler	STSci
	Dr. JJ Kavelaars	NRC-HIA
Atmospheres	Dr. Orenthal Tucker (Lead)	GSFC
	Dr. Leslie Young	SwRI
Engineering/Science Liaison	Mr. Adam Thodey	CSU
	Mr. Jon Pineau	Stellar Solutions
APL Technical Team		
APL Science Interface	Dr. Mark Perry	APL
	Dr. Hari Nair	APL
Program Manager	Mr. James Leary	APL
Systems Engineering	Mr. Karl Fielhauer	APL
	Mr. Clint Apland	APL
Mission Design	Mr. Fazole Siddique	APL
Cost Estimation	Ms. Rachel Sholder	APL

Role	Name	Organization
Operations	Mr. Mark Holdridge	APL
	Ms. Samantha Walters	APL
Instruments	Mr. Bruce Andrews	APL
	Mr. Clint Edwards	
Propulsion	Mr. Stewart Bushman	APL
Mechanical	Mr. Jimmy Kuhn	APL
Design	Mr. David Napolillo	APL
Thermal	Mr. Bruce Williams	APL
Radio Frequency	Mr. Adam Crifasi	APL
Power	Mr. Dan Gallagher	APL
	Mr. David Frankford	APL
	Mr. Doug Crowley	APL
Guidance, Navigation, and Control	Mr. Jack Hunt	APL
Avionics	Mr. Blair Fonville	APL
Software	Mr. Chris Krupiarz	APL

Acknowledgments

We thank NASA for its financial support through the Planetary Mission Concept Studies (PMCS) grant #18-PMCS18-0027 and contract task NNN06AA01C/80MSFC19F0097. We also thank SwRI and APL for their financial support through internal research funding (SwRI #R6007).

Data Release, Distribution, and Cost Interpretation Statements

This document is intended to support the 2023–2032 Planetary Science and Astrobiology Decadal Survey.

The data contained in this document may not be modified in any way.

Cost estimates described or summarized in this document were generated as part of a preliminary concept study, are model-based, assume an APL in-house build, and do not constitute a commitment on the part of APL.

Cost reserves for development and operations were included as prescribed by the NASA ground rules for the Planetary Science Decadal Survey. Unadjusted estimate totals and cost reserve allocations would be revised as needed in future more-detailed studies as appropriate for the specific cost risks for a given mission concept.

A Pluto-System Orbiter & Kuiper Belt Explorer Concept Mission

A large strategic mission to determine the habitability and evolution of the Kuiper Belt

SCIENCE OBJECTIVES

- What are the internal structures of Pluto and Charon?
—What is the evidence for a subsurface ocean on Pluto?
- How have surfaces and atmospheres in the Pluto system evolved?
- How has the KBO population evolved?

KEY PERSONNEL

Dr. Carly Howett (PI, SwRI)

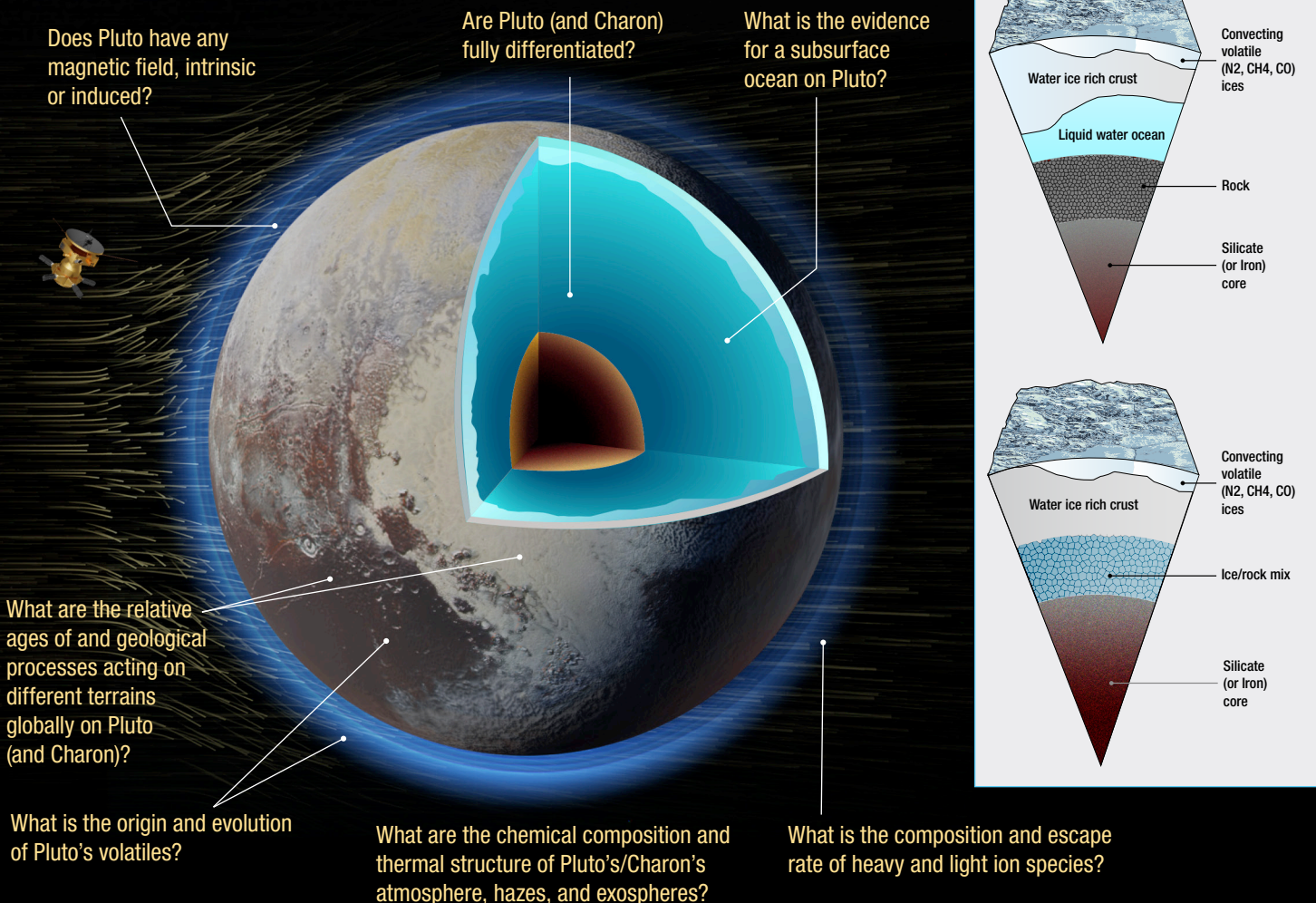
Dr. Stuart Robbins (DPI, SwRI)

Karl Fielhauer
(APL Study Lead)

MISSION OVERVIEW

Launch 2031, KBO flyby 2050,
Pluto-system tour 2058-2061

- Launch vehicle: SLS Block 2 with Centaur kick stage
- Cost: Phase A–F mission cost is \$3.0B FY25
- Total Data Volume: 806 MB/day maximum
- Propulsion:
 - Electronic Propulsion (xenon, main-system)
 - Chemical Propulsion (hydrazine, mainly for housekeeping and instrument pointing)
- Power: 5 Next-Generation RTGs



What can binary fraction, density, and shapes of KBOs tell us about their formation and the collisional environment in the primordial Kuiper Belt? Do they support current streaming instability models?

What do the surface features of encountered KBOs reveal about the origin, evolution and geologic history of KBOs?



Pluto



Charon



Styx

Nix

Hydra

Kerberos

What is the origin and evolution of Charon's surface composition?

What constraints do the small satellites in the Pluto system place on its evolution?

How do the detailed surface properties, compositions, volatiles, (and atmospheres, if present) of KBOs vary?

MISSION TIMELINE

Launch: Feb 2031
Jupiter flyby: May 2032
KBO flyby: Feb 2050

Pluto arrival: Oct 2058
Pluto-system tour: 2058–2061
Extended mission KBO encounter: 2069

INSTRUMENTS

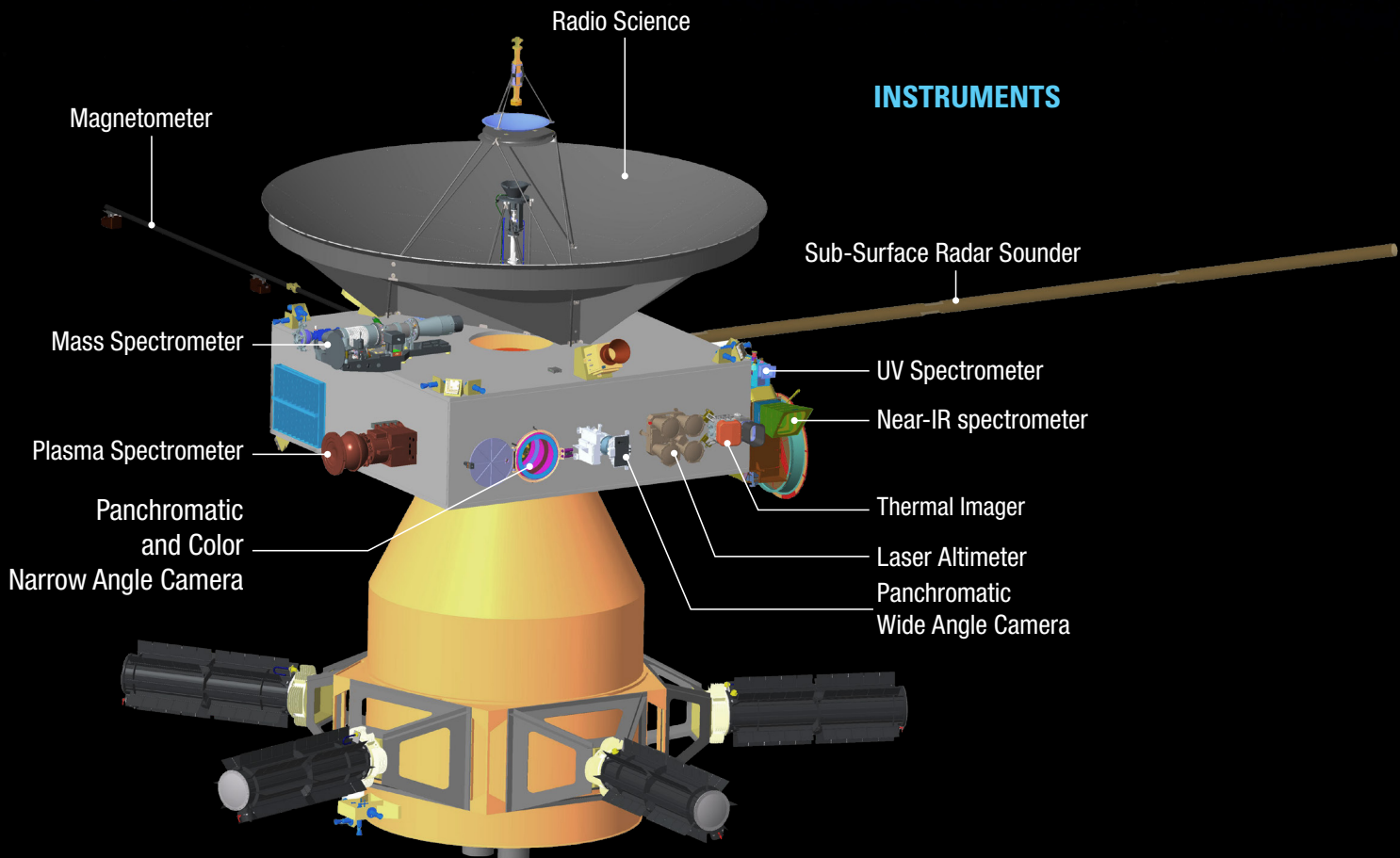


Table of Contents

STUDY PARTICIPANTS	I
ACKNOWLEDGMENTS	II
DATA RELEASE, DISTRIBUTION, AND COST INTERPRETATION STATEMENTS	II
FACT SHEET	III
TABLE OF CONTENTS	V
LIST OF FIGURES	VII
LIST OF TABLES	VIII
EXECUTIVE SUMMARY	X
1. SCIENTIFIC OBJECTIVES	1
The Case for Returning to the Kuiper Belt	1
Science Objectives	2
Technical Implementation	7
2. HIGH-LEVEL MISSION CONCEPT	15
Overview	15
Concept Maturity Level	16
Technology Maturity	16
Key Trades	17
3. TECHNICAL OVERVIEW	18
Instrument Payload Description	18
Flight System	22
Concept of Operations and Mission Design	28
Risk List	33
4. DEVELOPMENT SCHEDULE AND SCHEDULE CONSTRAINTS	34
High-Level Mission Schedule	34
Technology Development Plan	35
Development Schedule and Constraints	35
5. MISSION LIFE-CYCLE COST	35
Introduction	35
Mission Ground Rules and Assumptions	36
Cost Benchmarking	37
Methodology and Basis of Estimate	37
Confidence and Cost Reserves	39
APPENDIX A. ACRONYMS	A-1
APPENDIX B. REFERENCES	B-1
APPENDIX C. STATISTICAL MODELING	C-1
Background	C-1
Pre-Pluto KBO Encounter Modeling	C-1
Post-Pluto KBO Encounter Modeling	C-1

APPENDIX D. ADDITIONAL INSTRUMENTATION INFORMATION	D-1
Panchromatic and Color Camera	D-1
Infrared Spectrometer (LEISA).....	D-4
Thermal Imager (THEMIS)	D-6
Mass Spectrometer	D-7
Radio Science.....	D-8
UV Spectrometer	D-9
Occultation Opportunities	D-9
Magnetometer.....	D-10
Plasma Spectrometer	D-14

List of Figures

Figure 1. The diversity of KBOs: Pluto, its largest moon Charon, and the cold classical KBO Arrokoth.	4
Figure 2. Persephone external spacecraft overview featuring payload locations.	22
Figure 3. Persephone external equipment layouts.	22
Figure 4. Persephone flight system block diagram.	23
Figure 5. Electrical Power System block diagram.	27
Figure 6. (left) Prime launch period and (right) Earth-Jupiter-KBO-Pluto interplanetary transfer. ...	29
Figure 7. Science orbits, plotted in Pluto/Charon rotating frame.	30
Figure 8. Ground tracks of the four chosen orbits on Pluto and Charon.	31
Figure 9. Post-Pluto transfer time and the required xenon to achieve the science goal of a 100- to 150-km-class KBO.	32
Figure 10. The Persephone risk list requires significant external (to the program) efforts to be completed.	34
Figure 11. The schedule for Persephone satisfies all APL guidelines.	35
Figure 12. Mission-level cost comparison to other Flagships.	37
Figure 13. S-curve summary.	40
Figure 14. Distance and closest approach date of the spacecraft to the modeled KBO population (for pre-Pluto encounter).	C-1
Figure 15. Deflection angle at Pluto (i.e., how modified the nominal trajectory would have to be) to encounter KBOs of different brightness.	C-2
Figure 16. Relationship between brightness (H_v) and the predicted diameter of an object assuming geometric albedo, p_v , of 0.08.	C-2
Figure 17. The time-of-flight penalty for nominal trajectory deviations to visit a pre-Pluto KBO.	C-2
Figure 18. The nominal trajectory with (blue) and without (red) a 1 AU deviation.	C-3
Figure 19. Panchromatic and color imager’s (NAC) surface coverage of Pluto.	D-2
Figure 20. Panchromatic and color imager’s (NAC) surface coverage of Charon.	D-2
Figure 21. Minimum emission angles taken by the panchromatic and color imager (NAC) of Pluto.	D-3
Figure 22. Maximum emission angles taken by the panchromatic and color imager (NAC) of Pluto.	D-3
Figure 23. Range of available emission angles taken by the panchromatic and color imager (NAC) of Pluto.	D-4
Figure 24. Pluto’s surface coverage by the panchromatic (WAC) low-light camera.	D-4
Figure 25. Pluto’s surface coverage by the infrared spectrometer (LEISA).	D-5
Figure 26. The surface coverage of Pluto by the thermal infrared instrument (THEMIS).	D-6
Figure 27. The local time coverage of Pluto that the infrared spectrometer (THEMIS) will obtain.	D-7

Figure 28. Earth and solar occultation opportunities of Pluto.....	D-10
Figure 29. An example of stellar occultation opportunities.	D-10
Figure 30. Simulations of Pluto’s interaction with the solar wind.....	D-11
Figure 31. Orbital tour shown from different perspectives, and different distances from Pluto.	D-14
Figure 32. Example of mass resolutions for the CoDICE time of flight (TOF).....	D-15

List of Tables

Table 1. PSDS’ Key and Important Questions and Heliophysics’ Key Goals that Persephone addresses.....	2
Table 2. Measurement requirements for instruments for SQ1.1.....	8
Table 3. Measurement requirements for instruments for SQ1.2.....	9
Table 4. Measurement requirements for instruments for SQ1.3.....	10
Table 5. Measurement requirements for instruments for SQ2.1 to SQ2.3.....	11
Table 6. Science Traceability Matrix.....	13
Table 7. Key mission-driving requirements for the Persephone mission.....	15
Table 8. Persephone key trades.....	17
Table 9. Payload overview table.....	20
Table 10. Payload mass and power table.....	21
Table 11. Flight system neutral mass summary.....	23
Table 12. Flight system power modes.....	24
Table 13. Flight system element parameters.....	24
Table 14. Persephone mission events table.....	29
Table 15. Pluto/Charon tour events.....	30
Table 16. Persephone mission design table.....	32
Table 17. Mission operations and Ground Data Systems table.....	33
Table 18. Key phase duration table.....	34
Table 19. Estimated Phase A–F Persephone mission costs by level-2 Work Breakdown Structure (WBS) element.....	36
Table 20. WBS 5 costs in FY\$25K.....	38
Table 21. WBS 6 costs in FY\$25K.....	38
Table 22. Inputs to cost distributions in FY\$25K.....	39
Table 23. Cost risk analysis.....	40
Table 24. List of known KBO post-Pluto targets that could be reached.....	C-3
Table 25. System observing requirements for NAC and WAC cameras.....	D-1
Table 26. Requirements on the NAC and WAC camera systems.....	D-1
Table 27. Observing requirements of the infrared spectrometer.....	D-5

Table 28. Requirements on the thermal spectrometer observing strategy.	D-6
Table 29. Mass spectrometer key parameters.	D-8
Table 30. Observing requirements for radio science.	D-8
Table 31. UV spectrometer observing strategy.....	D-9
Table 32. Requirements on the UV spectrometer.....	D-9

Executive Summary

Persephone is a concept mission study that will address key questions raised by New Horizons' encounters with Kuiper Belt objects (KBOs), with arguably the most important being "*Does Pluto have an ocean?*" which has critical astrobiological impacts. More broadly, Persephone will answer three significant science questions: What are the internal structures of Pluto and Charon? How have the surfaces and atmospheres in the Pluto system evolved? How has the KBO population evolved? The questions we address here directly contribute to four Key Questions (KQs) and six Important Questions (IQs) outlined in the 2013–2022 Planetary Science Decadal Survey (PSDS; Vision and Voyages, 2011). Although not a driver for this study, we note that because of the nature and payload of this concept mission, the final mission would also address two Key Goals (KGs) from the Heliophysics Decadal Survey (SSP, Solar and Space Physics, 2013).

To answer these questions, Persephone has a comprehensive payload, and will both orbit within the Pluto system and have other planned KBO encounters. Specifically, the nominal mission is 30.7 years long, with a planned launch on an SLS then using existing electric propulsion (EP) technology and a Jupiter gravity assist to reach Pluto orbit in 27.6 years. En route to Pluto, Persephone will have one 50- to 100-km-class KBO encounter before starting its 3.1-year orbital campaign of the Pluto system. The mission also includes the potential for an extended mission, with a recommendation of an additional 8-year campaign, which would enable the exploration of another KBO in the 100- to 150-km-class.

The two largest risks to the mission are the power (currently five Radioisotope Thermoelectric Generators [RTGs] are required, which could increase if more power is required) and launch vehicle (if the SLS does not have the expected performance, then the mission may have to be modified to reduce the total mass). The nominal cost of this mission is \$3.0B, making it a large strategic science mission.

The mission's only required technology developments are the completion of an SLS-class launch vehicle and an advanced RTG, both considered external and critical to the program. The mission includes 11 instruments: Panchromatic and Color High-Resolution Imager (narrow-angle camera [NAC]), Low-Light Camera (wide-angle camera [WAC]), UV Spectrometer, Near-IR Spectrometer, Thermal IR Camera, RF Spectrometer, Mass Spectrometer, Altimeter, Sounding Radar, Magnetometer, and Plasma Spectrometer.

This report documents the results of a mission study that has been developed to concept maturity level 4 through a strong collaboration between the science team led by Southwest Research Institute (SwRI) and the technical team from Johns Hopkins Applied Physics Laboratory (APL).

Returning to Pluto and the Kuiper Belt is critical to answer key planetary science questions, including those about solar system formation, ocean-world habitability, atmospheres, and geophysics.

1. Scientific Objectives

The Case for Returning to the Kuiper Belt

NASA's New Horizons spacecraft blazed the trail of Kuiper Belt (KB) exploration with an encounter of the Pluto system in 2015 and a close flyby of Arrokoth, a cold classical Kuiper Belt object (CCKBO), in 2019. Resultant spacecraft data led to several important discoveries: KBOs are very diverse (see Figure 1), Pluto has a currently active surface, Charon has had an active geologic history, and CCKBO Arrokoth is a contact binary. The data returned raised new questions that can only be answered by a return to the Pluto system with an orbiter, and yet understanding the diversity of the KB and other dwarf planets also beckons. The Persephone mission would achieve both of these desires: to put an orbiter into the Pluto system and to explore the KB.

Images from New Horizons showed Pluto is unexpectedly active with vigorous surface geology, including a convecting ice sheet filling an ancient basin known as Sputnik Planitia (SP; Stern et al., 2015; Moore et al., 2016; McKinnon et al., 2016). One possible explanation for the formation of SP requires a subsurface ocean, sparking the debate about whether one could exist on Pluto (Nimmo et al., 2016), a body that spends most of its time >40 AU from the Sun. Determining whether Pluto does indeed have a subsurface ocean is one of the key drivers for this mission, because a subsurface ocean would have important astrobiological implications for our solar system (and, by extension, other systems too) (e.g., Hendrix et al., 2019).

Our detailed knowledge of other KBOs is lacking because of the difficulty in obtaining high signal-to-noise data for these faint, small objects from Earth. We do know that the KBO population has diverse surface colors, albedos, and compositions, implying that KBOs are intrinsically different, and/or that they experienced different resurfacing processes (e.g., Benecchi et al., 2019; Barucci et al., 2008). Different KB regions appear to have different binary fractions, with the CCKBOs having the highest percentage of non-contact binaries (~30% compared with ~15% for the remaining populations) (Noll et al., 2008) and plutinos having the highest (40%) fraction of contact binaries (Thirouin et al., 2018). CCKBOs having such a high fraction of binaries implies that their population is primordial, whereas the lower fraction of binaries of non-CCKBOs is consistent with a greater influence of dynamical evolution (gravitational scattering) and collisional processes (Parker and Kavelaars, 2012). Furthermore, the KB was thought to be fully collisionally evolved like the asteroid belt for objects less than ~100 km across, but data from New Horizons has called that assumption into question (Singer et al., 2019). Persephone's vantage point inside the KB provides it with a unique opportunity to resolve the surfaces of several KBOs and with unique phase coverage of targets. The proposed mission would improve our knowledge of KBOs, KB binaries, and the evolution of the KB as a whole (Bernstein et al., 2004; Benecchi et al., 2018).

Understanding the nature of Pluto has profound implications for the evolution of other bodies in our solar system (e.g., Neptune's captured-KBO moon, Triton) and would provide critical information on heat and volatile transport mechanisms in the KB. Furthermore, understanding the diversity of the KB would allow us to understand its complex evolution, and the context of the KB within the solar system's small body population.

Our report shows that the science case for returning to the KB, and in particular the Pluto system, is compelling. However, a Pluto-system orbiter and KB explorer is shown to be a multi-decadal mission requiring many Next-Generation Radioisotope Thermoelectric Generators (NGRTGs). This type of mission (i.e., orbiter rather than a single or even multi-spacecraft flyby) was selected because the science return would be groundbreaking rather than incremental. It is important to point out that other mission architectures may result in decreased mission duration and cost—for example, another New Horizons-like spacecraft flyby of the non-encountered hemisphere. While any exploration of the KB would increase our knowledge of this enigmatic region, the science return from such a mission would be greatly diminished. For example, without an orbiter, it would be very difficult to answer conclusively whether Pluto has a subsurface ocean or fully understand the workings of Pluto's active geologic-climatologic engine.

Instead of a different mission architecture, which is explored in Robbins et al. (2020), we strongly support the development of new technologies that would decrease the risk posture of this mission. The most signif-

icant technological development would be the development of a nuclear electric propulsion system (NEP; cf. Casani et al., 2020), which would substantially decrease the cruise time to Pluto. Casani et al. (2020) show that a 10-kWe NEP spacecraft can deliver 67% more payload with 2.4 years shorter flight time compared to the current radioisotope electric propulsion (REP) system. They also showed that a kilowatt-electric system would enable greater than four times the data rate at Pluto compared with the REP option.

New Horizons revealed Kuiper Belt objects to be incredibly interesting and diverse, and returning there is the only way to answer many of the questions it raised. For a spacecraft to explore the Kuiper Belt in the next 50 years, a mission needs to be selected soon, because the cruise time to these distant worlds is multi-decadal. Persephone could be that mission.

Science Objectives

Introduction

Persephone has three overarching Level 1 science questions (SQs): (SQ1.1) What are the internal structures of Pluto and Charon? (SQ1.2) How have surfaces and atmospheres in the Pluto system evolved? (SQ1.3) How has the KBO population evolved? These questions are complemented by another three Level 2 science questions: (SQ2.1) What is Pluto’s internal heat budget? (SQ2.2) What is Charon’s magnetic field environment? (SQ2.3) How do KBOs and the heliosphere interact? All of these science questions are addressed by a larger number of science objectives (SOs), which are discussed below and outlined in the Science Traceability Matrix (STM) (Table 6).

Persephone’s science objectives directly address many of the questions raised in the 2013–2022 Planetary Science Decadal Survey (PSDS; Vision and Voyages, 2011). Specifically, we address four of PSDS’ Key Questions (KQs), six of its Important Questions (IQs), and two of the Heliophysics Decadal Survey’s (SSP, 2013) Key Goals (KGs), which are outlined in Table 1.

Table 1. PSDS’ Key and Important Questions and Heliophysics’ Key Goals that Persephone addresses.

KQ1	1: What were the initial stages, conditions, and processes of solar system formation and the nature of the interstellar matter that was incorporated?
KQ2	2: How did the giant planets and their satellite systems accrete, and is there evidence that they migrated to new orbital positions?
KQ4	4: What were the primordial sources of organic matter , and where does organic synthesis continue today?
KQ10	10: How have the myriad chemical and physical processes that shaped the solar system operated, interacted, and evolved over time ?
IQ9	9: What are the abundances and distributions of different classes of asteroids, comets, and KBOs ?
IQ10	10: How do the compositions of Oort cloud comets differ from those derived from the Kuiper Belt?
IQ13	13: What is the relationship between large and small KBOs ? Is the population of small KBOs derived by impact disruption of the large KBOs?
IQ14	14: How do the impact histories of asteroids compare to those of comets and KBOs?
IQ18	18: Were there radial or planetesimal size limits on differentiation , and were KBOs and comets formed too late to have included significant amounts of live aluminum 26 as a heat source?
IQ19	19: What are the internal structures of Trojans and KBOs?
KG1	1: Determine the interaction of the Sun with the solar system and the interstellar medium.
KG4	4: Discover and characterize fundamental processes that occur both within the heliosphere and throughout the universe.

Details of the Science Objectives

SQ1.1: What are the internal structures of Pluto and Charon?

SO1.1: Is Pluto an ocean world? The internal structure of Pluto is particularly intriguing because it could currently host a subsurface ocean. Such an ocean could help explain how SP was formed: if the SP basin was created by an impact, Pluto could have reoriented to its current position from tidal and rotational torques. These torques require the basin to be a positive gravity anomaly (despite being negative topography), which is best explained if Pluto has a subsurface ocean (from shell thinning and ocean uplift; Nimmo et al., 2016). The heat within such an ocean could be insulated and maintained by a thin layer of clathrate hydrates (Kamata et al., 2019). However, other possible explanations for SP's formation do not require a subsurface ocean. For example, Hamilton et al. (2016) argue that SP was formed by the natural accumulation of ice at latitudes 30°S/N because they are Pluto's coldest regions. The only way to determine whether Pluto does, indeed, harbor an ocean is to return to the Pluto system so that its gravity and activity signatures can be determined.

SO1.2: Are Pluto and Charon fully differentiated? Pluto's bulk density indicates that its internal composition is roughly two-thirds rock and one-third ice, but how the rock and ice are distributed is unclear. The reason the distribution is important is that the extent to which rock and ice/water have separated can tell us about how much heat was released as Pluto accreted, and thus how accretion and evolution proceeded. The absence of compressional features indicates Pluto is not a homogeneous rock-ice mixture (McKinnon et al., 2017) but rather a partially or fully differentiated body, or it might have a Titan-like hydrated rock core. Meanwhile, Charon's smooth plains and vast tectonics are evidence of early heating, global expansion, and potential melting (Beyer et al., 2019; Robbins et al., 2019), indicating that partial or full differentiation also may be possible for Pluto's companion. Pluto's and Charon's differentiation states can be inferred from their moment of inertia (MoI). If the shape has relaxed to that of a fluid body, then either the present-day rotational or tidal bulges or the equivalent gravity coefficient (J_2 and C_{22}) could be used to deduce the MoI. No sign of "fossil bulges" was detected by New Horizons (Nimmo et al., 2017), but the limits derived are not very stringent (<0.6%, or 7 km).

Pluto's ratio of rock to ice is large enough to power low levels of internal heat for the duration of the solar system (McKinnon et al., 2017; Robuchon and Nimmo, 2011). However, it is surprising that Pluto displays the transfer of this internal heat to the surface when larger bodies (such as Callisto) do not. By studying other large KBOs (>50 km) (if possible, ones also with higher percentages of rock to ice than the Galilean satellites, and especially with ammonia and other volatile ices) Persephone will be able to determine whether this is typical behavior of KBOs.

SO1.3: Does Pluto have any magnetic field, intrinsic or induced? New Horizons provided the first in situ particle and fields data of the Pluto system. However, it did not carry a magnetometer and so was only able to indirectly characterize Pluto's magnetic field environment. Thus, Persephone will be the first to do so for Pluto (and other encountered KBOs), the results of which could provide data about their interior, surface modification processes that influence their evolution, and (where feasible on non-Pluto KBOs) atmospheric escape. If the 21-day solar wind variability is large enough, it might be possible to deduce a liquid ocean by modeling the magnetic field perturbations it would cause under different phases of this 21-day cycle.

A potential internal ocean makes Pluto a candidate "ocean world" for NASA study, with important implications for defining the habitability of our own and other solar systems. Thus, this mission directly addresses NASA's strategic objective 1.1, "Are we alone?" (NASA, 2018).

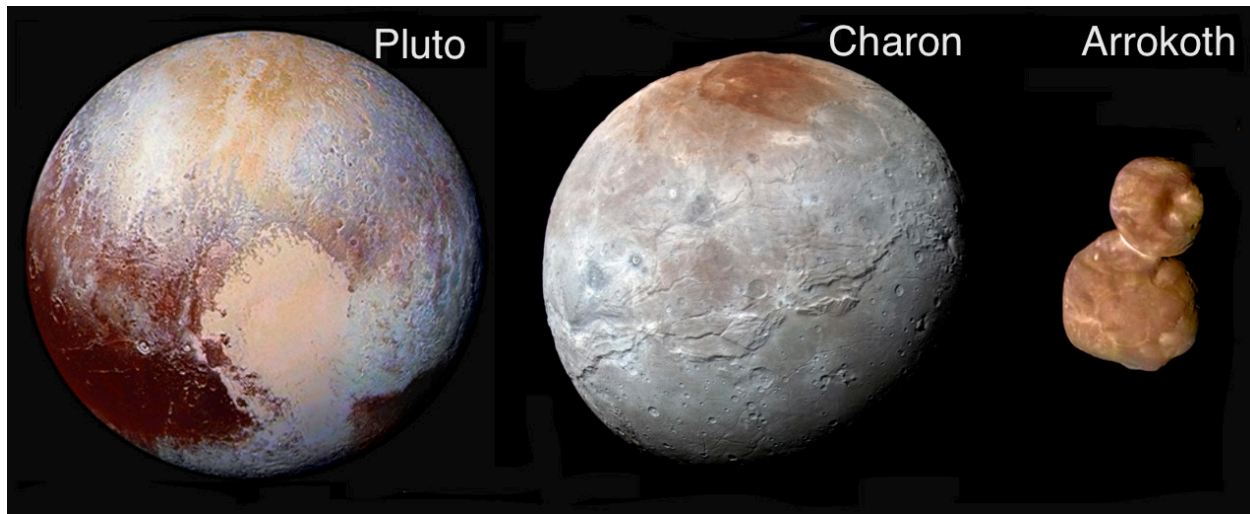


Figure 1. The diversity of KBOs: Pluto, its largest moon Charon, and the cold classical KBO Arrokoth. Note that the scale of these worlds are very different: the diameters of Pluto, Charon, and Arrokoth are 2377 km, 1212 km, and 34 km, respectively.

SQ1.2: How have the surfaces and atmospheres in the Pluto system evolved?

SO1.4: What are the relative ages of, and geological processes acting on, different terrains globally on Pluto and Charon (including current, internally derived activity)? Both endogenic and exogenic processes have sculpted the surfaces of Pluto and Charon. The creation and degradation of geologic features reveal information about the interiors of both bodies, including their heat flow history, and records surface-atmosphere interactions over time. Pluto and Charon both exhibit geologic features that are unique to those bodies. It is possible that Pluto was even more active in the past than it is now. For example, it has surface expressions of internal activity, such as its two possible cryovolcanoes (Moore et al., 2016; Singer et al., 2018), and the large-scale extensional fracturing, typical of freezing of a subsurface ocean. Furthermore, the tectonic structures east of SP known as Virgil Fossae may have been due to eruptive $\text{NH}_3\text{-H}_2\text{O}$ emissions (Cruikshank et al., 2019). This hypothesis supported by the spectroscopic detection of ammonia (NH_3) in this area, and because ammonia is geologically short-lived if exposed to solar radiation, this implies it is either recently deposited or uncovered (Dalle Ore et al., 2019).

A big difference between Pluto and Charon is that Charon's near surface is more porous (Verbiscer et al., 2019). Furthermore, this porous ice might be much thicker on Charon than Pluto. Another difference is that because most geological activity occurred early, the lithospheric thickness recorded may be quite different from the present-day value (as at Mars). Charon's Vulcan Planitia is a remnant of this early activity, for its smooth surface is thought to be due to an early subsurface ocean that reflowed and resurfaced the area (Beyer et al., 2019). Understanding these targets will broaden our knowledge of how geologic processes operate on icy worlds.

SO1.5: What is the origin and evolution of Pluto's volatiles (surface and atmospheric)? The composition of Pluto at sub-kilometer scales is unknown, because New Horizons mapped its composition to ~ 3 km/pixel on the encounter (and 70 km/pixel on the non-encounter) hemisphere. However, the color of Pluto (for example, across the bladed terrain of Tartarus Dorsa) varies over sub-kilometer distances, implying the composition might too (Moore et al., 2018). High-spatial-resolution (<1 km/pixel) compositional mapping will enable the composition of previously unexplored terrains to be determined. The composition of Pluto's darkening surface materials is still a mystery because New Horizons was unable to probe the diagnostic 2.5- to 5.0- μm region. It is thought that the materials are organics, but exactly what type and how they compare to those seen on other KBOs (e.g., Charon's North polar region) are unknown. Therefore, mapping Pluto's composition at high spatial resolution (<1 km/pixel) over a longer wavelength range than New Horizons (i.e., up to 5.0 μm) is key to understanding the composition and evolution of Pluto's surface.

New Horizons' observations of Pluto's surface ice and atmosphere showed how the two are inextricably connected: sublimation and condensation of N₂ create a kilometer-deep daily piston of cold N₂ gas, directly detected by New Horizons at dusk over SP via radio occultation, and likely are the cause of the layering imaged in Pluto's global photochemical haze layer. Over Pluto's orbit, changes in solar insolation due to eccentricity and obliquity govern the surface pressure (currently 11 μbar) of its primarily N₂ atmosphere, which is in vapor pressure equilibrium with the surface ice (e.g., Meza et al., 2019).

Over longer, ~3–4 Myr, time periods often referred to as mega-seasons, cycles of Pluto's precession have influenced global volatile transport about its surface and volatile loss (Stern et al., 2017; Bertrand et al., 2018). Volatile loss from Pluto is governed by solar heating of the upper atmosphere due to the absorption of solar ultraviolet (UV)/extreme ultraviolet (EUV) radiation primarily by CH₄. Pluto's upper atmosphere is much cooler (~70 K instead of ~90 K) than expected for a N₂-CH₄-dominated atmosphere (e.g., Young et al., 2018). The principal cooling agent affecting the thermal balance of energy in the upper atmosphere remains an enigma (e.g., Young et al., 2018). Nevertheless, the atmosphere is currently undergoing significant volatile loss via thermal escape due to Pluto's low gravity. In fact, light, minor species, such as CH₄, populate Pluto's extended corona, and a small fraction of the volatiles are eventually shared with Charon (e.g., Grundy et al., 2016).

SO1.6: What are the chemical composition and thermal structure of Pluto's/Charon's atmosphere, hazes, and exospheres? Upon arrival in 2058, we expect Pluto's atmospheric pressure to be lower than in 2015, but still global in extent and likely higher than at the time of discovery of the atmosphere in 1988, based on post-encounter models and ongoing ground-based stellar occultations (Olkin et al., 2014; Meza et al., 2019). Thus, studying Pluto's atmosphere (and Charon's, should one exist), particularly the first direct determination of its composition by mass spectrometry, remains a key objective.

Pluto's atmosphere and Charon's surface are known to be connected (Grundy et al., 2016), and it is expected that periods of significant volatile loss and atmosphere transfer to Charon can occur when Pluto and Charon are near perihelion, governed by increased UV/EUV heating of the upper atmosphere. Evidence of volatile loss and the origin of Pluto's volatiles can be inferred from the isotopic abundances (e.g., ¹⁴N/¹⁵N, ¹²C/¹³C, D/H and ⁴⁰Ar/³⁶Ar) of the atmosphere (Mandt et al., 2017; Glein and Waite, 2018). This science objective, in conjunction with SO1.5, aims to understand their atmosphere(s) and interconnectedness.

SO1.7: What is the origin and evolution of Charon's surface composition? The dark poles of Charon are thought to be cold-trapped volatiles (CH₄) from Pluto's extended atmosphere (CH₄) photolytically processed into more refractory material (Grundy et al., 2016). Measuring the composition of Charon's poles in the 2.5- to 5.0-μm region, and the isotopic abundance of Pluto's atmosphere (in conjunction with SO1.6), will enable this hypothesis to be tested. Charon's Vulcan Planitia is predicted to be formed by ammonia-rich cryovolcanism (Beyer et al., 2019), so mapping Charon's surface composition will enable such hypotheses to be tested.

SO1.8: What is the composition and escape rate of heavy and light ion species? New Horizons placed upper bounds on the densities in Pluto's ionosphere; however, its composition remains unknown (Hinson et al., 2018). With a Pluto orbiter, we can understand the dynamics of the neutral and charged particle environment within Pluto's atmosphere. Ultimately, these observations will inform the complex thermal balance of the atmosphere, essential to understanding the extent of atmospheric loss during Pluto's lifetime. Furthermore, in the unlikely event that Pluto's atmosphere is absent/contracted, or if Persephone's closest approach distance is too high, the ion plasma observations provide critical composition information.

The New Horizons mission obtained the best close-up view of Pluto currently available, but only as a snapshot in time. Therefore, its data are limited in describing the surface evolution, atmosphere dynamics, and history of volatiles on Pluto. Persephone offers the opportunity to detect temporal change in the Pluto system: the short-term changes that occur during its 3-Earth-year tour and the long-term changes that occurred during 43 Earth-years since the New Horizons flyby.

SQL3: How has the KBO population evolved?

SO1.9: What constraints do the small satellites in the Pluto system place on the evolution of that system? Understanding the detailed surface properties of Pluto's small satellites may offer key constraints on the Charon-forming impact and subsequent accretion process (Canup, 2005, 2011; Stern et al., 2006). High-resolution imagery of the small satellites will greatly enhance knowledge of the cratering record on their surfaces, which appears to be different from that of Arrokoth (Robbins et al., 2017; Singer et al., 2019; Spencer et al., 2020). Furthermore, by combining high-resolution imagery and altimetry, the shapes of the small satellites can be determined, which, in turn, will constrain their volumes better (Weaver et al., 2016). Combining this result with dynamical estimates from radio science of the masses of the small satellites would enable measurement of their bulk density (Brozović et al., 2015; Porter et al., 2017) and hence likely composition; for instance, a density in excess of 1 g/cc would require a significant rock fraction and be unusual given knowledge of gas giants' smaller moons.

The surface composition of Pluto's small satellites is largely unknown. Nix was the only satellite whose composition was determined from New Horizons, and it was shown to have intriguing signs of ammoniated ices similar to Charon (Cook et al., 2018). Persephone would be able to obtain high-signal-to-noise ratio (SNR), spatially resolved spectra for all four small satellites, allowing a direct comparison of their surface compositions. Thus, it would also enable an estimate of how much of their surfaces (and the surface of Charon) is contaminated with inter-satellite impact ejecta exchange (Stern et al., 2009; Porter and Grundy, 2015).

Finally, measuring the crater population on the smallest bodies within the Pluto system provides an important control on Pluto and Charon, because the small bodies should not be affected by the resurfacing on the larger bodies.

SO1.10: How do the detailed surface properties, compositions, volatiles (and atmospheres, if present) of KBOs vary? Images obtained by Persephone will enable the production of maps of photometric properties at a large range of wavelengths and phase angles, in order to understand Pluto's global surface variation. These could then be directly compared to both ground-based and derived photometric properties of other KBOs by New Horizons (Verbiscer et al., 2019; Porter et al., 2016) and Persephone to compare their surface properties.

SO1.11: What do the surface features (including the cratering record) of encountered KBOs reveal about the origin, evolution, and geologic history of KBOs? Small KBOs are some of the most unprocessed bodies in the solar system. Increasing our sample size beyond the one flyby of Arrokoth will greatly enhance our understanding of the diversity of KBOs and the processes that affect them.

Arrokoth has a highly uncertain crater population because of its illumination at flyby, although it, too, appeared to have relatively few impacts. Furthermore, different units across Pluto have different crater spatial densities because of resurfacing over time, and Charon appears to have a mostly ancient surface (with early resurfacing in the equatorial smooth plains), but it also does not have a saturated or extremely heavily cratered surface. It is not known whether this is a reflection of lower overall cratering rates in the KB?

Understanding KB craters has significant implications for the evolution of the KB as a whole. This is because measuring the crater population via imaging data, on a variety of terrains from all visited bodies, would give us numerous sample points for the crater population. This then informs on the impactor population that created them. This analysis can be performed for different KB locations and object types, and potentially in time (because of different terrain ages on Pluto and Charon).

SO1.12: What can binary fraction, density, and shapes of KBOs tell us about their formation and the collisional environment in the primordial Kuiper Belt? Do they support current streaming instability models? The close flyby of Arrokoth revealed a primitive world from the era of planetesimal formation (Stern et al., 2019; Lacerda and Jewitt, 2007). The shapes of other cold classical KBOs could reveal further clues to the formation mechanisms active in the primordial KB. For remote KBOs, time-domain imaging would provide well-sampled rotational light curves; one cause of a high-amplitude light curve is an irregular shape. Remote KBO observations would be possible from a Pluto orbiter and during the pre- and post-Pluto cruise. Pluto will be located near the inner edge of the classical KB in the 2050s, thus 2–10 AU

from classical KBOs; this much closer proximity than from Earth would resolve binaries separated by 1000 km (angular separation 460 milliarc-second [mas] from 3 AU versus 34 mas at 40 AU). Deep searches for binaries and faint satellites would be possible and important, and determining a satellite's orbit would ultimately lead to system masses and densities, informing models of binary formation in the primordial KB.

SQ2.1 to SQ2.4: What is Pluto's internal heat budget? What is the magnetic field environment in the Kuiper Belt?

SO2.1: What is Pluto's internal heat budget and surface heat flow? Are there current thermal anomalies (possibly associated with current activity)? How much internal heat Pluto has and how it reaches the surface in a global sense is unknown. Mapping all occurrences of water ice-based cryovolcanism across Pluto, with estimates for the ages from impact craters, will enable locating the source of these eruptions and measuring how much volume is released over time. We will also examine the convection patterns in SP, looking for any differences between the 2015 New Horizons observations and those from Persephone in ~2058, to estimate heat required to drive the speed of convection, and thereby obtain an estimate for global heat flow. Mapping Pluto's emission at long infrared (IR) wavelengths will enable estimation of its heat flow and searches for hot spots or other thermally anomalous regions associated with activity (e.g., Spencer et al., 2006).

SO2.2: Does Charon have any magnetic field, intrinsic or induced? SO2.3: Is there a Plutopause, tail, bow shock, and interaction region, and, if so, what are their shapes and motions? SO2.4: How do pickup ions affect shocks throughout the heliosphere and close to the Pluto system and other KBOs? New Horizons did not have a magnetometer, so the magnetic environment of the Pluto system is still somewhat unknown, and thus this aspect of the mission would be explorative. Sending a magnetometer and plasma spectrometer will, for the first time, allow mapping the extent of large KBOs' magnetic environment (like Pluto and Charon's), including the bow shock, Plutopause, and Pluto's ion tail. Including such instrumentation would also make this mission cross-disciplinary at NASA, between planetary science and helioscience.

Technical Implementation

In this section, we outline for each instrument the technical implementation required to achieve each of the science objectives outlined above. Unless stated otherwise, instrument parameters (e.g., wavelength coverage, spectral resolution) are the same as first listed.

SQ1.1: What are the internal structures of Pluto and Charon?

Persephone will determine the internal structures of Pluto and Charon using a technique similar to that applied to Saturn's moon Enceladus, whereby a combination of global gravity and topography measurements determine the MoI (which gives differentiation state) and potentially ice shell thickness (less et al., 2014). Two-way Doppler Radio Science measurements will determine the gravity field along with long-wavelength topography obtained through a combination of laser altimetry and stereo. Constraining Pluto's and Charon's interior structure using these observations requires knowledge of their global shape with an accuracy of <100 m. Furthermore, accurate regional topography across areas of interest, particularly SP, needs to be known to <100 m. If a subsurface ocean is present, then a substantial gravity anomaly is predicted from SP (Nimmo et al., 2016). Radio Science Doppler tracking during multiple close flybys over a range of latitudes and longitudes will determine the gravity coefficients J_2 and C_{22} of both targets. The magnetometer will be used to search for evidence of an induced or intrinsic magnetic field around Pluto, to determine whether subsurface exploration by induction is feasible.

Table 2. Measurement requirements for instruments for SQ1.1.

Observation Type	Measurement Requirement
Radio science	Resolution: The uncertainty of Doppler has to be >0.1 mm/s over 1 minute.
	Observing requirements: Seven passes with periapsis <1000 km; best if apoapsis is low and there are no maneuvers during series of five passes. <ul style="list-style-type: none"> • One of these passes must cover latitudes $>70^\circ$ at <1000 km (closer is better, but >500 km to avoid atmospheric drag). • Five high-latitude passes are required. These passes should be distributed in longitude. Two of these five passes should be over SP at least at 500-km altitude and not more than 700-km altitude.
	Additional requirements: Deep Space Network (DSN) contact is required for altitudes <3000 km. Requires the high-gain antenna (HGA) to be pointed at Earth during the periapsis pass. Measurements will be made via two-wave Doppler tracking during low-altitude ($<10,000$ km) periapses (no ultra-stable oscillator [USO] requirement).
Radar	Resolution: Vertical: 4 m and along track: 5 km at 1500-km altitude
	Observing requirements: Two passes over Pluto's SP are required, with one of the passes over its cellular portion; at least one pass over Charon's Vulcan Planitia is also required. Observing desirements: the ice mantles north and northeast of SP, smooth layered plains west and northwest of SP, the "bladed" terrain, and large north/south trough system.
Stereo imaging	Spatial resolution: <0.05 km/pix
	Observing requirements: Two images should be taken at the similar illumination but between 10° and 30° difference in emission angle over 75% of the illuminated surface.
Laser altimeter	Spatial resolution: Measurement spots are <100 μ rad in diameter, and the laser altimeter has a 30-Hz laser rate and 30 m between firings (i.e., laser spots on the surface).
	Vertical resolution: The instrument's vertical precision should be >0.1 m and be operated at altitudes <1200 km.
	Observing requirements: Five orbits with high-latitude periapses are required for global shape determination, and two-way Doppler (DSN) should be used for tracking on at least one of these orbits (to make orbit solution easier to determine). The ground tracks have to be well spaced in longitude and latitude and ensure coverage of the pits in SP, the mottled terrain on Charon, and the permanently dark regions.
Magnetometer	Range: -10 nT to $+10$ nT
	Resolution: 10 pT
	Observing requirements: Switched on continuously, with high-rate data (at least 64 Hz) within 5 Pluto radii of Pluto and elsewhere if feasible. Additional high-rate operations are required if Pluto magnetic field/bow shock/Plutopause is discovered in order to map it, particularly in conjunction with high-rate plasma measurements because the two datasets help with interpreting each other. North-south flybys at a range of longitudes are required to build a magnetic map (assuming an internal field exists), while additional flybys at different local times would help distinguish between internal and induced magnetic field.

SQ1.2: How have surfaces and atmospheres in the Pluto system evolved?

We will determine the surface ages of major regions of Pluto and Charon through cratering ages and crosscutting relationships. Furthermore, impact craters that formed at different times may show topographic and gravitational signatures of different degrees of relaxation, potentially probing the thermal history of the lithosphere, as at the Moon (Kamata et al., 2015). These analyses will be achieved by high-spatial resolution color and panchromatic surface imagery.

Gravity and topography data will be used in admittance analyses, which provide both the elastic (lithospheric) thickness and the density of the near-surface material (e.g., McGovern et al., 2002). If portions of Charon's shell experienced foundering as a result of density contrasts, associated gravity anomalies should be present. Gravity data will be obtained by radio science measurements, and topography will be obtained by stereo and radar altimeter.

IR spectra will map the surface composition of Pluto and Charon. The short-wavelength cutoff of the spectrometer should remain the same as New Horizons' LEISA ($1 \mu\text{m}$), but the long-wavelength cutoff should be extended to $5 \mu\text{m}$ (from $2.5 \mu\text{m}$) to differentiate organics (e.g., alkenes, alkanes) and tholins.

As previously discussed, one hypothesis to explain the smooth nature of Charon's Vulcan Planitia is an episode of large-scale, ammonia-rich cryovolcanism (Beyer et al., 2019). Altimetric and compositional measurements will test this hypothesis. We will also search for and map smaller putative cryovolcanic

constructs, similar to Pluto's Wright and Picard Montes on Pluto, for regions of recent (or evidence of on-going) activity.

In situ measurements of Pluto's atmosphere by a mass spectrometer will characterize the extent of volatile loss and transport in Pluto's atmosphere with measurements of the global and temporal variations of N₂, CH₄, C₂H_x, and the myriad photochemical products that have not been measured, such as H₂. UV and radio occultations, UV spectra, mass spectrometry, and ion data will be obtained to understand the dynamics of the neutral and charged particle environment within Pluto's atmosphere, and to determine the composition and densities of Pluto's ionosphere (if one exists) (Hinson et al., 2018). Volatile loss and the origin of Pluto's volatiles will be determined by isotopic abundances, which will primarily be measured by mass spectrometry (Mandt et al., 2017; Glein and Waite, 2018). Comparing these results to the compositional mapping of Charon's surface ice between 1 and 5 μm will enable us to test whether the dark poles of Charon are processed cold-trapped volatiles (CH₄) from Pluto's extended atmosphere. Ultimately this information will reveal the complex thermal balance of the atmosphere, key to understanding the extent of atmospheric loss during Pluto's lifetime.

Temporal variability would be monitored in two ways: (1) by comparing the change between 2015 (when New Horizons encountered the system) and Persephone's arrival in the late 2050s and (2) through monitoring change throughout Persephone's 3-Earth-year orbital tour of the Pluto system.

For reference: New Horizons' highest spatial resolution panchromatic observations of Pluto were acquired at 0.08 km/pixel, and at 0.66 km/pixel in color. The minimum altitude for operating the mass spectrometer is 500 km, consistent with the predicted density peaks of photochemical products and ions produced from the absorption of solar UV/EUV (Krasnopolsky, 2020). However, like Cassini INMS, this altitude can be adjusted during the mission after initial measurements (Waite et al., 2004).

The required sensitivity of the plasma spectrometer is $m/\Delta m > 8000$ to enable N₂ to be distinguished from CO. Its energy range reproduces full coverage of New Horizons' Solar Wind Around Pluto (SWAP) instrument range and the low end of New Horizons' Pluto Energetic Particle Spectrometer Science Investigation (PEPSSI) where most detections were near the bottom of its range (PEPSSI saw nothing at its high electron range). This sensitivity will resolve H⁺, He⁺, He⁺⁺, O⁺, and N⁺² and thus properly characterize the solar wind's interaction with Pluto's atmosphere, possible ionosphere, and possible magnetic field.

Table 3. Measurement requirements for instruments for SQ1.2.

Observation Type	Measurement Requirement
Illuminated Surface Imaging	Wavelength: Panchromatic 350 and 1050 nm in framing mode; color: 8 Time Delay Integration (TDI) color filters between 350 and 1050 nm, including narrow- and wide-band 890-nm CH ₄ filters
	Spatial resolution: <0.2 km/pixel for color, <0.05 km/pixel for panchromatic
	Coverage: 95% of the illuminated surface on Pluto and Charon
	Observing: Incidence angles <80° and emission angles <70°
Unilluminated Surface Imaging	Wavelength: Panchromatic 350 and 1050 nm in framing mode
	Spatial resolution: <1 km/pixel
	Coverage: 70% of the unilluminated surface on Pluto and Charon
Photometric Property Imaging	Spatial resolution: <2 km/pixel
	Coverage: 95% of the illuminated surface
	Observing: Phase angles between 0 and 140° and incidence angles <60°
Infrared Spectrometer (composition)	Wavelength: 1–5 μm
	Spatial resolution: <0.5 km/pixel
	Coverage: 90% global coverage of illuminated surface
	Observing desirements: Incidence angles between 10 and 30° and emission angles between 0° and 60°
Infrared Spectrometer (photometric properties)	Spatial resolution: <7 km/pixel
	Coverage: 90% global coverage of illuminated surface
	Observing desirements: Phase angles between 0° and 140° and emission and incidence angles between 0° and 80°
UV Spectrometer	Wavelength range: 570–2000 Å

Observation Type	Measurement Requirement
(surface)	Spectral resolution: 10 Å Observing: >50 surface scans are required for Pluto, and >10 for Charon.
UV Spectrometer (atmospheres)	Vertical resolution: 10 km for ranges ≤ 5000 km Observing: >100 limb and disk, solar and stellar occultation profiles. These profiles should be distributed in time, longitude, and latitude. Furthermore, 50 air glow spectra and 3 ring searches are also required.
Radio Frequency Spectrometer (surface)	Observing: >1 therm-scan of the surface is required, which must intersect with the region scanned by New Horizons (on Pluto and Charon). The therm-scan region should also be covered by the thermal instrument to allow cross-calibration.
Radio Frequency Spectrometer (atmosphere)	Observing: Earth-pointed with DSN contact over a minimum of two different locations (SP has to be one), and two different local times for each location (dawn and dusk). Note, a USO is required for REX to operate in this mode.
Mass Spectrometer	Resolution: $m/\Delta m > 8000$; a selectable resolution up to 25,000 is preferred. Vertical resolution: <20 km Observing: Large range (>20) of altitudes between 500 km and 2000 km to be sampled, with a preference that the instrument is operational for most/all of the orbital period.
Plasma Spectrometer	Energy range: 0.5 and 50 keV/q Energy resolution: $\Delta E/E$ of 5% Mass detection range: 1 and 60 amu Mass resolution: $m/\Delta m$ of 2–10 Angular resolution: >30° Number flux range: $1e2 \text{ cm}^{-2}\text{s}^{-1}$ (low Plutogenic fluxes in tail) to at least $5e7 \text{ cm}^{-2}\text{s}^{-1}$ (solar wind fluxes for $r > 5$ AU and Pluto ionospheric fluxes) Observing: Full data rate for one of the initial orbits with an apoapsis between 10,000 and 20,000 km, and then at least one orbit every 2 months at high data rate; the rest of the time lower data rates can be used.

SQ1.3: How has the KBO population evolved?

During its small satellite and KBO encounters, Persephone will map their surface geology, color, and composition; search for (and, if present, sample) atmospheres; and map their interaction with the heliosphere. Because the poles of Pluto's small satellites precess, it is hard to predict their orientation when the spacecraft arrives (Showalter and Hamilton, 2015); thus their local time coverage is also impossible to predict. Using both color and panchromatic imaging, Persephone will measure distant (<1 AU) KBO colors and acquire light curves that will be used to determine the rotation periods of the KBOs and model their shapes. No requirements are put on these observations because the KBOs will be unresolved and the signal-to-noise will depend on the target's size and albedo.

For reference, New Horizons resolved Arrokoth at 33 m/pixel using its panchromatic imaging (although because of smear and a lower SNR, the effective resolution is actually ~75 m/pixel) and at 130 m/pixel using its color imaging (Spencer et al., 2020). New Horizons' IR spectrometer imaged Arrokoth at 1.9 km/pixel and Pluto's small satellites between 3.6 km/pix (Nix) and 14.5 km/pixel (Hydra). Kerberos was unresolved by the IR spectrometer, and Styx was not imaged by the IR spectrometer (Cook et al., 2018).

Table 4. Measurement requirements for instruments for SQ1.3.

Observation Type	Measurement Requirement
Pluto's Small Satellites	
Illuminated Surface Imaging	Spatial resolution: <1 km/pixel for color, <0.5 km/pixel for panchromatic Coverage: 95% of the illuminated surface of each satellite
Unilluminated Surface Imaging	Spatial resolution: <2 km/pixel Coverage: 70% of the unilluminated surface on each satellite
Infrared Spectrometer	Spatial resolution: <2 km/pixel Coverage: >90% global coverage of illuminated surface
Altimeter	Vertical precision: <0.1 m

Observation Type	Measurement Requirement
	Observing: Operate at altitudes <1200 km
Radio Science (surface)	Resolution: Doppler uncertainty of <0.1 mm/s Observing: Operate at altitudes <3000 km
UV Spectrometer (surface)	Observing: >5 disk integrated scans of each satellite's surface
Magnetometer	Observing: Run continuously using the high-rate data for orbits with satellite encounters
KBO Flybys	
Illuminated Surface Imaging	Spatial resolution: <0.1 km/pixel for color, <0.03 km/pixel for panchromatic
	Coverage: As much as possible
	Observing: Preferred emission and incidence angles are between 0° and 80°, and preferred phase angles are between 0° and 140°
Unilluminated Surface Imaging	Spatial resolution: <4 km/pixel
	Coverage: As much as possible
Infrared Spectrometer	Spatial resolution: <1.5 km/pixel
	Coverage: >90% global coverage of illuminated surface
Altimeter	Vertical precision: <0.1 m
	Observing: Operate at altitudes <1200 km
Radio Science (surface)	Resolution: Doppler uncertainty of <0.1 mm/s
	Observing: Operate at altitudes <3000 km
UV Spectrometer (surface)	Observing: >5 disk integrated scans of the KBO's surface
UV Spectrometer (atmosphere)	Observing: >10 limb and disk, solar and stellar occultation profiles, and 3 ring searches
Mass Spectrometer	Observing: Operational when within 2000 km of the target
Plasma Spectrometer	Observing: In high-data-rate mode within <1200 km of the target, but also for as much of the encounter as possible
Magnetometer	Observing: Run continuously using the high-rate data at <1200 km (but for the whole encounter if possible)
Distant KBO Encounters	
Imaging Lightcurves	Wavelength: Panchromatic is expected to be of most use (use color when their signal-to-noise is >2)
	Observing: Obtain full rotational lightcurves for multiple solar phase angles (to constrain shape)
Imaging KBO Search	Observing: Obtain deep satellite searches for targets that the spacecraft flies within 0.3 AU of

SQ2.1 to SQ2.3: What is Pluto's internal heat budget? What is Charon's magnetic field environment? How do the Pluto system and heliosphere interact?

We note that the expected coldest surface temperatures on Pluto are between 35 and 55 K (Earle et al., 2017).

Table 5. Measurement requirements for instruments for SQ2.1 to SQ2.3.

Observation Type	Measurement Requirement
Pluto's Internal Heat Budget	
Thermal IR (surface mapping)	Minimum temperature to be detected: 35 K
	Spatial resolution: 20 km/pixel
	Surface coverage: 95% of both the illuminated and unilluminated surface
Thermal IR (thermal inertia mapping)	Spatial resolution: 10 km/pixel
	Local time coverage: At least one daytime (9 a.m. and 3 p.m.) and one nighttime (between 6 p.m. and 6 a.m. local time) at 10 geologically and compositionally diverse surface locations
Charon's Magnetic Field Environment	
Magnetometer	Operations: High data rates should be used when <1200 km.
	Observing: At least four periapses with one <600 km; these orbits should cover a range of longitudes.
Pluto/Heliosphere Interaction	
Magnetometer	Operations: Require full-orbit coverage for three orbits, with at least five periapses <1000 km and at least one <500 km. At least one set of equatorial equator and one set of polar orbits (>70° relative to the equator).

Instrument Performance and Observing Difficulties

For most instruments, the effect of not meeting the requirements is a sliding scale. For example, if one of the color channels fails, we will simply not be able to map in that color, or if the focal length/aperture is not to specification, then the signal-to-noise and/or resolution will be degraded. We note that much of the science will be addressed by multiple instruments, which provides some degree of redundancy. However, the radar instrument is not duplicated through other instruments, so it is uniquely capable of probing these questions. All of the measurement requirements outlined in this section (Table 1 to Table 4) can be met by the instruments selected (outlined in section 3).

None of the observations required is novel; all have been previously made either by New Horizons' or by other missions. The slow ground speeds and repeated ground tracks mean that there are many opportunities to obtain data and redo observations that have problems. Furthermore, few resources would be required to add an additional revolution to a given orbit, meaning additional observation opportunities could be added if required. We judge these planned observations to be about the same difficulty, with the most difficult probably being those to determine Pluto's gravity signature, because multiple target flybys with little/no station-keeping during that period are preferred. These observations must be planned carefully, to minimize the station-keeping but to ensure spacecraft safety.

Equity, Diversity, and Inclusion

We recommend that the decadal survey consider the critical role of team dynamics, equity, diversity, inclusion, and accessibility in planetary science. As demonstrated in this report, exploration of the KB requires drawing on perspectives spanning the gamut of planetary science, geoscience, astronomy, technology, engineering, and beyond over many decades. Studies of scientific teams have repeatedly demonstrated the importance of an integrated approach, where team members with diverse expertise develop synergies between their specialties and resources that result in an end product that adds up to more than the sum of its parts (Balakrishan et al., 2011). Sociological studies have demonstrated that groups that foster strong connections across subunits are more innovative (Burt, 2004; Powell et al., 1996; de Vaan et al., 2015) with higher impact outcomes that endure (de Vaan et al., 2015; Curral et al., 2001).

Additionally, it is critical that the planetary science community fosters an interdisciplinary, diverse, equitable, inclusive, and accessible environment. We strongly encourage the decadal survey to consider the state of the profession and the issues of equity, diversity, inclusion, and accessibility—not as separable issues but as critical steps on the pathway to understanding the KB and the entire solar system. Background information on the current lack of diversity in our community and specific, actionable, and practical recommendations can be found in Rivera-Valentin et al. (2020), Rathbun et al. (2020), Strauss et al. (2020), and Milazzo et al. (2020). We note that by 2050, demographics in the United States will have shifted to be less white: 47% white, 29% Hispanic, 13% Black, and 9% Asian (Passel and Cohn, 2008). Hence, if no action is taken, there will be a growing discrepancy between the diversity in the United States as a whole and the diversity of the planetary science workforce.

Table 6. Science Traceability Matrix.

Science Questions (SQs)	Detailed Science Objectives (SOs)	Measurement	Instrument	Functional Requirement
SQ1.1: What are the internal structures of Pluto and Charon? [KQ-1, IQ-10, IQ-18 & IQ-19]	SO1.1: What is the evidence for a subsurface ocean on Pluto?	Measure long-wavelength topography and gravity field to model the interior structure	Radio science & altimeter	Seven passes with periapsis less than 1000 km, including high-latitude passes for altimeter global shape determination; two-way Doppler (DSN) on at least one of these orbits
		Measure subsurface structure to 10-km depth; measure depth of ice and liquid in Sputnik Planitia	Radar	At least two passes over Sputnik Planitia, with one of the passes over its cellular portion; at least one pass over Vulcan Planitia on Charon
	SO1.2: Are Pluto and Charon fully differentiated?	Determine the J_2 and C_{22} of Pluto and Charon	Radio science	Multiple close Pluto and Charon passes over a range of latitudes and longitudes while Doppler tracking
	SO1.3: Does Pluto have any magnetic field, intrinsic or induced?	Measure Pluto magnetic environment	Magnetometer	Require at least four periapses with high-rate data below 1200 km, with at least one below 600 km that traverses a range of latitudes
SQ1.2: How have surfaces and atmospheres in the Pluto system evolved? [KQ-1, IQ-13, IQ-14]	SO1.4: What are the relative ages of, and geological processes acting on, different terrains globally on Pluto and Charon (including current, internally derived activity)?	Map surface geology of Pluto and Charon	Color and panchromatic imagers (NAC and WAC)	Incidence angles <80° and emission angles <70° for panchromatic; for color, phase angles 0–140° and incidence angles <60°
		Determine the topography of Pluto and Charon	Panchromatic imaging (NAC)	A series of images taken at the similar illumination but between 10° and 30° difference in emission angle
	SO1.5: What is the origin and evolution of Pluto's volatiles (surface and atmospheric)?	Map surface composition and photometric properties, and measure atmospheric composition	IR spectrometer, color imaging, Mass spectrometer, ultraviolet (UV)	Visible imaging + IR spectrometer (composition): global coverage with incidence angles between 10° and 30°, emission angles between 0° and 60°; mass spectrometer: passes at <500 km
				Visible imaging + IR spectrometer (photometric properties): regional observations with phase angles between 0° and 140°, emission and incidence angles between 0° and 80°
	SO1.6: What are the chemical composition and thermal structure of Pluto's/Charon's atmosphere, hazes, and exospheres?	Determine Pluto's and Charon's global atmospheric composition	Mass spectrometer, plasma, UV, color imager and infrared (IR) spectrometer	UV requirement: 100 solar and stellar occultations distributed over latitude and longitude; mass spectrometer: passes at <500 km; Plasma: instrument should be on during close (<2000 km) in sweeping mode, with $M/\Delta M$ of 2
				Visible imaging + IR spectrometer (composition): global coverage with incidence angles between 10° and 30°, emission angles between 0° and 60°; mass spectrometer: passes at <500 km
				Visible imaging + IR spectrometer (photometric properties): regional observations with phase angles between 0° and 140°, emission and incidence angles between 0° and 80°
	SO1.7: What is the origin and evolution of Charon's surface composition?	Map surface composition and photometric properties	IR spectrometer and color imaging	Visible imaging + IR spectrometer (composition): global coverage with incidence angles between 10° and 30°, emission angles between 0° and 60°; mass spectrometer: passes at <500 km
Visible imaging + IR spectrometer (photometric properties): regional observations with phase angles between 0° and 140°, emission and incidence angles between 0° and 80°				
SO1.8: What is the composition and escape rate of heavy and light ion species?	Determine escape rates	Mass spectrometer and plasma	Mass spectrometer: passes between 500 and 2000 km; at least five passes at <1000 km, plasma: and at least one below 500 km and add number flux range	

Science Questions (SQs)	Detailed Science Objectives (SOs)	Measurement	Instrument	Functional Requirement
SQ1.3: How has the KBO population evolved? [KQ-1, KQ-2, KQ-4, KQ-10, (KG-1, KG-4) IQ-9, IQ-10, IQ-13, IQ-14, IQ-18, IQ-19]	SO1.9: What constraints do the small satellites in the Pluto system place on the evolution of that system?	Map the surface, color, shapes, and composition of Pluto's small satellites	Color and panchromatic imager, altimeter, and IR spectrometer	Global high-resolution imaging and composition of encounter targets. Unresolved imaging and composition where possible. At least one close (3000 km) encounter with each satellite, with emission and incidence angles between 10° and 80°.
		Constrain the mass of at least one of Pluto's small satellites to 10%	Radio science	Encounters with each satellite at a closest approach <3000 km, with a velocity of <1 km/s and Doppler uncertainty of 0.1 mm/s
	SO1.10: How do the detailed surface properties, compositions, volatiles (and atmospheres, if present) of KBOs vary?	Map surface composition and photometric properties, and measure atmospheric composition if present	Color and panchromatic imaging, IR spectrometer (Mass spectrometer, plasma, UV for atmosphere)	KBO flybys at <10,000 km, with a preference for emission and incidence angles between 0° and 80° and preferred phase angles between 0° and 140°
	SO1.11: What do the surface features (including the cratering record) of encountered KBOs reveal about the origin, evolution, and geologic history of KBOs?	Map surface geology and color of encountered KBOs	Color and panchromatic imagers (NAC and WAC)	KBO flybys at a close approach distance <10,000 km
		Map surface composition, and determine photometric properties of KBOs	Color and panchromatic imaging, IR spectrometer	KBO flybys at <10,000 km, with a preference for emission and incidence angles between 0° and 80° and preferred phase angles between 0° and 140°
	SO1.12: What can binary fraction, density, and shapes of KBOs tell us about their formation and the collisional environment in the primordial Kuiper Belt? Do they support current streaming instability models?	Identify and characterize new KBO satellites	Panchromatic imaging (NAC)	Target of opportunity with no driving functional requirements
		Calculate KBO rotation periods from light curves	Panchromatic imaging (WAC)	Target of opportunity with no driving functional requirements
Level 2 SQ2.1: What is Pluto's internal heat budget? [KG-1, KQ-10, IQ-9, IQ-18, IQ-19] SQ2.2: What is Charon's magnetic field environment? [KQ-10, IQ-19] SQ2.3: How do the Pluto system and heliosphere interact? [KQ-10, KG-1, KG-4]	SO2.1: What is Pluto's internal heat budget and surface heat flow and search for thermal anomalies (possibly associated with current activity)?	Map surface temperature in conjunction with Science Questions 1 and 2	Thermal IR	Thermal emission to be determined at 10 geologically and compositionally diverse surface locations at local times between 9 a.m. and 3 p.m. and between 6 p.m. and 6 a.m.
	SO2.2: Does Charon have any magnetic field, intrinsic or induced?	Measure Charon magnetic environment	Magnetometer	Require at least four periapses with high-rate data below 1200 km, with at least one below 600 km that traverses a range of latitudes
	SO2.3: Is there a Plutopause, tail, bow shock, and interaction region, and if so, what are their shapes and motions?	Measure Pluto's extended magnetic field	Magnetometer, plasma	Require full-orbit coverage for three orbits, with at least five periapses below 1000 km and at least one below 500 km. At least one set of equatorial equator and one set of polar orbits (>70° relative to the equator).
		SO2.4: How do pickup ions affect shocks throughout the heliosphere and close to the Pluto system and other KBOs?	Measure the extended magnetic field at Pluto and during other KBO encounters	Magnetometer, plasma

2. High-Level Mission Concept

Overview

As part of NASA’s support to the National Research Council (NRC) and its 2023 Planetary Decadal Survey, APL was assigned the task of developing a mission and flight system architecture suitable to perform a scientifically viable Persephone mission responsive to STM requirements formulated by the Principal Investigator.

The Principal Investigator was specifically interested in a mission that would probabilistically encounter a KBO before and after entering Pluto orbit while accommodating the shortest Earth/Pluto transfer time technically feasible. Architecture trade-space analyses as well as detailed point designs were to be performed by APL. To meet the study’s needs, the work was divided into two phases: (1) an initial examination of the architecture trade space, specifically focused on initial mass and power, by a stand-alone study team staffed by generalists and specialists chosen for their knowledge relevant to the problem, and (2) detailed point design and cost estimating of the mission architectures emerging from the stand-alone team’s analyses by APL’s concurrent engineering team. This arrangement allowed for a free-ranging exploration of possible mission architectures by the stand-alone team, followed by a detailed point design phase leveraging the efficiency and experience designing spacecraft and costing total mission architectures, areas routinely handled by APL’s concurrent engineering team. The work was done in close coordination with the Principal Investigator and the Persephone Science Team, with the Principal Investigator and Science Team actively engaged throughout the process in the design decisions leading to the Persephone mission described in this study report.

Table 7 shows the key requirements and constraints identified by the study team to guide the Persephone mission design. The requirements and constraints in Table 7 were selected on the basis that they were (1) required by the NASA Decadal Survey ground rules, (2) identified by the Principal Investigator as critical to achieving the mission science objectives, or (3) identified by the Persephone study team as essential to the achievement of an affordable, low-risk flight system design.

Table 7. Key mission-driving requirements for the Persephone mission.

Requirement/Constraint	Origin/Comment
Project/Systems Engineering	
Limit the Earth-Pluto transfer duration to a minimum	Principal Investigator 1. Persephone will require five (5) Radioisotope Thermoelectric Generators (RTGs) to achieve. 2. RTG design life exceeded as outlined in the Decadal Guidelines—waiver submitted and approved by NASA HQ. 3. Requires use of an SLS-Block 2 with high-energy kick stage. Not part of the Decadal Guidelines—waiver submitted and approved by NASA HQ.
Launch Schedule Constraint #1 Optimal phasing with Jupiter ends in May 2032	Use a Jupiter flyby to allow a faster arrival time to the Pluto/Charon system. Limits launch to 2030, 2031, and 2032. Optimal phasing with Jupiter does not return until 2042.
Launch Schedule Constraint #2 Next-generation RTG availability	Decadal ground rules/flight-qualified next-generation RTG unit will not be available until 2030.
Encounter a 100- to 150-km-class KBO with a deviation of no greater than 1 AU from the nominal Pluto/Charon ingress trajectory	Persephone Science Team
Encounter a 100- to 150-km-class KBO within 8 years of leaving the Pluto/Charon system	Persephone Science Team
Apply APL design principles	APL Persephone Design Team
Mission class: large strategic science missions	Large strategic science mission based on mission cost and complexity

Requirement/Constraint	Origin/Comment
Mission Design	
Accommodate minimum 24-month Pluto/Charon orbital tour, with a minimum of four tour options of the Pluto/Charon system	Persephone Science Team
Payload	
Accommodate Persephone and KBO science team defined payload	Persephone Science Team Affects flight system pointing, instrument duty cycles, coverage strategy, and mission design
Operations	
Accommodate science data acquisition requirements	Persephone Science Team Accommodate observation plan for 10 instruments from Persephone Science Team and use SciBox (MESSENGER) build observation plan that satisfies requirements.
Flight System	
No new technology	Goal: Reduce mission risk and cost
Accommodate a mission Δ -V of >10 km/s	Persephone Design Team Electric propulsion is the most mass-efficient technology that can satisfy this requirement.
Use Ka-band for data downlink	Decadal ground rules
Accommodate spacecraft pointing error of $\pm 0.05^\circ$	Ka-band spacecraft pointing to accommodate fixed HGA operations
Accommodate downlink data rate at Pluto/Charon to fully return required science observations	Principal Investigator Use dual polarization and simultaneous right-hand circular polarization (RHCP) and left-hand circular polarization (LHCP) (New Horizons) to achieve full science return requirement with >3-dB link margin.
Accommodate instruments and instrument duty cycles	Principal Investigator
Support radio science modes of operation	Principal Investigator Add New Horizons class USO and REX capability to radio frequency (RF) subsystem.
Ground System	
34-m DSN antenna	Decadal ground rules
One antenna at each DSN complex (no antenna arraying)	Decadal ground rules

Concept Maturity Level

Upon completion of the Persephone study, with point designs in place, the concept is at concept maturity level (CML) 4 as defined by Wessen et al. (2013). The architectures studied were defined at the subsystem level with estimates developed for mass, power, data volume, link rate, and cost using APL's institutionally endorsed design and cost tools. Risks were also identified and assessed as to their likelihood and mission impact, as discussed.

Technology Maturity

All flight system elements—subsystems and instruments—are currently at or above technology readiness level (TRL) 5. For the spacecraft, the integration Radioisotope Power System (RPS) with ion electronic propulsion currently has not been tested or flown in a flight system. The integration of these two technologies should represent a low-risk integration. RPSs to increase the TRL would not be available until 2028 given the current RPS Program Office.

The instruments are all based on technology that either is highly developed or has already flown, as shown in Table 9. For the instruments, only engineering development necessary to accommodate the mission life and the specific enhancements of performance would be required.

Key Trades

Multiple solutions were considered for each design decision, with final selections primarily motivated by the prioritization of maximized landed mass. Key trade studies that drove the design are listed in Table 8.

Table 8. Persephone key trades.

Area	Trade Space, Result (Bold)	Rationale
Solar Electric Propulsion (SEP) Stage	SEP	
	No SEP Stage	Notional SEP stages did not result in decreased Earth-Jupiter-Pluto transit time, because of added mass of the stage; the additional mass resulted in the spacecraft being made heavier and harder to slow down.
Delta-Velocity Earth Gravity Assist (DVEGA)	DVEGA	
	No DVEGA	The DVEGA increases the Earth-Jupiter-Pluto transit time by 3 years. In addition, launch must occur by 2028 to arrive at Jupiter by 2031 for proper flyby phasing. No RTGs will be available at that time per the Decadal Guidelines. The mission would not be viable.
Direct Earth-Jupiter-Pluto Transfer	Direct Pluto Transfer	
	Earth-Jupiter-Pluto Transfer	This trade resulted in significantly shortened transit time and delivered mass when coupled with a high-energy upper stage. It was chosen as the mission concept baseline.
Launch Vehicles	Falcon Heavy vs. Falcon Heavy Expendable vs. SLS-Block 1 vs. SLS-Block 2	SLS-Block 2 has the lowest Earth-Jupiter transit time and highest delivered mass and was chosen as the mission concept baseline.
High-Energy Upper Stages	Centaur vs. Castor30B	Centaur significantly increases delivered mass to the Pluto/Charon system. Science goals could not be achieved without added mass.
Electric Propulsion Systems	NEXT-C, Qinetiq T5, Busek BHT-600, XR-5 , and Apollo ACE Max	XR-5 is chosen because it has maximum thrust at minimum power.
Performing Mission under Decadal Guidelines	STM Met	To meet science goals, waivers were submitted and approved by NASA HQ for deviations from the decadal ground rules.
	STM Not Met	The trade concluded that the mission goals could not be met using the given decadal ground rules. In addition, mission duration would increase by multiple decades.
Attitude Control during Cruise Phase	Spin	
	3-Axis	Three-axis stabilized was selected to be compatible with the electric engine gimbal system.
Periodic Pluto/Charon Tour	Orbiting	
	Lagrange Transfers	Periodic orbital design based on using Lagrange point transfers provided the best ground-track options to achieve science goals.
Power Density	Fission	The cost and availability of fission sources are currently unknown; however, a fission source would be a significant mission enabler, potentially reducing Earth-Pluto transit time by decade or more.
	RTG	RTG power was chosen to allow the report to be completed to CML 4.
Number of RTGs	1, 2, 3, 4, or 5	A trade study was conducted to decrease the transfer time to the Pluto/Charon system to an acceptable period per the Persephone Science Team. To decrease the transfer time, operating the EP system at the most efficient operating point is required. This requires optimization of electrical power to the EP engine. The study team analyzed the required number of RTGs to achieve peak efficiency over the thrusting lifetime. Increasing the number of RTGs to five allowed the most efficient operation of the EP engine over the thrusting time period.
Number of Redundant Reaction Wheels	1 or 2	Reliability analysis concluded that two additional reaction wheels would increase mission reliability. Further analysis will be required to support the extended mission.

3. Technical Overview

Instrument Payload Description

The entire science payload is based on existing instruments. None require new technologies, but some have modifications that improve their performance for this mission. All of the instruments are body mounted to the spacecraft or to a fixed boom. The imagers, imaging spectrometers, and altimeter are mounted on the same side of the spacecraft and will be facing nadir during most low-altitude passes. A perpendicular side of the spacecraft faces in the ram direction, toward the direction of motion. The in situ instruments are mounted on this deck. None of the instruments articulate, and the spacecraft attitude provides instrument pointing. Although the spacecraft can accept data at high rates, the instruments will have embedded storage so that they can perform compression or higher-level processing, if desired.

Most of the imaging and spectroscopic instruments can achieve the required spatial resolution at altitudes of 5000–10,000 km. Because the spacecraft will dwell in this altitude range for thousands of hours over the mission lifetime, the instruments can perform their global mapping from this range. There is a range of illumination and viewing geometry available, which enables high-quality imaging and photometric studies. The observation plan requires only slow slews and low acceleration, well within the torque capability of the spacecraft reaction wheels. The in situ instruments—magnetometer, plasma spectrometer, and mass spectrometer—operate primarily within 2000 km of the surface but will also be used for several surveys of the entire Pluto/Charon system. The altimeter and radar sounder gather data at altitudes <1200 km. Stellar occultations are available at a full range of local times and locations. UV and radio occultations cover dawn and dusk at several longitudes.

The instruments in this study were selected to verify the feasibility of the measurements required to meet the science goals. Because of the high mass and power required for the electronic propulsion system that brings the payload to Pluto, overall mission performance is much less sensitive to payload mass and power than for most missions. Table 9 is a summary of each payload instrument, and Table 10 provides details on the payload mass and power. The data rates are averages when taking data. The radio frequency (RF) communications system provides the downlink rate necessary to return all required data, with margin.

Instrument 1: Panchromatic and Color High-Resolution Imager

The panchromatic and color high-resolution imager provides global maps for high-resolution panchromatic, eight colors, and stereo for a total of 10 global maps. The operation plan also includes measurements with different illumination and viewing geometry for phase-function calibration. The instrument will operate in a push-broom mode for Pluto and Charon, capturing both panchromatic and color bands simultaneously with color filters on eight strips that are 4000 pixels wide. There is also a framing mode for optical navigation and for long-range imaging of KBOs. The spacecraft provides the pointing and the 50 μ rad/s scan rate.

The pixel size is 5 μ rad for all data. Spatial resolution exceeds the 50-m requirement at altitudes <10,000 km, and the surface scans occur between 7000 and 11,000 km. Spatial resolution for color data is lower, 200 m, and those data will be binned 2×2 to reduce data volume while still outperforming the requirement. High-performance lossy compression is also possible.

Instrument 2: Low-Light Camera

Because of Pluto's obliquity, latitudes between 50°S and the south pole will be in shadow during the mission. The low-light camera uses reflected light from Pluto to image this otherwise-hidden terrain on Charon (and similarly Charon-light on Pluto). The low-light camera is a version of the Europa Imaging System (EIS) WAC (Europa Clipper) modified with an aperture increased to 25 mm, the size needed to obtain the required SNR.

Instrument 3: UV Spectrometer

The UV spectrometer measures Pluto's atmosphere by providing column density versus wavelength during solar or stellar occultations. There are two apertures. The one that is used for stellar occultations is aligned with the nadir-facing instruments and can also be used for characterizing surfaces of the airless targets (Charon, the small satellites, and other KBOs). A second aperture has a restricted throughput designed for solar occultations and can be used at the same time as REX measurements of occultations with Earth transmissions. The data rate is calculated based on the maximum expected count rate during solar occultations.

Instrument 4: Near-IR Spectrometer

The near-IR spectrometer provides hyperspectral coverage from 0.8 to 5 μm , an extension of the wavelength coverage of both New Horizons and Lucy LEISA. The spectral regions are selectable, with ~ 250 of the 2000 spectral elements stored and transmitted to Earth. This enables high spectral resolution for important features across a wide range of wavelengths. The instrument is capable of higher angular (spatial) resolution than the required 60 μrad .

Instrument 5: Thermal IR Camera

The Thermal IR camera provides temperature measurements of a target's surface. The camera is based on the THEMIS instrument (Mars Odyssey) with different wavelength filters, similar to the thermal wavelengths on Diviner (LRO). Measurements at several local times provide information on the thermal inertia of the surface.

Instrument 6: RF Spectrometer (REX)

The RF spectrometer is integrated into the RF communications system. It consists of electronics that monitor the RF transmissions from Earth while Pluto's atmosphere occults the signals. The resulting change in amplitude provides density and temperature information about a target's surface to the lowest few scale heights. The REX electronics are unchanged from REX on New Horizons. REX requires that the RF system include a USO.

Instrument 7: Mass Spectrometer

The mass spectrometer measures neutrals at densities $>10^4$ molecules/ cm^3 and is based on MAss SPectrometer for Planetary EXploration/Europa (MASPEX) (Europa Clipper) but without the extra radiation shielding required for the Jovian environment and without the cold trap, which is unnecessary in the Pluto/Charon system. We also add an open aperture, which enables measurements of ions. Measurements up to 1000 μ are possible, but most neutral molecules will be below 200 μ . Mass resolution will be at least 2500 and is adjustable to 25,000.

Instantaneous data rate is high, but there are tens of seconds of integration time between measurements. Onboard processing selects the scientifically useful mass ranges to reduce the data volume for downlink.

Instrument 8: Altimeter

The altimeter is a version of the Mercury laser altimeter (MLA) modified to increase pulse rate from 8 Hz to 30 Hz. It measures along-track topography with high accuracy (range accuracy of 0.1 m) at 30 Hz, which corresponds to <30 m between measurements on the surface. The data are used to anchor elevations from stereo and to provide the shape accuracy required for inferring internal structure from gravity. The maximum range is at least 1200 km.

Instrument 9: Sounding Radar

The sounding radar is a very-low-frequency (VLF), single-frequency (50 Hz) active radar based on SHARAD. This frequency is a balance between depth resolution of 3–5 m, depending on the layer composition, and the deepest penetration, which will be ~10 km. Pluto's ionosphere is too thin to interfere with the sounding radar measurements. The boom is two linear dipole antennas. Radiated power is 100 W. Spatial resolution is ~4 km but can be shorted along track to 1 km. The raw data rate is 20 Mb/s, but instrument processing reduces the output to 300 kb/s to the spacecraft.

Instrument 10: Magnetometer

Two boom-mounted three-axis fluxgate magnetometers measure the magnetic field. The boom is 3.6 m (MESSENGER) with one magnetometer mounted at the end and one approximately half way down the boom. The instrument will operate continuously and can store data at a normal or lower rate.

Spacecraft rolls will be used to augment the ground calibration.

Instrument 11: Plasma Spectrometer

The plasma spectrometer measures the composition, energies, angular and spatial distributions, and densities of pickup ions, solar wind ions, and ionosphere ions. If a bow shock is present, the plasma spectrometer will quantify the densities. Energy range is 3 eV to 50 keV. Both electrostatic analyzers and time of flight are used to determine composition. There are several existing instruments that can be flown. CoDICE-Lo (IMAP) is a recent example. A FIPS (MESSENGER) type instrument has a large field of view (FOV) that is well suited for non-spinning spacecraft.

The instrument will operate when near the predicted bow shock and magnetotail and when within 3000 km of Pluto's surface. It will also gather data throughout the Pluto/Charon system to check for additional sources and flows.

Table 9. Payload overview table.

	Panchromatic and Color High-Resolution Imager	Low-Light Camera	UV Spectrometer	Near-IR Spectrometer	Thermal IR Camera	RF Spectrometer (REX)	Mass Spectrometer	Altimeter	Sounding Radar	Magnetometer	Plasma Spectrometer
Instrument #	1	2	3	4	5	6	7	8	9	10	11
Type of instrument	Optical	Optical	Optical	Optical	Optical	Passive EM	Particle	Optical	Active EM	Fields	Particles
Number of channels	9	1	1	1	1	1	1	1	1	2	1
Size/dimensions (mm × mm × mm)	ø314.5 × 593.9	264 × 239 × 270	463 × 213 × 132	852 × 728 × 560	333 × 240 × 288	(in radio)	1054 × 443 × 290	297 × 297 × 285	Ø76.2 × 5048	100 × 200 × 50	524 × 443 × 290
Instrument mass without contingency, CBE* (kg)	8.8	14	4.5	10.5	9	0.2	15	11	10	5	11
Instrument mass contingency (%)	15	15	15	15	15	15	15	15	15	15	15
Instrument mass with contingency (CBE + Reserve) (kg)	10.1	16.1	5.2	12.1	10.3	0.2	17.25	12.65	11.5	5.75	12.65
Instrument average payload power without	5.8	6	4.4	7.1	28	1.6	45	25	25	10	16

	Panchromatic and Color High-Resolution Imager	Low-Light Camera	UV Spectrometer	Near-IR Spectrometer	Thermal IR Camera	RF Spectrometer (REX)	Mass Spectrometer	Altimeter	Sounding Radar	Magnetometer	Plasma Spectrometer
contingency (W)											
Instrument average payload power contingency (%)	15	15	15	15	15	15	15	15	15	15	15
Instrument average payload power with contingency (W)	6.7	6.9	5.1	8.2	32.2	2.3	51.7	28.7	28.7	11.5	18.4
Instrument average science data rate [^] without contingency (Kbps)	4320	1000	16	1600	1	2.5	1000	5	300	5	2
Instrument average science data [^] rate contingency (%)	0	0	0	0	0	0	0	0	0	0	0
Instrument average science data [^] rate with contingency (Kbps)	4320	1000	16	1600	1	2.5	1000	5	300	5	2
Instrument FOVs (degrees)	1.15 × 0.57	48	0.1 × 2.0	0.9	4.6	N/A	45	0.006	N/A	N/A	150
Pointing requirements (knowledge) (degrees)	0.017	1	0.02	0.01	0.05	N/A	5	0.01	1	2	5
Pointing requirements (control) (degrees)	0.017	5	0.05	0.05	0.1	N/A	10	0.05	5	2	10
Pointing requirements (stability) (degrees/s)	0.00278	10	0.01	0.00278	0.001	N/A	N/A	N/A	N/A	N/A	N/A

*CBE = Current Best Estimate

[^]Instrument data rate is defined as science data rate before onboard processing.

Table 10. Payload mass and power table.

	Mass			Average Power		
	CBE (kg)	% Cont.	MEV (kg)	CBE (W)	% Cont.	MEV (W)
Panchromatic and color high-resolution imager	8.8	15	10.1	5.6	15	6.4
UV spectrometer	4.5	15	5.2	4.4	15	5.1
Near-IR spectrometer	10.5	15	12.1	7.1	15	8.2
Low-light camera	14	15	16.1	6	15	6.9
Thermal IR camera	9	15	10.4	28	15	32.2
RF spectrometer	0.16	15	0.2	1.6	15	1.84
Mass spectrometer	15	15	17.2	45	15	51.7
Altimeter	11	15	12.7	25	15	28.7
Sounding radar	10	15	11.5	25	15	28.7
Magnetometer	5	15	5.8	10	15	11.5
Plasma spectrometer	11	15	12.7	16	15	18.4
Total payload mass	99		114	173.7		199.6

MEV = Maximum Expected Value

Flight System

The flight system would consist of a single Persephone spacecraft that enters the Pluto/Charon system after a long cruise and KBO encounter. Refer to the mission design section for the proposed timeline and trajectory. The spacecraft uses its large, nuclear-powered, electric propulsion system for the Pluto/Charon Δ -V maneuvers, and later for orbit adjustment and KBO tour Δ -V maneuvers. The flight system would employ three-axis stabilization and feature the following: a body-fixed Earth-pointing HGA and body-fixed payload suite, X- and Ka-band science data downlinks, five NGRTGs to provide power, and a small monopropellant blowdown (hydrazine) propulsion system for orbit maintenance and attitude control.

The flight system would be dual string with cold spares and a 3-m-diameter HGA. The equipment layout and thermal design are intended to minimize heater power required. All of the bus equipment and much of the payload share a highly insulated single enclosure. Figure 2 and Figure 3 illustrate the payload and equipment layouts, respectively. Figure 4 shows the flight system block diagram. Table 11 represents the neutral mass summary of the Persephone spacecraft.

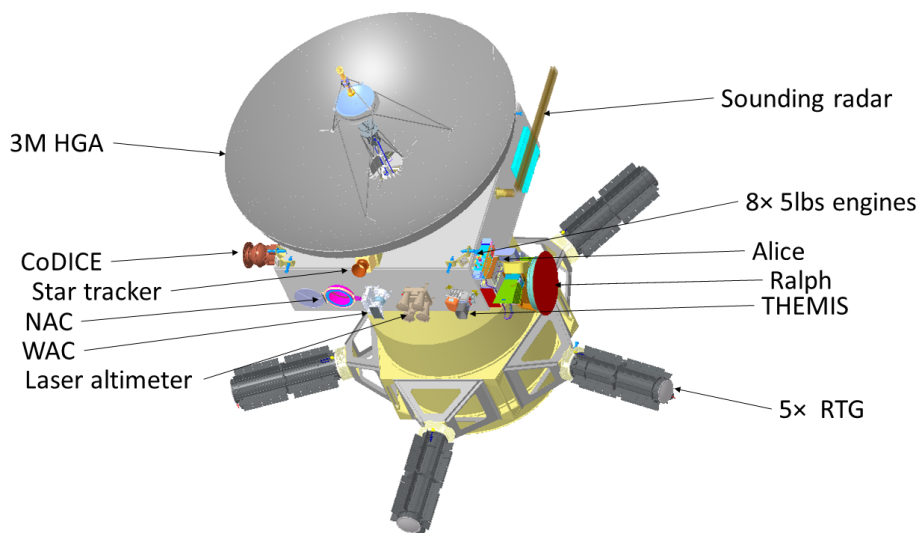


Figure 2. Persephone external spacecraft overview featuring payload locations.

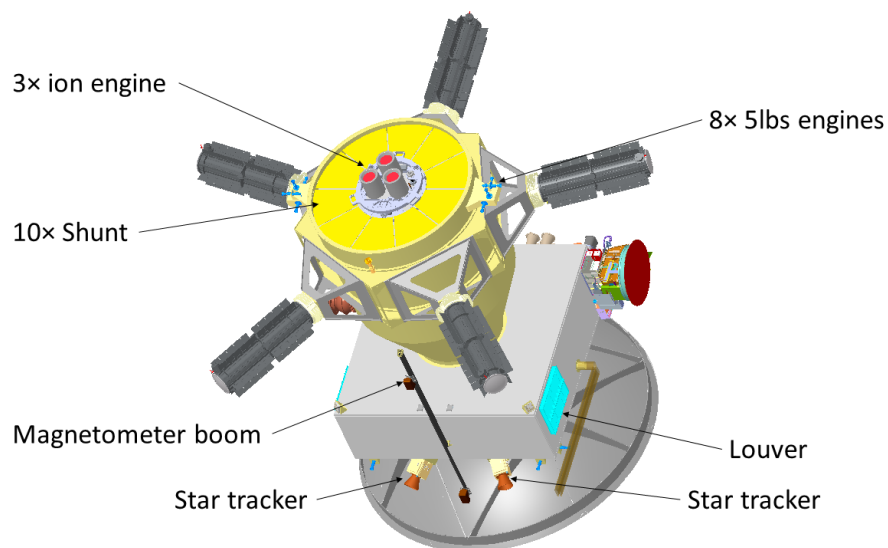


Figure 3. Persephone external equipment layouts.

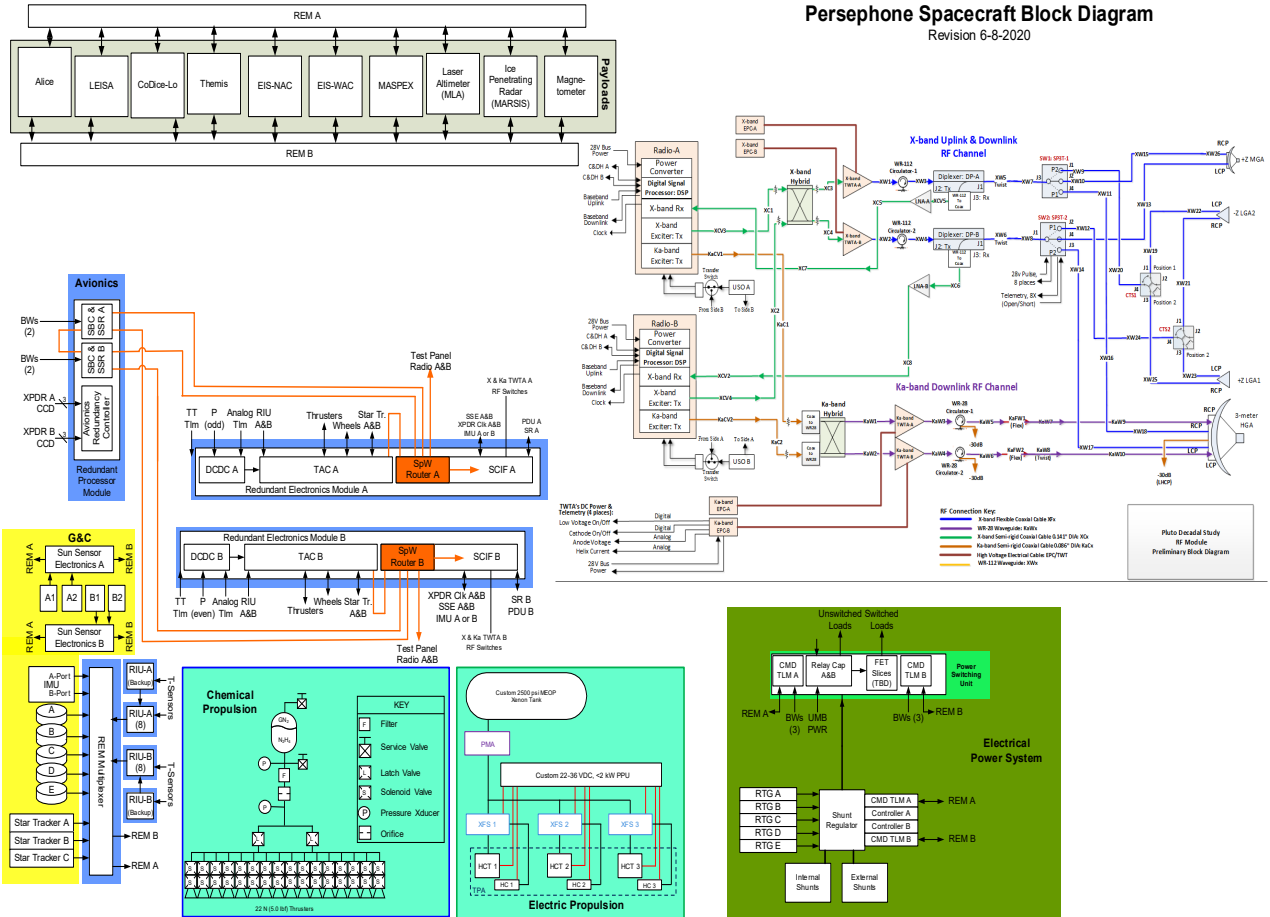


Figure 4. Persephone flight system block diagram.

Table 11. Flight system neutral mass summary.

Pluto-KBO Flight System Neutral Mass Summary (kg)			
Subsystem	CBE	Cont.	MEV
Avionics	17	10%	18
Guidance, Navigation, and Control	64	9%	70
Power	346	15%	397
Harness	116	15%	133
Thermal	107	15%	123
RF Communications	59	14%	67
Electric Propulsion	486	14%	555
Propulsion	64	9%	69
Mechanical	460	15%	529
Spacecraft Bus Total	1718	14%	1963
Payload	99	15%	114
Flight System Dry Mass (CBE, cont., MEV)	1817	14%	2076
Hydrazine Mass (CBE, cont., MEV)	100	4%	104
NEUTRAL MASS (CBE, MEV), kg	1917		2180
DRY MASS MPV, kg			2699.0
DRY MASS MARGIN, kg			622.6
DRY MASS MARGIN, %			32%

Hydrazine CBE mass is calculated using the MEV wet mass of the space vehicle upon entry to the Pluto/Charon system and 120% of the Δ -V number (in meters per second), plus estimated Attitude Control System (ACS) propellant.

The spacecraft team evaluated a number of power modes that were potential hot- or cold-case thermal drivers or total load power drivers. Non-EP loads have at least 30% margin. Because the baseline EP system has flight heritage, we are allocating 10% contingency to the EP-related loads. Required margin for the EP system can be lower than for non-EP loads, as suggested in *Analysis of System Margins on Missions Utilizing Solar Electric Propulsion* (Oh et al., 2008). A power mode summary is in Table 12. Table 13 provides an overall summary of the flight system characteristics.

Table 12. Flight system power modes.

Subsystem/Instrument	Science	EP Burn-End of Pluto Insertion	EP Burn-End of Planned KBO Tour	Chemical Δ -V Prep	Chemical Δ -V	Data Link Active	Radio Science
Payload Instruments MEV	198	1	1	1	1	1	1
Command and Data Handling (C&DH) MEV	20	20	20	20	20	19	19
Guidance, Navigation, and Control (GNC) MEV	45	45	45	84	84	63	63
Electrical Power Subsystem (EPS) MEV	31	31	31	31	31	31	31
Thermal MEV	22	6	20	62	62	21	62
Telemetry, Tracking and Control (TT&C) MEV	15	15	15	9	9	551	316
Propulsion MEV	18	18	18	137	108	18	18
MEV TOTALS (payload plus non-EP bus loads)	349	136	150	344	315	705	510
Non-EP Margin	30%	30%	30%	30%	30%	30%	30%
Non-EP Power with Margin	454	177	195	447	409	917	663
Electric Propulsion MEV	0	844	560	0	0	0	0
Total RTG Years	41	30	41	41	41	33	41
Available Power	857	1059	857	857	857	1000	857
Total Non-EP Power with Margin	454	177	195	447	409	917	663
Remaining Power for EP	404	882	663	410	448	83	194
Required EP Power	N/A	760	504	N/A	N/A	N/A	N/A
EP Power Margin, W	N/A	122	159	N/A	N/A	N/A	N/A
EP Power Margin, %	N/A	16%	32%	N/A	N/A	N/A	N/A

Table 13. Flight system element parameters.

Flight System Element Parameters	Value/Description
General	
Design Life, Years, Cruise	28
Design Life, Years, Pluto/Charon	28 + 3 = 31
Design Life, Years, Extended Mission	28 + 3 + 8 = 39
Structure	
Structure Material	Aluminum
Number of Articulated Structures	None
Number of Deployed Structures	Two (magnetometer boom, ice-penetrating radar antenna)
Thermal Control	
Type of Thermal Control Used	Mostly passive thermal control with heaters and louvers utilized to protect the minimum temperature of the system
Propulsion	
Systems	Electric propulsion (xenon), chemical propulsion (hydrazine)

Flight System Element Parameters	Value/Description
Electric Propulsion Δ -V	9164 m/s
Electric Propulsion Isp and thrust	1266–1009 s; 74 mN – 36 mN
Electric Propulsion Thrusters and Tanks	Single custom tank, three XR-5 thrusters, single power processing unit (PPU) with internal redundancy, thrusters articulated with electrically redundant biaxial gimbal
Chemical Propulsion Δ -V	30 m/s + 50 kg (ACS)
Chemical Propulsion Isp	232 s (steady-state)
Chemical Propulsion Thrusters and Tanks	Single diaphragm tank, 16 5-lbf thrusters, used for small Δ -V and ACS
Attitude Control	
Control Method	Three-axis
Control Reference	Solar (safe), stars (all other modes)
Pointing Control Capability, Degrees	61.9 arcsec; 0.52-arcsec jitter, 0.1 s
Pointing Knowledge Capability, Degrees	61.9 arcsec
Agility Requirements (maneuvers, scanning, etc.)	0.006°/s
Articulation	All elements body-fixed
Sensor and Actuator Information (precision/errors, torque, momentum storage, etc.)	Two fine Sun sensors, three star trackers with <10-arcsec accuracy, single Scalable Space Inertial Reference Unit (SSIRU), five reaction wheel assemblies (RWA) with 75-mNm torque, 68-Nms angular momentum storage, and 0.06-Nm capability
Command and Data Handling	
Flight Element Housekeeping Rate	≤20 kbps
Data Storage Capacity	256 Gb
Maximum Storage Record Rate	>2 Mbps
Maximum Storage Playback Rate	>2 Mbps
Power	
Power Source	Five NGRTGs
Beginning of Life and End of Life Load Power Capability	1811 W at launch; 857 W at 39 years postlaunch (end of extended mission)

Attitude Control

The Pluto Orbiter guidance, navigation, and control (GNC) provides a three-axis-controlled platform that satisfies all requirements set by science, navigation, communication, and propulsion. All GNC components are available commercial off-the-shelf (COTS) with multiple potential vendors.

Reaction wheels are generally designed for the 15-year life typical of a geosynchronous satellite, although there are many missions and wheels that have been operated well beyond that time to 20 years or more. Because of the very long lifetime required for this mission, five wheels have been baselined to provide adequate redundancy and wheel operating life. Three wheels will be used at any one time to maintain attitude control with two wheels in storage. At a cadence to be determined in the future and in consultation with the reaction wheel vendor, the reaction wheels in storage will be rotated into the control system while two active wheels are moved to storage to balance the operating life among the wheels and maximize bearing life.

RF Communications

The telecommunications system will feature a fully redundant design, including two radios, all necessary redundant RF cabling and switching, and two USOs. The radios are connected to a suite of antennas: two low-gain antennas (LGAs), one medium-gain antenna (MGA), and one HGA. The HGA is a 3-m dish, mimicking the Europa Clipper HGA. The USOs are in an active cross-strapped configuration; both clocks will be powered on and available to provide clocking to the radios. The USOs provide the radios with a precision clock source capable of radio science, as well as standard communications exchange. The Ka-band transmission will be supported by a 150-W amplifier, and the X-band will be supported by a 12.5-W amplifier.

The spacecraft will communicate to the DSN family of 34-m beam waveguide antennas. Upon arriving at Pluto, the Ka-band downlink will provide a 28-kbps link with the DSN. This will allow for 800+ MB/day of science data from the spacecraft to Earth. The extended mission sees a data rate of ~350 MB/day.

Propulsion

There are two propulsion subsystems baselined across the spacecraft. Both propulsion systems will be purchased from a propulsion system supplier who will integrate them onto an APL-furnished spacecraft structure. The REP subsystem will accomplish the low-thrust trajectory to Pluto. Any necessary higher-thrust maneuvers, including instrument pointing, will be performed using the chemical propulsion system.

Radioisotope Electric Propulsion (REP) Subsystem

The cruise stage will baseline three Aerojet Rocketdyne XR-5 Hall Current Thrusters (HCTs) to accomplish a low-thrust trajectory to Pluto. HCTs use an electron-emitting cathode to ionize xenon propellant, which is then electromagnetically accelerated to provide thrust. The XR-5 was developed by the U.S. Air Force and Lockheed Martin for the Advanced Extremely High Frequency series.

The XR-5 engines are capable of operating from 300 to 4500 W and will require a delta-qualification to demonstrate necessary throughput. Although this study closed using the XR-5 engine, other flight-proven electric propulsion engines exist, such as BepiColombo's Qinetiq T6 Hall Engine.

The REP subsystem will include a custom composite-overwrapped xenon tank with a 4000-kg usable capacity at 2500 psi. The tank will be thermally controlled to keep the stored xenon in its supercritical phase at >20°C. The system will also feature a plume-neutralizing hollow cathode (HC), high-pressure propellant management assembly (PMA), low-pressure xenon flow systems (XFSSs), a custom PPU, and a multi-axis thruster pointing assembly (TPA).

Chemical Propulsion System

The chemical propulsion subsystem is a blowdown monopropellant hydrazine system that provides Δ -V capability and attitude control for the spacecraft. The system consists of 16 22-N (5-lbf) thrusters and components required to control the flow of propellant and monitor system health and performance. The propellant and helium pressurant are stored in a single tank separated by a silicon-free elastomeric diaphragm. As propellant is expelled, the pressure declines; therefore, the thrust and specific impulse of the thrusters decrease as the mission progresses.

The thrusters are of the catalytic monopropellant hydrazine type; when the thruster valves open, propellant flows through the thruster into a catalyst bed, where the hydrazine spontaneously decomposes into hot gases, which then expand through a nozzle and exit the thruster, producing thrust. For the purposes of this study, mission-averaged performance data for the MESSENGER-heritage Aerojet Rocketdyne MR-106E 22-N thrusters were used, but alternate options exist.

The propellant and pressurant will be stored in a titanium tank manufactured by Northrop Grumman Innovation Systems. The remaining components used to monitor and control the flow of propellant will be selected from a large catalog of components with substantial flight heritage on APL and another spacecraft.

Avionics Architecture

The Persephone avionics architecture is designed for block redundancy with full interface cross-strapping. The avionics hardware is separated into two primary housings: the Redundant Processor Module (RPM) and the Redundant Electronics Module (REM). This approach is consistent with previous APL spacecraft programs and will take advantage of extensive heritage hardware.

Redundant Processor Module

Command and data handling (C&DH), guidance and control (G&C), and spacecraft fault protection functions will be performed in a single radiation-hardened, quad-core, GR740 processor. A cold redundant processor and solid-state recorder (SSR) will serve as backup and can be placed in a warm-spare state as needed. The Avionics Redundancy Controller (ARC) will continually monitor the status and health of the single board computer (SBC) and SSR systems and switch or change power states of the equipment if necessary.

The SSR board will form eight 32-Gbit memory banks for a recorder size of 256 Gb. This design leverages existing technologies developed for the Parker Solar Probe mission.

Redundant Electronics Module

The REM consists of the Spacecraft Interface Card (SCIF), the Thruster/Actuator Controller (TAC), and the Multiplexer Card. The REM incorporates cross-strapped redundancy for payload and navigation interfacing as well as SpaceWire links to the RPM through a nine-port SpaceWire router. The SpaceWire and payload routing will be performed by an RTG4 field-programmable gate array (FPGA) onboard the SCIF.

Power

The Electrical Power Subsystem (EPS) provides power generation, regulation, and distribution for the vehicle through all mission phases. Figure 5 presents a block diagram of the EPS. The subsystem is designed to provide a 30% margin in all load cases (see Table 12).

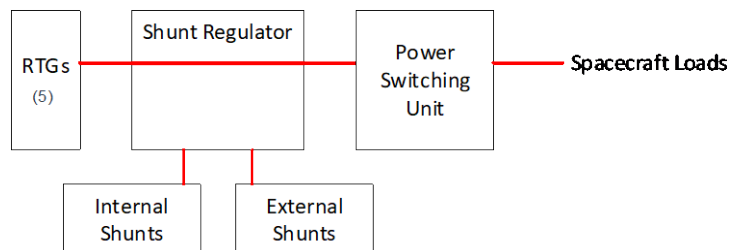


Figure 5. Electrical Power System block diagram.

Power Generation

Five NGRTGs provide power to the vehicle. Together the NGRTGs provide 2000 W when initially loaded with fuel and are estimated to provide 910 W at the end of the extended mission (after distribution, regulation, and switching losses, available power at power switching unit output is 857 W at the end of the extended mission), assuming the RTGs are loaded 2 years¹ before launch. The RTGs are provided by NASA and will be installed at the launch base. Spacecraft testing will be achieved using RTG simulators, which are similar in form, fit, and function to the RTGs, but the thermocouples are heated using electrical heaters rather than plutonium.

Mechanical

The mechanical design of the spacecraft consists of two main sections: a lower section that primarily houses the propulsion tanks (xenon and hydrazine) and the five RTGs, and an upper section that accommodates most other components, including the instruments.

The lower section is an aluminum assembly consisting of a 1.6-m-diameter cylinder to house the large xenon tank, a conical adapter section, and a smaller cylinder that provides the interface between the lower section and the upper section. The lower section provides the interface to the launch vehicle and accommodates the five RTGs, which are supported by titanium brackets to provide thermal isolation. The -Z face of the lower section accommodates the three ion engines on a two-axis gimbal. This face has an array of shunts used to dissipate waste RTG heat.

¹ The timeline of 2 years prior to launch for fueling the NGRTGs is for the purposes of calculating the degradation rate of the fuel source over the course of the mission lifetime.

The upper section is a rectangular prism of honeycomb construction with dimensions $2.1 \times 2.1 \times 0.6$ m. One side of the upper section accommodates the in situ instruments, facing them in the ram direction, to limit contamination from the rest of the spacecraft. The nadir side of the upper section accommodates the nadir-facing instruments with their FOVs unobstructed. The sounding radar instrument's boom deploys off of the upper section and points anti-ram. The magnetometer boom also deploys off the upper section and points anti-nadir. The +Z face of the upper section accommodates most of the antennas, HGA, MGA, and one LGA (the other LGA is located adjacent to the launch vehicle interface facing -Z). The antennas are stacked on each other in a configuration that was used on New Horizons.

Eight reaction control engines are located on each main section (16 total). The eight on the lower section are positioned toward the -Z to maximize separation from the engines on the upper section. The five reaction wheels are accommodated inside the upper section.

The overall dimensions of the spacecraft are approximately 5 m in height and 4.8 m in diameter. In the launch configuration, there is ample clearance for the spacecraft inside the launch vehicle fairing.

Thermal

The Persephone thermal design accommodates the range of mission solar distances. All instruments are thermally isolated from the spacecraft and blanketed to minimize heater power usage. For the spacecraft bus, Persephone uses the same approach as New Horizons. All spacecraft hardware including instrument electronics and propulsion module components are thermally coupled together and covered with VDA Kapton multilayer insulation, using electronics waste heat to maintain temperature. The spacecraft bus will maintain a constant internal heat dissipation, providing a set thermal load to the system. As electronics boxes are turned off, makeup heaters will be enabled to maintain the bus temperature. Heat pipes will be selectively utilized to transport the concentrated heat from the traveling wave tubes (TWTs) and PPU to a nearby radiator for rejection to space. Louvers maintain the spacecraft core between 10°C and 50°C as the external environment varies because of solar distance, along with bus internal heat variations.

The RTGs are mounted on brackets in a ring around the propulsion module section, where the large xenon tank is housed. Although the RTGs are thermally isolated from the structure via the titanium brackets, enough heat soaks back into the structure to help maintain the xenon tank within the limits of 20°C to 50°C with only a small amount of heat need to keep the tank from freezing. When the EP engines are in use, the majority of the electricity generated by the RTGs will be consumed by the EP engines and the PPU. When the EP engines are not firing, the excess electricity will be dissipated at the main shunts, which are mounted to and thermally isolated from the aft deck of the spacecraft. Special internal shunt heaters could be enabled inside the spacecraft bus and on the xenon tank should extra heat be needed.

Flight Software

The Persephone flight software (FSW) is built upon software successfully flown on multiple APL missions, including the most recent Parker Solar Probe. The FSW uses a layered architecture to encapsulate functionality into multiple distinct applications. This ensures that functionality is self-contained and readily maintainable.

Concept of Operations and Mission Design

The mission design is broken into three primary phases: the interplanetary transfer phase, the Pluto orbit phase, and the post-Pluto phase.

We note that our original proposal indicated that a 12-year interplanetary cruise was feasible, based on the work of Finley et al. (2018). However, this study assumed a $\Delta\text{-V}$ that was above the ability of any existing launch vehicle. The work in this study, using predicted launch profiles, shows the minimum cruise time to Pluto is 18 years. However, to get our required mass into orbit (and to include a pre-Pluto KBO flyby), this cruise time is increased even further.

Interplanetary Transfer Phase

The interplanetary transfer trajectory involves a high-energy launch on an SLS-Block 2 with Centaur kick stage and Jupiter gravity assist (JGA) en route to Pluto. Potential launch opportunities exist annually from 2029 to 2032, after which unfavorable geometry with Jupiter prevents subsequent launch opportunities until 2042. Performing a JGA is required to deliver the required mass into Pluto orbit.

Figure 6 shows the 21-day launch period opens on 19 February 2031 with a maximum C_3 of $141 \text{ km}^2/\text{s}^2$. The backup launch period occurs 1 year later in 2032. Deterministic xenon required for this phase is capped at 3450 kg.

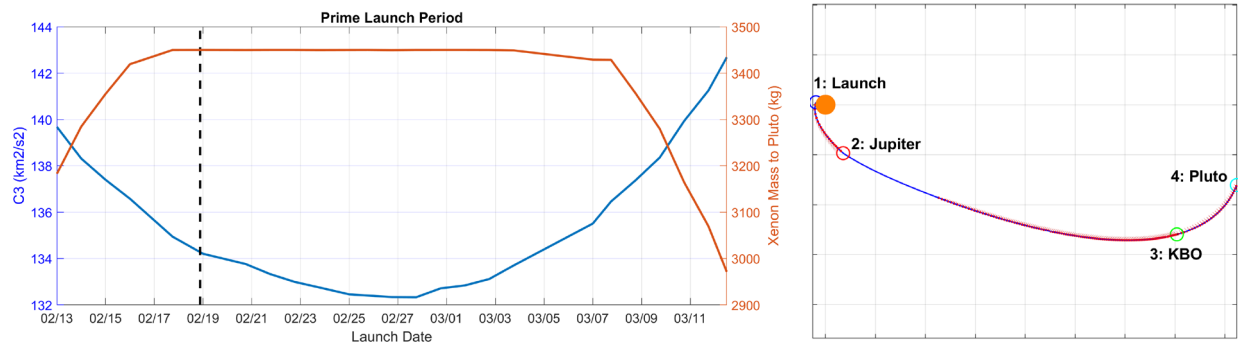


Figure 6. (left) Prime launch period and (right) Earth-Jupiter-KBO-Pluto interplanetary transfer.

Thrusting is primarily done using a single XR5 EP engine at a time tuned for maximum thrust powered by the five NGRTGs. The JGA is set to a lower bound altitude of 17.8 rJ. In addition to the JGA, the trajectory accommodates a KBO flyby before arriving at the Pluto system. The mission design has sufficient margin built into the transfer to accommodate for missed thrust periods.

Pluto Orbit Phase

Because of the premium placed on the mass required to deliver into Pluto orbit, the science orbit consists of multiple periodic orbits designed in the Pluto/Charon restricted three-body dynamics model. These orbits leverage the simultaneous gravitational pull from both Pluto and Charon and effectively eliminate the need for deterministic high-thrust chemical propulsion maneuvers during the Pluto orbit phase (a small amount is allocated for station-keeping). The Pluto/Charon system, with mass proportions an order of magnitude greater than the Earth/Moon system, gives an unprecedented opportunity to exploit restricted three-body dynamics to find very chaotic orbits that span very large radial distances both in and out of the moon plane, enabling close encounters with Pluto and all its moons. These orbits, when viewed in a Pluto-centered inertial frame, do not follow standard Keplerian motion because of gravitation perturbations from the secondary body, but, when viewed in a frame that has both primary and secondary bodies fixed, can reveal insightful characteristics. The periodic nature of these orbits in the Pluto/Charon rotating frame, coupled with the fact that Pluto and Charon are tidally locked, have repeating ground tracks naturally built in to the trajectory. The periodic orbits found in the study fell into two primary categories: a high out-of-plane component to enable high-latitude global mapping and low altitude to enable in situ sampling. Four distinct periodic orbits—two from each category—consisting of the complete Pluto orbit tour were selected. The orbits also have varying maximum radial extents from Pluto, enabling encounter opportunities with the smaller moons. The XR5 EP engine will utilize low-energy transfer arcs to transfer between periodic orbits. The total xenon required for all three transfers is 62.3 kg, 50% of which results from the transfer between the inclined high-latitude Orbit 2 to the equatorial low-altitude Orbit 3. The total science orbit mission duration, including time spent performing multiple revolutions on certain periodic orbits and the transfer arcs between orbits, is 3.1 years.

Table 14. Persephone mission events table.

Major Event	Date	Time (years)
Launch	Feb 2031	0
Jupiter Flyby	May 2032	1.2
KBO Flyby	Feb 2050	19.0
Pluto Arrival	Oct 2058	27.6

Table 15. Pluto/Charon tour events. Phasing refers to the time between departing (Dep) or arriving (Arr) into an orbit and the start of that orbit. This phasing time can be used for science. During the transfer (Xfer) time, all available power will go to the EP system, and thus no/little science data can be obtained.

Leg	Duration (days)	Revolutions	Start Time (EpDays)	End Time (EpDays)	Propellant Used (kg)
Entire Tour	1131		0.0	1130.5	62.3
Orbit 1 Science	46	4	0.0	184.5	
Orbit 1 Dep Phasing	1		184.6	185.4	
Orbit 1 to 2 Xfer	28		185.4	213.7	16.1
Orbit 2 Arr Phasing	28		213.7	242.0	
Orbit 2 Science	69	3	242.0	449.8	
Orbit 2 Dep Phasing	39		449.8	488.7	
Orbit 2 to 3 Xfer	30		488.7	518.7	29.8
Orbit 3 Arr Phasing	78		518.8	596.3	
Orbit 3 Science	154	1	596.3	750.2	
Orbit 3 Dep Phasing	0		750.2	750.2	
Orbit 3 to 4 Xfer	16		750.2	766.3	16.4
Orbit 4 Arr Phasing	89		766.3	855.5	
Orbit 4 Science	91	3	855.5	1130.5	

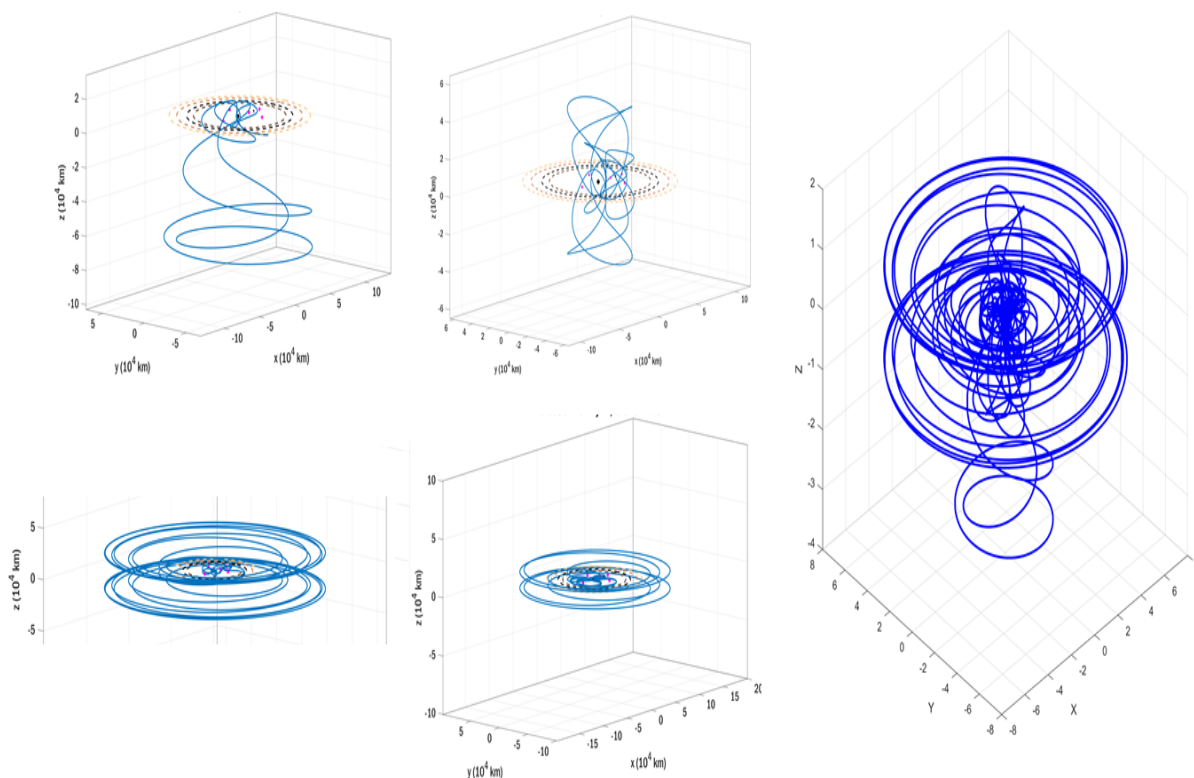


Figure 7. Science orbits, plotted in Pluto/Charon rotating frame. Four left panels: Orbit 1 (top left), Orbit 2 (top right), Orbit 3 (bottom left), and Orbit 4 (bottom right). Right panel: Complete science tour. The dotted lines indicate the orbits of Pluto's small satellites, the black dots show the location of Pluto and Charon, and the pink dots indicate the Lagrangian points. Axes are distance from Pluto (in 10^4 km).

Target Coverage

The global coverage of Pluto and Charon provided by each of the four orbits is given in Figure 8. The first two orbits provide global coverage of both targets, while Orbits 3 and 4 provide low-altitude and low-latitude coverage that is optimized for the in situ instruments.

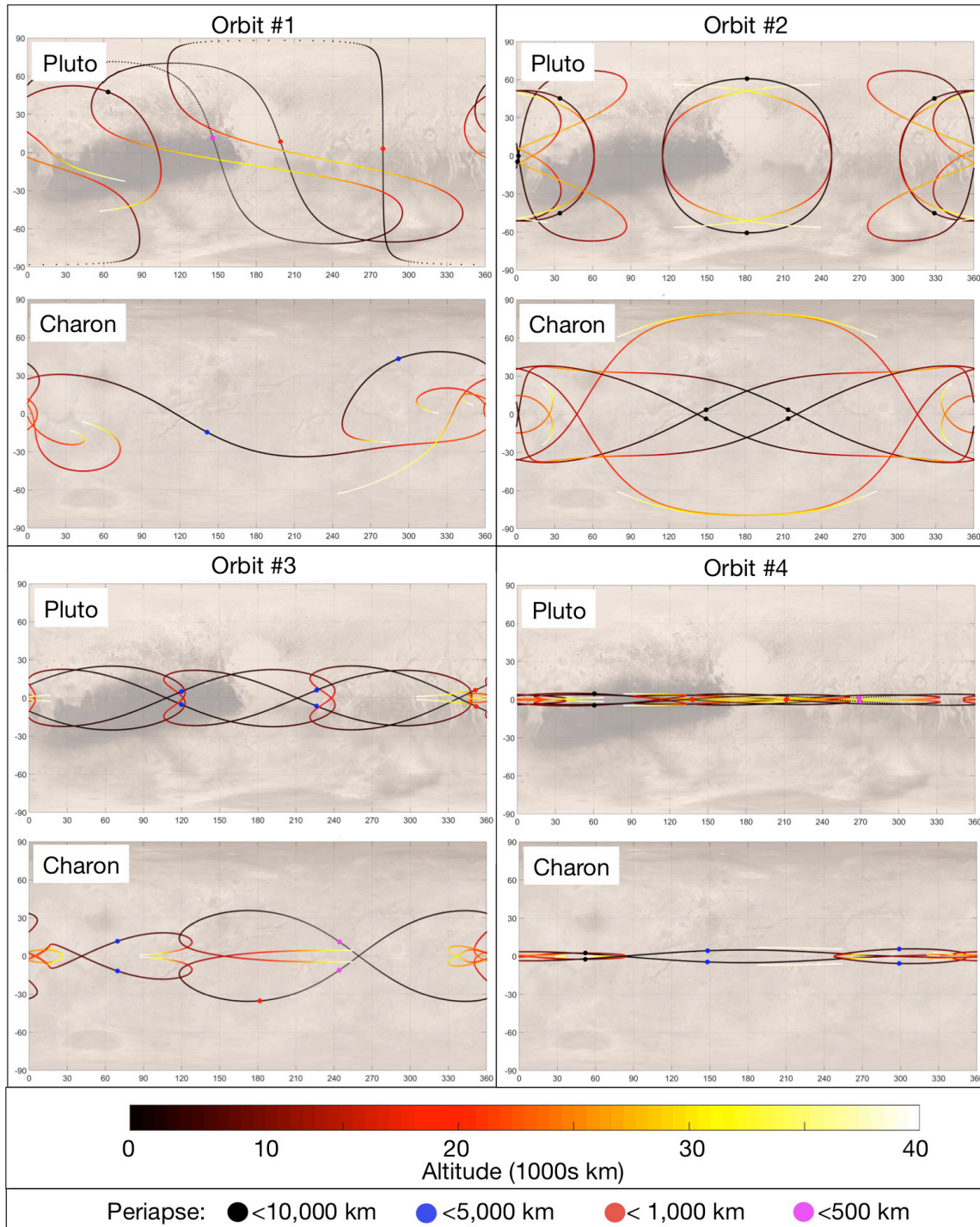


Figure 8. Ground tracks of the four chosen orbits on Pluto and Charon. The color indicates the altitude (see color bar), and the ground-track locations at periastrons are depicted as colored dots, with the color indicative of altitude (see subfigure keys for details).

While the Pluto-Charon tour is relatively insensitive to the arrival time at the Pluto system, this is not true for the small satellites. Once the arrival time is defined, the mission would be able to define the small satellite tour, by seeing when the closest approaches are to each satellite. Generally, the closer a small satellite is to Pluto, the more and closer potential encounters there are with it. Thus, the best coverage will likely be obtained for Styx, and the worst for Hydra. Encounters with Styx and Nix will happen fairly easily but are less common with Hydra and Kerberos. Depending on the timing, it may be possible to have a Hydra or Kerberos close flyby during the propulsive transition period between orbital configurations. The encounter velocity of the small satellites will be <300 m/s.

Persephone’s expected (New Horizons’ achieved) resolution for the small satellites is: Styx, 80 m/pixel (3157 m/pixel); Nix, 80 m/pixel (306 m/pixel); Kerberos, 110 m/pixel (1982 m/pixel); Hydra, 175 m/pixel (1155 m/pixel) (cf. Weaver et al., 2016). In addition, Persephone will be able to image the small satellites at more geometries than were visible during the New Horizons flyby. Persephone will almost certainly be able to expand the global imaging coverage for all of the satellites.

Post-Pluto Phase

As a potential extended mission option, a Charon flyby can be executed to depart the Pluto system. The XR5 EP engine can then be used to target a KBO flyby. Xenon propellant available at the end of the Pluto orbit phase limits Pluto departure velocity and thus transfer time to more distant KBOs. Robust amounts of xenon margin in the mission propellant budget can accommodate access to many targets. For example, using 250 kg of Xe from margin enables reaching a target 3 AU from Pluto after ~8 years, which based on analysis of KBO statistical position models, could be a flyby of a 100- to 150-km target.

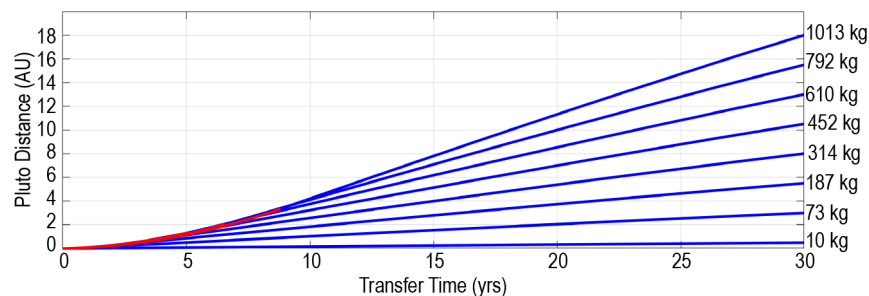


Figure 9. Post-Pluto transfer time and the required xenon to achieve the science goal of a 100- to 150-km-class KBO.

Table 16. Persephone mission design table.

Parameter	MEV Mass	MPV Mass
Mission lifetime (years)	30.7	30.7
Transfer time to Pluto (years)	27.6	27.6
Launch site	Cape Canaveral Air Force Station	Cape Canaveral Air Force Station
Total flight element #1 mass (kg)	2076	2699
Xenon propellant mass without contingency (kg)	3512	3756
Xenon propellant contingency (%)	14	5
Xenon propellant mass with contingency (kg) (Oh et al., 2008)	3991	3935
XR5 EP engine duty cycle (%)	85	95
Hydrazine propellant mass without contingency (kg)	100	100
Hydrazine propellant contingency (%)	4	4
Hydrazine propellant mass with contingency (kg)	104	104
Launch adapter mass with contingency	106	106
Total launch mass	6277	6844
Launch vehicle	SLS-Block 2 + Centaur	SLS-Block 2 + Centaur

Parameter	MEV Mass	MPV Mass
Launch C ₃ (km ² /s ²)	136.5	129.7
Launch vehicle lift capability (kg)	6278	6847
Launch vehicle mass margin (kg)	1	3
Launch vehicle mass margin (%)	0	0

The baseline science tour, using multi-body dynamics in the Pluto/Charon system, enables both high-latitude and low-altitude science observation and makes for a compelling mission concept. The mission design also has robust propellant margin to enable both pre-Pluto and post-Pluto KBO flybys. The challenge for this mission is the 27.6-year transfer time to Pluto. There is a direct correlation to Pluto transfer time and delivered mass into the Pluto system. Because of the limited power available, the EP engine is running extremely inefficiently, and thus the heavier the spacecraft, with the limited amount of thrust available, the longer it takes to brake into Pluto orbit. Having multiple kilowatts of power available, thereby running the EP engine at full power, would be a game changer for a Persephone concept. Space fission reactors were explored to see how much of an enabler this type of future technology could be. A 10-kW space fission reactor (1068 kg of added dry mass) would reduce the flight time to Pluto by 25–30%.

Table 17. Mission operations and Ground Data Systems table.

Downlink Information	Pre-Pluto		Pluto Operations	Extended Mission	
	Earth/ Jupiter Cruise	Cruise Extended + KBO		Post-Pluto Cruise	KBO Operation
Number of contacts per week	3	1	7	1	7
Number of weeks for mission phase, weeks	63	1373	104	416	52
Downlink frequency band, GHz	Ka-band, 31.8–32.3				
Telemetry data rate(s), kbps	>28	>14	28	12	12
Transmitting antenna type(s) and gain(s), dBi	3 m, X/Ka-band parabolic HGA X-band = 45.5; Ka-band = 57.0				
Transmitter peak power, watts	Dual band, 300				
Downlink receiving antenna gain, dBi	34-m beam waveguide (BWG), 78.7				
Transmitting power amplifier output, watts (RF)	150 W for Ka-band, 12.5 W for X-band				
Total daily data volume, MB/day	806	403.2	806	345	345
Uplink information					
Number of uplinks per day	3	0.25	7	0.1	7
Uplink frequency band, GHz	X-band, 7.145–7.190				
Telecommand data rate, kbps	0.5	0.25	0.25	0.25	0.25
Receiving antenna type(s) and gain(s), dBi	3 m, X-band parabolic HGA = 44.7; 0.4 m, X-band parabolic MGA = 27.2				

Risk List

Persephone risks are identified using APL's standard risk management process (Figure 10.). The risks are dominated by external factors; all risk factors under program control have had mitigation plans included in the baseline concept (e.g., limited technology development required). The external dependencies (launch vehicle and RPS performance) are critical items that would need to have development plans tied to the program milestones.

ID	Name	Risk Statement	Likelihood	Consequence – Impact	Risk Rating
1	Lifetime	If the reliability associated with a lifetime of >15 years cannot be demonstrated adequately, then spacecraft complexity and program cost may increase. (McNutt et al., 2019)	2 Unlikely	3 Moderate	6
2	RPS Performance	If the mission implementation requires significant power (margin), then more NGRTGs (total of five for current design point) than are planned for development may be required.	5 Likely	3 Moderate	15
3	Launch Vehicle Availability and Performance	If a launch vehicle with the performance necessary is unavailable (in particular for an RPS-powered spacecraft) because of development schedule or the cost assumed, then the mission will have to be modified.	4 Probable	4 Critical	16
4	Project Schedule	If the mission has to launch by May 2032 to facilitate a JGA, then the necessary project start date to provide sufficient schedule margin may not be far enough in the future if backup launch windows are desired.	4 Probable	3 Moderate	12

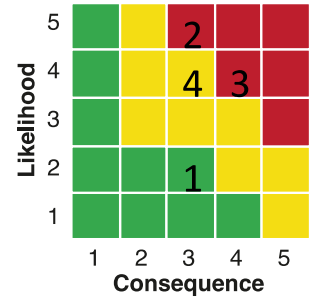


Figure 10. The Persephone risk list requires significant external (to the program) efforts to be completed.

4. Development Schedule and Schedule Constraints

High-Level Mission Schedule

The program development schedule is constrained on both ends. The start date of 1 January 2023 is specified by the study guidelines. Orbital dynamics and the JGA constrain the latest possible launch window to April 2032. A second possible launch window was also identified to ensure a backup opportunity ~1 year earlier. Therefore, the program phasing is constrained as shown in Table 18 and Figure 11, with 98 months between Phase A start and launch. The phase durations compare favorably to Parker Solar Probe, a mission of comparable development (more technology development but less overall complexity). However, the program is constrained to 3.4 months of schedule margin on the critical path. The critical path follows the propulsion subsystem through system integration and testing (I&T) to RTG integration at the launch site. The critical path schedule margin is set at the minimum recommended by APL guidelines. Additional margin could be allocated with an earlier start date, or by a more aggressive (shorter in duration) Phase A plan. Shortening Phase A is feasible because of the limited amount of technology development for the mission.

Table 18. Key phase duration table.

Project Phase	Duration (Months)
Phase A – Conceptual Design	23
Phase B – Preliminary Design	23
Phase C – Detailed Design	25
Phase D – Integration and Testing	29
Phase E – Primary Mission and Extended Operations	592
Start of Phase B to Preliminary Design Review	23
Start of Phase B to Critical Design Review	36
Start of Phase B to Delivery of All Instruments	48
Start of Phase B to Delivery of All Flight Elements	48
System-Level Integration and Testing	21
Project Total Funded Schedule Reserve	3.4
Total Development Time Phase B–D	69

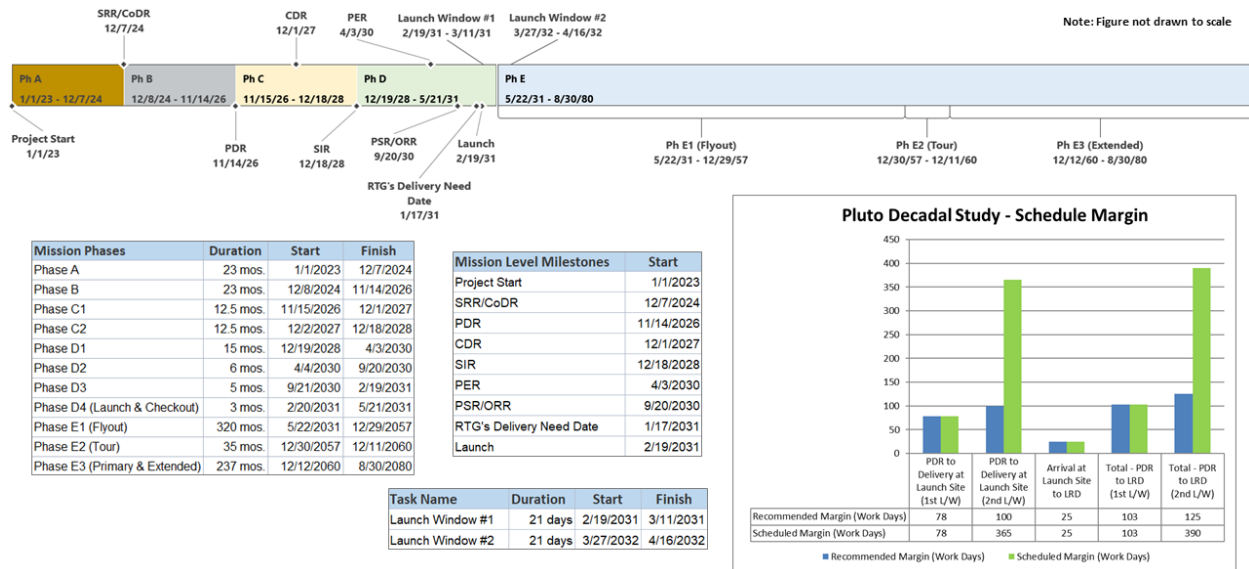


Figure 11. The schedule for Persephone satisfies all APL guidelines.

Technology Development Plan

No new technology, with the exception of the NGRTGs (which is beyond the purview of this report), would be required for the mission. However, because of the complexity and number of the instruments, additional time would be allocated for instrument design and testing.

Development Schedule and Constraints

No long-lead-time procurements would be required.

It will take significant schedule to meet the requirements set forth in the National Environmental Policy Act of 1969 (NEPA). There is no alternative to RTG power to support the Persephone mission.

Launch can occur no earlier than 2030 because of the availability of flight-qualified NGRTGs (source: Ground Rules for Mission Concept Studies in Support of Planetary Decadal Survey, November 2019).

Launch window #1 is 19 February 2031 to 11 March 2031, if a slip occurs.

Final launch window is 27 March to 16 April 2032.

After 2032, a 10-year Earth-Pluto transfer time penalty occurs.

Jupiter does not come back into phase until 2042.

5. Mission Life-Cycle Cost

Introduction

The cost estimate prepared for the Persephone mission is at CML 4. The payload and spacecraft estimates capture the resources required for a preferred point design and take into account subsystem level mass, power, and risk. Our estimate also takes into account the technical and performance characteristics of components. Estimates for Science, Mission Operations, and Ground Data System elements whose costs are primarily determined by labor take into account the Phase A–D schedule and Phase E timeline.

The result is a mission estimate that is comprehensive and representative of expenditures that might be expected if the Persephone mission is executed as described. The Persephone Phase A–F mission cost, including unencumbered reserves of 50% (A–D, excluding launch vehicle costs) and 25% (E–F, excluding DSN charges), is \$3.4B in fiscal year 2025 (FY\$25) dollars, as shown in Table 19. Excluding all launch-vehicle-related costs, the Persephone Phase A–F mission cost is \$2.9B FY\$25.

Table 19. Estimated Phase A–F Persephone mission costs by level-2 Work Breakdown Structure (WBS) element.

Pluto Orbiter (FY25\$K)					
WBS		Phases A–D	Phases E–F	Total	Notes
1	Project Management (PM)	\$143,608	\$-	\$143,608	15.9% of payload, spacecraft, I&T (average of historical missions) E–F in WBS 7
2	Systems Engineering (SE)				
3	Mission Assurance (MA)				
4	Science	\$26,081	\$181,833	\$207,914	Cost per month of historical missions
5	Payload	\$366,840	\$-	\$366,840	Average of analogy and two parametric estimates (SEER/NICM)
6	Spacecraft (SC)	\$434,832	\$-	\$434,832	Parametrically estimated spacecraft bus with propulsion Rough Order of Magnitude (ROM)
7	Mission Operations (MOps)	\$46,917	\$720,273	\$767,190	Cost per month of historical missions DSN charges of \$29M
8	Launch Vehicle (LV)	\$566,000	\$-	\$566,000	\$500M SLS-Block 2, \$40M Upper Stage, \$26M RTG surcharge
9	Ground Data Systems (GDS)	\$47,675	\$-	\$47,675	Cost per month of historical missions. Postlaunch GDS is in WBS 7
10	Integration and Testing (I&T)	\$101,526	\$-	\$101,526	12.7% of payload and spacecraft (average of historical missions)
	Total (without reserves and with LV)	\$1,733,479	\$902,106	\$2,635,585	
	Total (without reserves and without LV)	\$1,167,479	\$902,106	\$2,069,585	
	Reserves (50% A–D, 25% E–F)	\$583,739	\$218,327	\$802,066	Per Decadal guidelines
	Total (with reserves and with LV)	\$2,317,218	\$1,120,433	\$3,437,651	
	Total (with reserves and without LV)	\$1,751,218	\$1,120,433	\$2,871,651	

Mission Ground Rules and Assumptions

- Estimating ground rules and assumptions are derived from revision 4 of the “Decadal Mission Study Ground Rules” dated 22 November 2019.
- Mission costs are reported using the level-2 (and level-3 where appropriate) work breakdown structure (WBS) provided in NPR 7120.5E.
- Responsibility for the mission is spread throughout the NASA community. SwRI will lead the Persephone science investigation, while APL will lead the mission and design, develop, manufacture, integrate, and test the spacecraft. It will also lead MOps during Phase E. A number of organizations, including APL, will design, develop, and deliver instruments.
- Cost estimates are reported in FY\$25 dollars.
- The NASA New Start inflation index provided by the Planetary Mission Concept Studies Headquarters (PMCS HQ) was used to adjust historical cost, price data, and parametric results to FY\$25 dollars if necessary.
- The mission does not require Technology Development dollars to advance components to TRL 6 because all Persephone mission components will be at or above TRL 6 when required.

- A launch vehicle of sufficient capability to support the Persephone mission is in development. Our assumption is that a launch vehicle meeting mission requirements will be available by 2030. Launch vehicle costs are estimated based on the expected capability.
- This estimate assumes no development delays and an on-time launch in February 2031.
- Phase A–D cost reserves are calculated as 50% of the estimated costs of all components excluding the launch vehicle. Phase E–F cost reserves are calculated as 25% of the estimated costs of all Phase E elements excluding DSN charges.

Cost Benchmarking

The cost and scope of the Persephone concept corresponds well to a NASA Flagship-class mission (see Figure 12). The estimated cost to develop and operate Persephone compares favorably to current Flagship missions under development as well as past flagship missions with an average cost of \$3.1B, excluding launch vehicle costs, as shown in red.

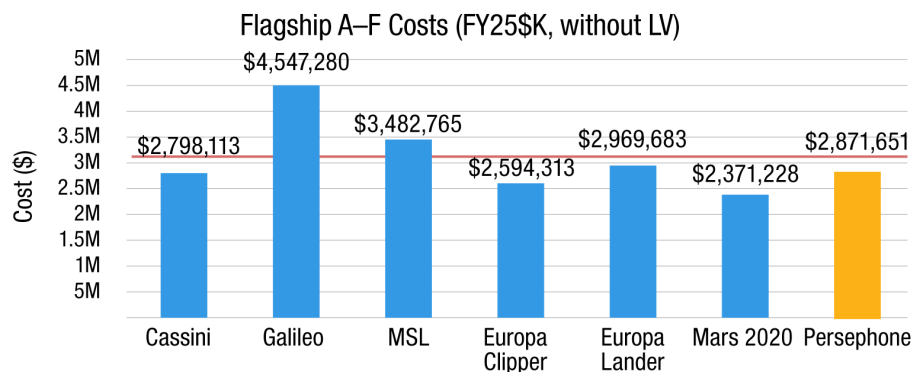


Figure 12. Mission-level cost comparison to other Flagships.

Methodology and Basis of Estimate

The Persephone CML 4 mission cost estimate is a combination of high-level parametric and analog techniques and incorporates a wide range of uncertainty in the estimating process. No adjustments were made to remove the historical cost of manifested risk from the heritage data underlying the baseline estimate. Therefore, before reserves are applied, the estimated costs already include a historical average of the cost of risk. This approach is appropriate for capturing risk and uncertainty commensurate with early formulation stages of a mission. The following describes the basis of estimate for each element.

WBS 1, 2, 3 Project Management, Systems Engineering, Mission Assurance (PM/SE/MA)

Because these functions depend on multiple mission- and organization-specific characteristics (Hahn, 2014), cost analogies to analogous historical missions are preferred over cost model output, which does not take the mission into account. Existing analyses demonstrate that hardware costs are a reliable predictor of these critical mission function costs. APL has conducted thorough and rigorous analyses of PM/SE/MA costs, both for historical APL missions and for analogous missions. The PM/SE/MA estimate for Persephone relies on APL's analysis of historical PM, SE, and MA practices on Van Allen Probes, Parker Solar Probe, and New Horizons. Van Allen Probes and Parker Solar Probe in particular include costs associated with current NASA requirements (e.g., Earned Value Management System [EVMS], NPR 7120.5E). Persephone's total mission PM/SE/MA cost is 15.9% of the flight system (payload + spacecraft + I&T). This percentage is allowed to vary along with hardware costs as part of the mission cost risk analysis, discussed below, to capture uncertainty (particularly given CML-4-level design phase).

WBS 4 Science

This element covers the management, direction, and control of the science investigation. It includes the costs of the Principal Investigator, Project Scientist, Science Team members, and activities. The Phase A–D and E–F science estimate is an analogous estimate based off of the cost per month of New Horizons, MESSENGER, Cassini, Dragonfly, OSIRIS-REx, and Juno. New Horizons is the predecessor mission to Persephone, MESSENGER is APL’s most recent historical data point for planetary orbital science, and Cassini is a recently completed outer-planets flagship mission. The analogy costs are representative of expenditures for science on a typical New Frontiers or Flagship mission. The estimate reflects the manpower needed to ensure production of various data products as well as ensure closure to science objectives.

WBS 5 Payload

The WBS 5 estimate includes a science payload of 10 instruments and payload-level PM/SE/MA (Table 20). Costs for the REX instrument plus the USO are carried within the RF subsystem cost because they are not part of the science payload. The 8.2% cost-to-cost factor for estimating payload PM/SE/MA costs is based on the Van Allen Probes, New Horizons, MESSENGER, and Parker Solar Probe payload suite cost data with PM/SE/MA costs estimated as a percentage of the payload hardware. Technical management and systems engineering costs for individual instruments are carried in their respective instrument development costs.

Given the early design phase, multiple approaches are used to estimate each instrument to capture the potential range in cost. This includes two parametric estimates that rely on different sets of input variables (SEER Space and NICM 8.5), and historical analogous costs to specific heritage instruments where available. The mass spectrometer and sounding radar are modeled as “Modification-Major” in SEER, and NICM output is adjusted (Armon and Smoker, 2010) to reflect TRL 5. The Plasma Spectrometer and Magnetometer both draw heritage from IMAP (CoDICE-Lo and MAG), the NEAR-IR Spectrometer and UV Spectrometer both draw heritage from New Horizons (Ralph/LEISA and Alice), the Laser Altimeter draws heritage from MESSENGER (MLA), the sounding radar draws design heritage from MRO (SHARAD), and the NAC, WAC, and mass spectrometer all draw heritage from Europa Clipper (NAC, WAC, and MASPEX). An average of the historical analogy and two parametric estimates is used as the point estimate to prevent estimate bias (high or low). These estimates are subject to a cost risk analysis (discussed below) to further quantify uncertainty.

Table 20. WBS 5 costs in FY\$25K.

Payload	\$366,840
Payload Management	\$27,645
Plasma Spectrometer	\$43,725
Laser Altimeter	\$32,745
Thermal IR Camera	\$18,340
Near-IR Spectrometer	\$39,007
NAC	\$40,096
UV Spectrometer	\$13,893
WAC	\$26,807
Mass Spectrometer	\$78,407
Sounding Radar	\$37,532
Magnetometer (and boom)	\$8,642

WBS 6 Spacecraft

The WBS 6 estimate includes the spacecraft bus and NGRTG (Table 21). Spacecraft PM/SE/MA is carried in WBS 1, 2, and 3 consistent with APL in-house builds (Hahn, 2015). The basis of estimate relies primarily on SEER Space. SEER Space is the primary estimating methodology because it was designed specifically for missions in early formulation stages. SEER Space allows for a reasonably robust estimate with fewer input parameters, which is ideal for a CML-4-level study. No major technology development is required for the spacecraft. To increase fidelity, the estimate is cross-checked with a secondary parametric estimate, the results of which validate to within 21% (which is a reasonable range given different input variables). To maintain conservatism given the early formulation stage, the higher SEER Space estimate serves as the primary estimating methodology.

Table 21. WBS 6 costs in FY\$25K.

Spacecraft	\$434,832
Spacecraft Bus	\$264,832
NGRTGs (5)	\$170,000

WBS 7 and 9 Mission Operations (MOps) and Ground Data Systems (GDS)

The Persephone MOps estimate includes MOps planning and development, network security, data processing, and mission management. The pre- and postlaunch GDS estimate and the pre- and postlaunch MOps cruise estimate are based off of the cost per month of New Horizons, MESSENGER, OSIRIS-REx, Dawn, and Cassini. The orbital operations cost estimate is based off of the cost per month of MESSENGER. These missions represent GDS/MOps costs associated with New Frontiers- and Flagship-class missions, particularly outer-planet missions with orbital operations (except New Horizons).

WBS 8 Launch Vehicle and Services

The mission requires a launch vehicle that will meet the launch C₃ requirements. This corresponds with an SLS-Block 2, allowed under an addendum to the Decadal Survey Study Guidelines. Without specific costing guidance for the cost of an SLS-Block 2, we assume at least \$500M for a launch using a standard-sized fairing based on past pricing to NASA missions of evolved expendable launch vehicles (EELVs). The price to add an upper stage would likely be no more than \$40M. NEPA and Nuclear Launch Approval costs are covered by the cost of the RTGs in WBS 6. The \$26M RTG surcharge is included.

WBS 10 System Integration and Testing (I&T)

This element covers the efforts to assemble and test the spacecraft and instruments. The Persephone I&T effort is estimated as 12.7% of the hardware. This percentage is based on a detailed analysis of cost actuals from previous APL missions, including MESSENGER, New Horizons, STEREO, Van Allen Probes, and Parker Solar Probe. This percentage is allowed to vary along with hardware costs as part of the mission cost risk analysis to capture the risk historically manifested during I&T.

Deep Space Network (DSN) Charges

This element provides for access to the DSN infrastructure needed to transmit and receive mission and scientific data. Mission charges are estimated using the Jet Propulsion Laboratory (JPL) DSN Aperture Fee tool. The DSN cost estimate covers pre- and post-contact activity for each linkage.

Confidence and Cost Reserves

The cost risk ranges by major WBS element as inputs for the Persephone probabilistic cost risk analysis to quantify total cost risk are found in Table 22 and are described below.

Table 22. Inputs to cost distributions in FY\$25K.

WBS	Cost Element	Project Estimate	70th Percentile
1, 2, 3	Mission PM/SE/MA	\$143,608	\$190,333
4	Science	\$207,914	\$259,893
5	Payload	\$366,840	\$531,165
6	Spacecraft	\$434,832	\$531,004
7	Mission Operations	\$767,190	\$958,987
9	GDS	\$47,675	\$59,594
10	I&T	\$101,526	\$134,896

PM/SE/MA

Given the use of cost-to-cost factors to estimate these functions, both the cost estimating relationship and underlying cost drivers are allowed to range so that all sources of uncertainty can be quantified.

Science, GDS, and MOps

These are low-risk cost elements but are subject to cost growth as part of the cost risk analysis.

Payload

Given that the point estimate is an average of two parametric models and a historical analogy for each of the 10 instruments, the highest value of the three primary estimate inputs is used to inform the Persephone payload risk model to capture the uncertainty given the CML-4-level design phase.

Spacecraft

Each subsystem is subject to a data-driven risk analysis based on historical APL cost growth. Mass input also varies in the SEER space model consistent with early design programs to 30% over CBE.

I&T

I&T as a percentage of the payload and spacecraft from the point estimate is used to inform the risk analysis, allowing I&T to vary with hardware cost.

Per the Decadal Study Ground Rules, the estimate includes unencumbered cost reserves of 50% of the estimated costs of all Phase A–D elements except for the launch vehicle plus 25% of the estimated costs of Phase E–F elements, excluding DSN charges. A probabilistic cost risk analysis shows 76% confidence that the Phase A–F mission is achievable within the estimated costs of this study (see Table 23 and Figure 13). The high confidence level is driven primarily by the robustness of the required reserves posture for this pre-proposal concept. Given a typical competitive pre-Phase A NASA environment with 25% reserves on Phase A–D elements and 10% reserves on Phase E–F elements, the probabilistic cost risk analysis shows 65% confidence that the Phase A–F mission would be achievable with the less robust reserves posture. A 50th- to 70th-percentile confidence level is expected and reasonable for a pre-Phase A concept with this level of reserves.

Table 23. Cost risk analysis.

Description	Value (FY\$25K)	Confidence Level
Point Estimate	\$2,635,585	47%
Mean	\$2,888,676	
Standard Deviation	\$905,392	
Cost Reserves	\$802,066	
PI-Managed Mission Cost	\$3,437,651	76%

A coefficient of variation (standard deviation/mean) of ~31% indicates appropriate levels of conservatism given the early formulation phase. The model confirms the point estimate and provides a reasonable basis for the Persephone CML-4 study.

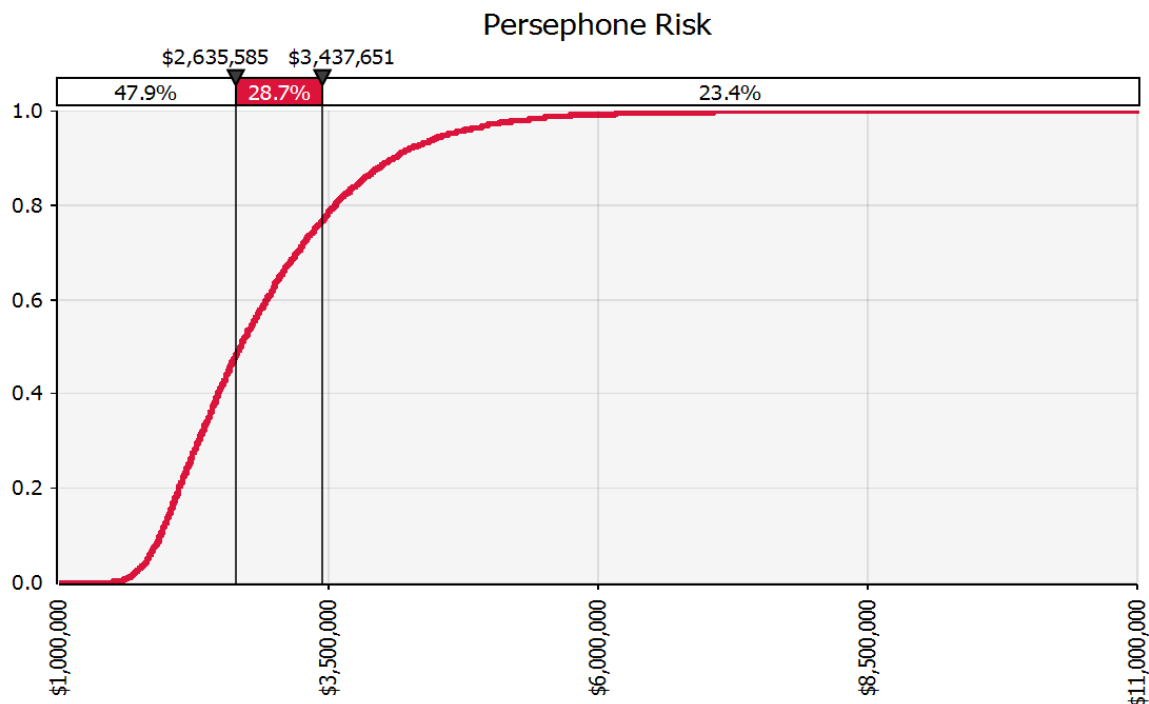


Figure 13. S-curve summary.

Appendix A. Acronyms

ACS	Attitude Control System
ALMA	Atacama Large Millimeter Array
APL	Johns Hopkins Applied Physics Laboratory
ARC	Avionics Redundancy Controller
BWG	Beam Waveguide
C&DH	Command and Data Handling
CBE	Current Best Estimate
CCKBO	Cold Classical Kuiper Belt Object
CML	Concept Maturity Level
CMOS	Complementary Metal–Oxide–Semiconductor
COTS	Commercial Off-the-Shelf
DART	Double Asteroid Redirection Test
DSN	Deep Space Network
DVEGA	Delta-Velocity Earth Gravity Assist
EELV	Evolved Expendable Launch Vehicle
EIS	Europa Imaging System
EP	Electric Propulsion
EPS	Electrical Power Subsystem
EUV	Extreme Ultraviolet
FOV	Field of View
FPGA	Field-Programmable Gate Array
FSW	Flight Software
FY	Fiscal Year
G&C	Guidance and Control
GDS	Ground Data Systems
GNC	Guidance, Navigation, and Control
HC	Hollow Cathode
HCT	Hall Current Thruster
HGA	High-Gain Antenna

I&T	Integration and Testing
IQ	Important Question
JGA	Jupiter Gravity Assist
KB	Kuiper Belt
KBO	Kuiper Belt Object
KG	Key Goal
KQ	Key Question
LEISA	Linear Etalon Imaging Spectral Array
LGA	Low-Gain Antenna
LHCP	Left-Hand Circular Polarization
LRO	Lunar Reconnaissance Orbiter
LV	Launch Vehicle
MA	Mission Assurance
MEV	Maximum Expected Value
MGA	Medium-Gain Antenna
MLA	Mercury Laser Altimeter
Mol	Moment of Inertia
MPV	Maximum Possible Value
NAC	Narrow-Angle Camera
NGRTG	Next-Generation Radioisotope Thermoelectric Generator
NRC	National Research Council
PEPSSI	Pluto Energetic Particle Spectrometer Science Investigation
PI	Principal Investigator
PMA	Propellant Management Assembly
PM/SE/MA	Project Management, Systems Engineering, Mission Assurance
PPU	Power Processing Unit
PSDS	Planetary Science Decadal Survey
REM	Redundant Electronics Module
REP	Radioisotope Electric Propulsion
RF	Radio Frequency
RHCP	Right-Hand Circular Polarization
RPM	Redundant Processor Module

RPS	Radioisotope Power System
RTG	Radioisotope Thermoelectric Generator
SBC	Single Board Computer
SC	Spacecraft
SCIF	Spacecraft Interface Card
SEP	Solar Electric Propulsion
SNR	Signal-to-Noise Ratio
SO	Science Objective
SP	Sputnik Planitia
SSR	Solid-State Recorder
STM	Science Traceability Matrix
SWAP	Solar Wind Around Pluto
TAC	Thruster/Actuator Controller
TDI	Time Delay Integration
THEMIS	Thermal Emission Imaging System
TPA	Thruster Pointing Assembly
TRL	Technology Readiness Level
TWT	Traveling Wave Tube
USO	Ultra-Stable Oscillator
UV	Ultraviolet
VLF	Very Low Frequency
WAC	Wide-Angle Camera
WBS	Work Breakdown Structure

Appendix B. References

- Armon and Smoker, An Integrated Approach to Managing Technology Maturation Costs, NDIA 13th Annual Systems Engineering Conference, 2010.
- Balakrishnan et al., Research Team Integration: What It Is and Why It Matters, CSCW '11: Proceedings of the ACM 2011 Conference on Computer Supported Cooperative Work, 523–532, doi:10.1145/1958824.1958905, 2011.
- Barucci et al., Composition and Surface Properties of Transneptunian Objects and Centaurs, in *The Solar System Beyond Neptune* (Barucci, Boehnhardt, Cruikshank, and Morbidelli, eds.), Tucson, AZ: University of Arizona Press, pp. 143–160, 2008.
- Benecchi et al., K2 Precision Lightcurve: Twelve Days in the Pluto-Charon System, *Icarus*, 314, 265–273, 2018.
- Benecchi et al., The Color and Binariness of (286958) 2014 MU₆₉ and Other Long-Range New Horizons Kuiper Belt Targets, *Icarus*, 334, 22–29, 2019.
- Bernstein et al., The Size Distribution of Trans-Neptunian Bodies, *The Astronomical Journal*, 128, 1364–1390, 2004.
- Bertrand et al., The Nitrogen Cycles on Pluto Over Seasonal and Astronomical Timescales, *Icarus*, 309, 277–296, 2018.
- Beyer et al., The Nature and Origin of Charon's Smooth Plains, *Icarus*, 323, 16–32, 2019.
- Bird et al., Radio thermal emission from Pluto and Charon During the New Horizons Encounter, *Icarus*, 322, 192–209, 2019.
- Brockwell et al., The Mass Spectrometer for Planetary Exploration (MASPEX), 2016 IEEE Aerospace Conference, 1–17, 2016.
- Brozović et al., The Orbits and Masses of Satellites of Pluto, *Icarus*, 246, 317–329, 2015.
- Burt, Structural Holes and Good Ideas, *American Journal of Sociology*, 110, 349–399, 2004.
- Canup, A Giant Impact Origin of Pluto-Charon, *Science*, 307, 546–550, 2005.
- Canup, On a Giant Impact Origin of Charon, Nix, and Hydra, *The Astronomical Journal*, 141, article id. 35, 2011.
- Casani et al., Enabling a New Generation of Outer Solar System Missions: Engineering Design Studies for Nuclear Electric Propulsion, White Paper for Decadal Survey, 2020.
- Clark et al., Compositional Mapping of Surfaces in the Saturn System with Cassini VIMS: The Role of Water, Cyanide Compounds and Carbon Dioxide, American Geophysical Union, abstract id. P22A-02, 2005.
- Cook et al., Composition of Pluto's Small Satellites: Analysis of New Horizons Spectral Images, *Icarus*, 315, 30–45, 2018.
- Cruikshank et al., Recent Cryovolcanism in Virgil Fossae on Pluto, *Icarus*, 330, 155–168, 2019.
- Currall et al., It's What You Do and the Way That You Do It: Team Task, Team Size, and Innovation-Related Group Processes, *European Journal of Work and Organizational Psychology*, 10:2, 187–204, 2001.

Dalle Ore et al., Detection of Ammonia on Pluto's Surface in a Region of Geologically Recent Tectonism, *Science Advances*, 5:5, eaav5731, doi:10.1126/sciadv.aav5731, 2019.

Delamere, Hybrid Code Simulations of the Solar Wind Interaction with Pluto, *Journal of Geophysical Research: Space Physics*, 114, doi:10.1029/2008JA013756, 2009.

de Vaan et al., Game Changer: The Topology of Creativity, *American Journal of Sociology*, 120, 1144–1194, 2015.

Earle, A. et al., Long-Term Surface Temperature Modeling of Pluto, *Icarus*, 287, 37–45, 2017.

Elliot et al., Temporal and Radial Variation of the Solar Wind Temperature-Speed Relationship, *Journal of Geophysical Research*, 117(A), A09102, <https://doi.org/10.1029/2011JA017125>, 2012.

Elliot et al., The New Horizons Solar Wind Around Pluto (SWAP) Observations of the Solar Wind From 11–33 au, *The Astrophysical Journal Supplement Series*, 223(2), 19, <https://doi.org/10.3847/0067-0049/223/2/19>, 2016.

Elliot et al., Determining the Alpha to Proton Density Ratio for the New Horizons Solar Wind Observations, *The Astrophysical Journal*, 866(2), 85, <https://doi.org/10.3847/1538-4357/aadba6>, 2018.

Elliot et al., Slowing of the Solar Wind in the Outer Heliosphere, *The Astrophysical Journal*, 885(2), 156, <https://doi.org/10.3847/1538-4357/ab3e49>, 2019.

Finley et al., A Pluto Orbiter Tour Preliminary Results, Presented at DPS meeting #50, 2018.

Gladman et al., The Resonant Trans-Neptunian Populations, *The Astronomical Journal*, 122, 1051–1066, 2012.

Glein and Waite Jr., Primordial N₂ Provides a Cosmochemical Explanation for the Existence of Sputnik Planitia, Pluto, *Icarus*, 313, 79–92, 2018.

Grundy et al., Surface Compositions Across Pluto and Charon, *Science*, 351, 1283, 2016.

Hahn, Higher Fidelity Estimating: Program Management, Systems Engineering, & Mission Assurance, 2014 NASA Cost Symposium, 2014.

Hahn, In-House Build Efficiencies: PM, SE, & MA, 2015 NASA Cost Symposium, 2015.

Hamilton et al., The Rapid Formation of Sputnik Planitia Early in Pluto's History, *Nature*, 540, 97–99, 2016.

Hendrix et al., The NASA Roadmap to Ocean Worlds, *Astrobiology*, 19, 1–27, 2019.

Hinson et al., An Upper Limit on Pluto's Ionosphere From Radio Occultation Measurements with New Horizons, *Icarus*, 307, 17–24, 2018.

less et al., The Gravity Field and Interior Structure of Enceladus, *Science*, 344, 78–80, 2014.

Kamata et al., Tidal Resonance in Icy Satellites with Subsurface Oceans, *Journal of Geophysical Research*, 120, 1528–1542, 2015.

Kamata et al., Pluto's Ocean Is Capped and Insulated by Gas Hydrates, *Nature Geoscience*, 12, 407–410, 2019.

Kavelaars et al., The Canada-France Ecliptic Plane Survey – L3 Data Release: The Orbital Structure of the Kuiper Belt, *The Astronomical Journal*, 137, 4917, 2009.

Krasnopolsky, A Photochemical Model of Pluto's Atmosphere and Ionosphere, *Icarus*, 335, 113374, <https://doi.org/10.1016/j.icarus.2019.07.008>, 2020.

- Lacerda and Jewitt, Densities of Solar System Objects From Their Rotational Light Curves, *The Astronomical Journal*, 133, 1293, 2007.
- Mandt et al., Photochemistry on Pluto: Part II. HCN and Nitrogen Isotope Fractionation, *Monthly Notices of the Royal Astronomical Society*, 472, 118–128, 2017.
- Mastrapa et al., Optical Constants of Amorphous and Crystalline H₂O-Ice in the Near Infrared From 1.1 to 2.6 Microns, *Icarus*, 197, 307–320, 2008.
- McComas et al., Solar Wind Observations Over Ulysses' First Full Polar Orbit, *Journal of Geophysical Research*, 105(A), 10419–10434, <https://doi.org/10.1029/1999JA000383>, 1999.
- McComas et al., Pluto's Interaction with the Solar Wind, *Journal of Geophysical Research: Space Physics*, 121(5), 4232–4246, 2016.
- McComas et al., Interstellar Mapping and Acceleration Probe (IMAP): A New NASA Mission, *Space Science Reviews*, 214(8), 116, <https://doi.org/10.1007/s11214-018-0550-1>, 2018.
- McGovern et al., Localized Gravity/Topography Admittance and Correlation Spectra on Mars: Implications for Regional and Global Evolution, *Journal of Geophysical Research*, 107, E12, 2002.
- McKinnon et al., Convection in a Volatile Nitrogen-Ice-Rich Layer Drives Pluto's Geological Vigour, *Nature*, 534, 82–85, 2016.
- McKinnon et al., Origin of the Pluto-Charon System: Constraints from the New Horizons Flyby, *Icarus*, 287, 2–11, 2017.
- McNutt Jr. et al., Near-Term Interstellar Probe: First Step, *Acta Astronautica*, 162, 284–299, 2019.
- Meza et al., Lower Atmosphere and Pressure Evolution on Pluto From Ground-Based Stellar Occultations, 1988–2016, *Astronomy and Astrophysics*, 625, A42, 2019.
- Milazzo et al., White Paper for Decadal Survey: DEIA 101: Why Is Diversity Important?, 2020.
- Moore et al., The Geology of Pluto and Charon Through the Eyes of New Horizons, *Science*, 351, 1284–1293, 2016.
- Moore et al., Bladed Terrain on Pluto: Possible Origins and Evolution, *Icarus*, 300, 129–144, 2018.
- NASA, NASA Strategic Plan 2018, https://www.nasa.gov/sites/default/files/atoms/files/nasa_2018_strategic_plan.pdf, 2018.
- Nimmo et al., Reorientation of Sputnik Planitia Implies a Subsurface Ocean on Pluto, *Nature*, 540, 94–96, 2016.
- Nimmo et al., Mean Radius and Shape of Pluto and Charon from New Horizons Images, *Icarus*, 287, 12–29, 2017.
- Noll et al., Binaries in the Kuiper Belt, in *The Solar System Beyond Neptune* (Barucci, Boehnhardt, Cruikshank, and Morbidelli, eds.), Tucson, AZ: University of Arizona Press, pp. 345–363, 2008.
- Oh et al., Analysis of System Margins on Missions Utilizing Solar Electric Propulsion, American Institute of Aeronautics and Astronautics, 2008.
- Olkin et al., Evidence that Pluto's Atmosphere Does Not Collapse From Occultations Including the 2013 May 04 Event, *Icarus*, 246, 220–225, 2014.
- Palumbo and Strazzulla, The 2140 cm⁻¹ Band of Frozen CO: Laboratory Experiments and Astrophysical Applications, *Astronomy and Astrophysics*, 269, 568–580, 1993.

Parker and Kavelaars, Collisional Evolution of Ultra-Wide Trans-Neptunian Binaries, *The Astrophysical Journal*, 744, 139, 2012.

Passel and Cohn, U.S. Population Projections: 2005–2050, Washington, DC: Pew Research Center, 2008.

Petit et al., The Canada-France Ecliptic Plane Survey – Full Data Data Release: The Orbital Structure of the Kuiper Belt, *The Astronomical Journal*, 142, 131, 2011.

Porter and Grundy, Ejecta Transfer in the Pluto System, *Icarus*, 246, 360–368, 2015.

Porter et al., The First High-Phase Observations of a KBO: New Horizons Imaging of (15810) 1994 JR1 from the Kuiper Belt, *The Astrophysical Journal Letters*, 828, L15, 2016.

Porter et al., Constraints on the Shapes and Rotational States of the Distant New Horizons Kuiper Belt Targets, American Geophysical Union Fall Meeting, abstract #P13F-07, 2017.

Powell et al., Interorganizational Collaboration and the Locus of Innovation: Networks of Learning in Biotechnology, *Administrative Science Quarterly*, 41, 116–145, 1996.

Protopapa et al., Water Ice and Dust in the Innermost Coma of Comet 103P/Hartley 2, *Icarus*, 238, 191–204, 2014.

Rathbun et al., White paper for Decadal Survey: Who Is Missing in Planetary Science?: Recommendations to Increase the Number of Black and Latinx Scientists, 2020.

Richardson et al., Statistical Properties of the Solar Wind, Proceedings of the Eighth International Solar Wind Conference: Solar Wind Eight, AIP Conference Proceedings, 382, 483–486, <https://doi.org/10.1063/1.51433>, 1996.

Rivera-Valentin et al., White Paper for Decadal Survey: Who Is Missing in Planetary Science?: Demographics Showing Black and Latinx Scientists Are the Most Underrepresented, 2020.

Robbins et al., Craters of the Pluto-Charon System, *Icarus*, 287, 187–206, 2017.

Robbins et al., Geologic Landforms and Chronostratigraphic History of Charon as Revealed by a Hemispheric Geologic Map, *Journal of Geophysical Research*, 124, 155–174, 2019.

Robbins et al., White Paper for Decadal Survey: Pluto System Follow-on Missions: Background, Rationale, and New Mission Recommendations, 2020.

Robuchon and Nimmo, Thermal Evolution of Pluto and Implications for Surface Tectonics and a Subsurface Ocean, *Icarus*, 216, 426–439, 2011.

Russo and Khanna, Laboratory Infrared Spectroscopic Studies of Crystalline Nitriles with Relevance to Outer Planetary Systems, *Icarus*, 123, 366–395, 1996.

Showalter and Hamilton, Resonant Interactions and Chaotic Rotation of Pluto's Small Moons, *Nature*, 522, 45–49, 2015.

Singer et al., Cryovolcanic Constructs on Pluto, American Astronomical Society, DPS meeting #50, id. 506.04, 2018.

Singer et al., Impact Craters on Pluto and Charon Indicate a Deficit of Small Kuiper Belt Objects, *Science*, 363, 955–959, doi:10.1126/science.aap8628, 2019.

Solar and Space Physics, National Research Council, Solar and Space Physics: A Science for a Technological Society, Washington, DC: The National Academies Press, <https://doi.org/10.17226/13060>, 2013.

Spencer et al., Cassini Encounters Enceladus: Background and the Discovery of a South Polar Hot Spot, *Science*, 311, 1401–1405, 2006.

Spencer et al., The Geology and Geophysics of Kuiper Belt Object (486958) Arrokoth, *Science*, 367, eaay3999, 2020.

Stern et al., A Giant Impact Origin for Pluto’s Small Moons and Satellite Multiplicity in the Kuiper Belt, *Nature*, 439, 946–948, 2006.

Stern, Ejecta Exchange and Satellite Color Evolution in the Pluto System, with Implications for KBOs and Asteroids with Satellites, *Icarus*, 199, 571–573, 2009.

Stern et al., The Pluto System: Initial Results From Its Exploration by New Horizons, *Science*, 350, 292, 2015.

Stern et al., Initial Results From the New Horizons Exploration of 2014 MU69, a Small Kuiper Belt Object, *Science*, 364, eaaw9771, doi:10.1126/science.aaw9771, 2019.

Strauss et al., White Paper for Decadal Survey: Non-binary Inclusion in Planetary Science, 2020.

Thirouin et al., The Mission Accessible Near-Earth Objects Survey: Four Years of Photometry, *The Astrophysical Journal Supplement Series*, 239, 14, 2018.

Tyler et al., The New Horizons Radio Science Experiment (REX), *Space Science Reviews*, 140, 217–259, 2008.

Verbiscer et al., The Pluto System at True Opposition, EPSC-DPS, id. EPSC-DPS2019-1261, 2019.

Vision and Voyages, National Research Council, *Vision and Voyages for Planetary Science in the Decade 2013–2022*, Washington, DC: The National Academies Press, <https://doi.org/10.17226/13117>, 2011.

Waite Jr. et al., The Cassini Ion and Neutral Mass Spectrometer (INMS) Investigation, *Space Science Reviews*, 114, 113–231, 2004.

Warren and Brandt, Optical Constants of Ice From the Ultraviolet to the Microwave: A Revised Compilation, *Journal of Geophysical Research*, 113, D14220, doi:10.1029/2007JD009744, 2008.

Weaver et al., The Small Satellites of Pluto as Observed by New Horizons, *Science*, 351, aae0030, doi:10.1126/science.aae0030, 2016.

Wessen et al., Space Mission Concept Development Using Concept Maturity Levels, AIAA Space 2013 Conference and Exposition, 2013.

Young et al., Structure and Composition of Pluto’s Atmosphere From the New Horizons Solar Ultraviolet Occultation, *Icarus*, 300, 174–199, 2018.

Zanchet et al., Optical Constants of NH₃ and NH₃:N₂ Amorphous Ices in the Near-Infrared and Mid-Infrared Regions, *The Astrophysical Journal*, 777, 26, 2013.

Appendix C. Statistical Modeling

Background

Dr. JJ Kavelaars led the statistical modeling effort to identify locations in inertial space where KBOs would exist along the nominal trajectory to Pluto. The model used was based on the Canada-France Ecliptic Plane Survey (CFEPS) studies of the inner, main, and outer classical belt and the resonant populations that have at least one detection (cf. Kavelaars et al., 2009; Petit et al., 2011; Gladman et al., 2012). The model is de-biased to predict true orbital distributions to an Hg magnitude of 8.5, and includes Centaur populations.

Pre-Pluto KBO Encounter Modeling

The model results are shown in Figure 14 and Figure 15, and the assumed relationship between brightness and object size is given in Figure 16. These results indicate that a 0.2,AU deviation from the nominal trajectory would enable a ~30-km-sized KBO (i.e., approximately the same size as Arrokoth), and a >0.5-AU deviation would be required to visit a larger target. Analysis of the trade space between the time-of-flight penalty of a trajectory deviation and the magnitude of the deviation itself (Figure 17) led us to assume a 1-AU deviation, which would add 1 Earth-year to our cruise time but would enable a ~50- to 100-km-sized KBO to be visited. The final and original tour are compared in Figure 18.

Post-Pluto KBO Encounter Modeling

Similar modeling to the pre-Pluto KBO encounter was done for the post-Pluto encounter as well. The results, shown in the main report (in the Concept of Operations and Mission Design section) show the trade space between post-Pluto distance traveled, time, and xenon used. A 1 (3) AU deviation would enable a ~40 km (~70 km) diameter object to be visited. This trade is included in the report because additional xenon would have to be carried through the nominal mission to facilitate it, affecting the cruise duration. We selected 250 kg of xenon as the sweet spot to enable a 150 km statistical object to be visited in ~8 years. Additionally, a list of possible known KBO targets that could be reached is given in Table 24.

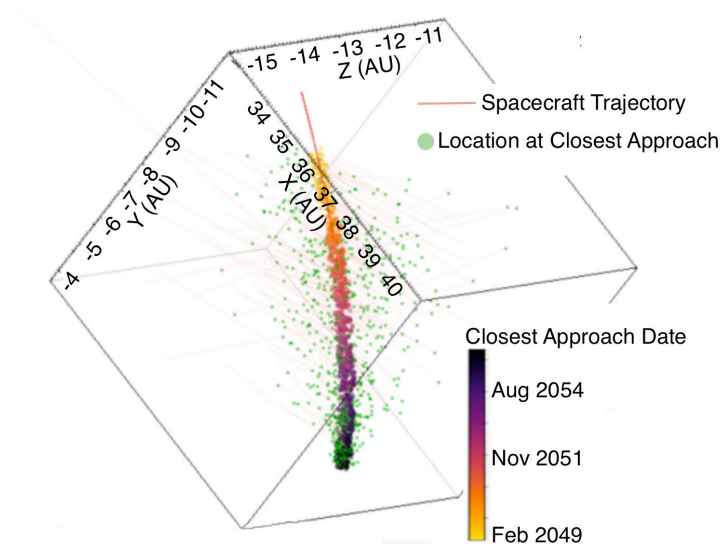


Figure 14. Distance and closest approach date of the spacecraft to the modeled KBO population (for pre-Pluto encounter).

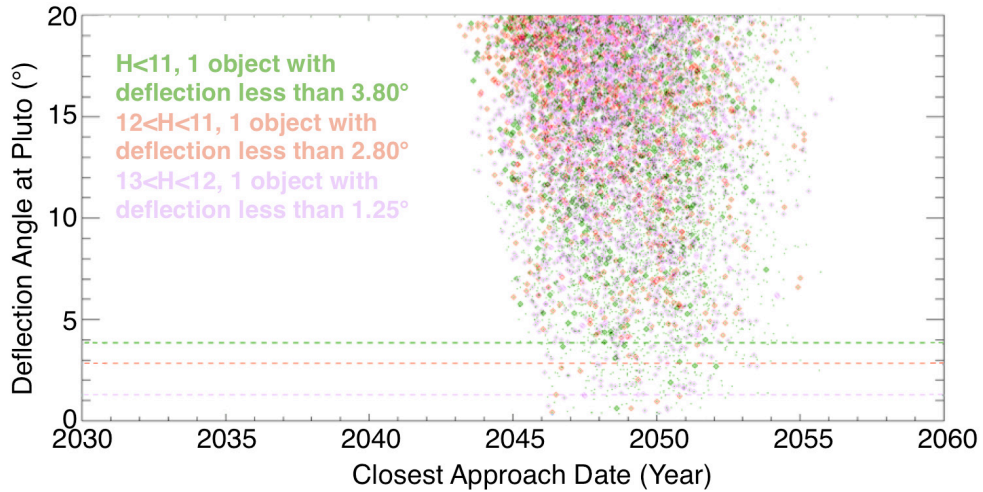


Figure 15. Deflection angle at Pluto (i.e., how modified the nominal trajectory would have to be) to encounter KBOs of different brightness.

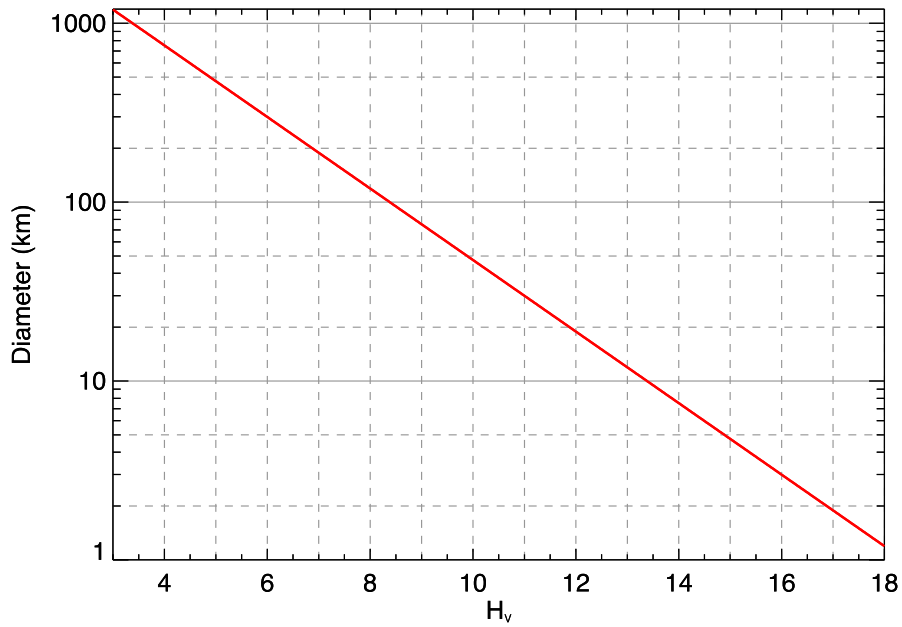


Figure 16. Relationship between brightness (H_v) and the predicted diameter of an object assuming geometric albedo, p_v , of 0.08.

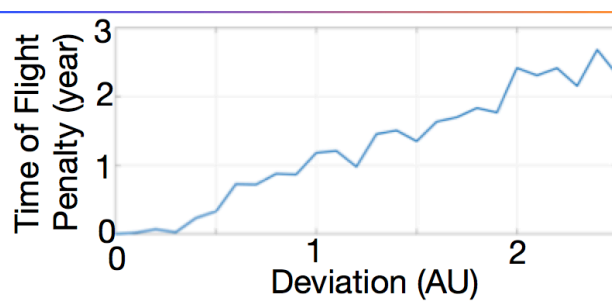


Figure 17. The time-of-flight penalty for nominal trajectory deviations to visit a pre-Pluto KBO.

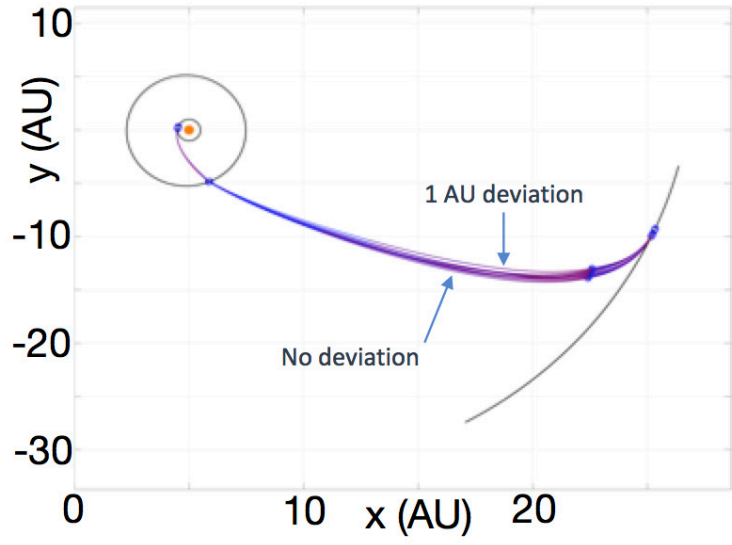


Figure 18. The nominal trajectory with (blue) and without (red) a 1 AU deviation

Table 24. List of known KBO post-Pluto targets that could be reached.

Name	H_v	Estimated diameter (km) ¹	Approx. departure	Transit duration (years)	Min. & Max. distance (AU)
(470308) 2007 JH43	4.5	600	2061–2066	20	4.39–4.46
(182294) 2001 KU76	6.6	230	2060–2066	17–20	3.02–4.37
2004 HN79	7.1	180	2060–2066	18–20	2.63–4.27
2004 HZ78	7.3	165	2060–2061	16–19	3.37–4.29
2015 KD176	7.4	160	2060–2070	20	3.93–4.05
(523704) 2014 HB200	7.5	150	2060–2061	17–20	3.61–4.27
2013 JR65	7.9	125	2060–2067	13–17	2.26–3.73
2000 FT53	8.3	100	2060–2066	17–20	2.09–4.35
2004 HY78	8.3	100	2060–2064	15–20	2.55–4.48
2015 KO173	8.8	80	2060–2070	12–19	0.41–4.26
2015 KQ175	8.9	75	2060–2070	20	3.60–3.83
2015 GH54	9.7	55	2060–2070	18–20	1.47–4.04

¹Assuming a visible geometric albedo, p_v , of 0.08.

Appendix D. Additional Instrumentation Information

This appendix provides additional information on the payload as deemed necessary; a small amount of duplication of the main text is included where necessary for context. Additional information is only outlined for instruments that required it, so not all of the payload is included in this appendix.

Panchromatic and Color Camera

The camera will image the surface of each target with as much spatial coverage and resolution as possible. The camera is modeled after the Europa Clipper Europa Imaging System (EIS) narrow-angle camera (NAC) and wide-angle camera (WAC). The NAC will provide panchromatic optical navigation capabilities working in framing mode, as well as color and panchromatic coverage of surfaces and/or atmospheres. The requirements, driven by Pluto-observational strategy, are outlined in Table 25.

Table 25. System observing requirements for NAC and WAC cameras.

Instrument	Driving Requirements
NAC Spatial Resolution for Global Coverage	Color: 0.2 km/pix over 95% of illuminated surface
	Color: 2 km/pix over 95% of illuminated surface at 0–140° phase angles and incidence angles < 60°
	Panchromatic: 0.05 km/pix over 95% of the illuminated surface, preferably with incidence angles < 80° and emission angles < 70°
WAC Spatial Resolution	Panchromatic: 1 km/pix over 70% of the unilluminated surface (~50°S to 90°S on Pluto and Charon, and anti-Pluto hemisphere of Charon)
Stereo Coverage	Panchromatic: Two images at 0.05 km/pix taken at the similar illumination but between 10° and 30° difference in emission angle over 75% of the illuminated surface

The details of the filters required are given in Table 26. We prefer complementary metal–oxide–semiconductor (CMOS) detectors to be used because they provide the flexibility to observe in framing and time delay integration (TDI) mode. They may also perform better in the likely high-radiation environment created by flying five RTGs.

The NAC detector is similar to EIS, and the NAC telescope is similar to New Horizons LORRI, but shrunk by a factor of 0.77 in linear dimension to produce the same pixel scale as LORRI with the smaller EIS detector pixels. Unlike EIS, the NAC is fixed rather than on a gimbal, with pointing accomplished by spacecraft motion.

The WAC is similar to the EIS WAC but with faster optics (e.g., f2 rather than f5.8 for the EIS WAC) in order to provide adequate signal to noise on dark-side terrain illuminated by Charon or Pluto, or by Pluto's haze. This requires the aperture be increased from 8 to 25 mm, while keeping the same focal length. Exposure times of ~10 s will be required for dark-side imaging. We will retain the current EIS WAC instantaneous field of view (IFOV) (0.25 mrad) and detector array (2k by 2k).

Table 26. Requirements on the NAC and WAC camera systems.

Parameter	NAC	WAC
Focal length, mm	2100	50
Aperture, mm	170	25
IFOV, μ rad	5	200
FOV, mrad	20 × 10	400 × 400
FOV, pixels	4000 × 2000	2000 × 2000
Detector	CMOS, 10- μ m pixel pitch	CMOS, 10- μ m pixel pitch
Filters	8 TDI color filters between 350 and 1050 nm, including narrow- and wide-band 890-nm CH ₄ filters, plus panchromatic framing mode	None
Sensitivity (pan), 10-s exposure	Stellar limiting magnitude > 17 with signal-to-noise ratio (SNR) >7	SNR > 20 for I/F = 4e-5 at 40 AU

Figure 20 shows the expected surface coverage of Pluto and Charon, respectively, obtained by the NAC, which provides panchromatic and color images. The emission angles covered by this camera are shown in Figure 21 to Figure 23. The panchromatic surface coverage of Pluto provided by the WAC is given in Figure 24. The WAC will primarily be used to image regions in winter darkness.

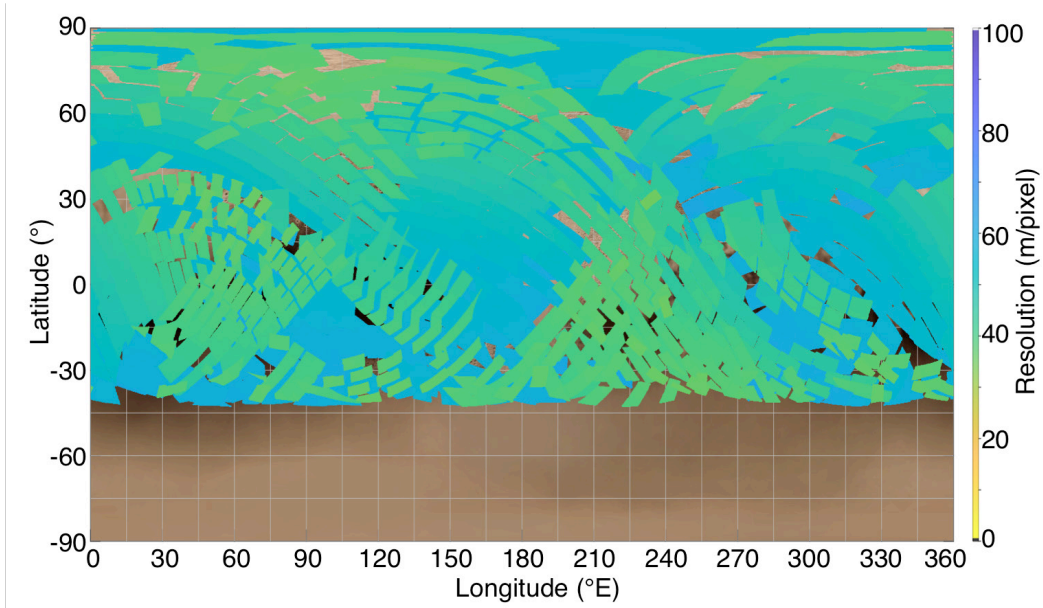


Figure 19. Panchromatic and color imager's (NAC) surface coverage of Pluto.

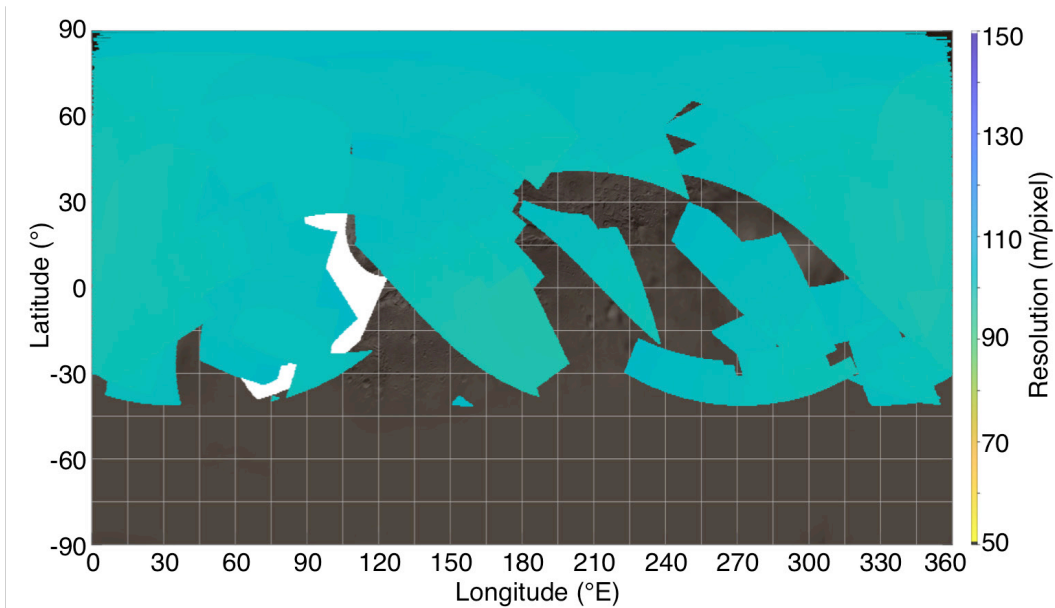


Figure 20. Panchromatic and color imager's (NAC) surface coverage of Charon. Note that this mosaic has not been optimized, and with additional work, full coverage of the illuminated surface is expected.

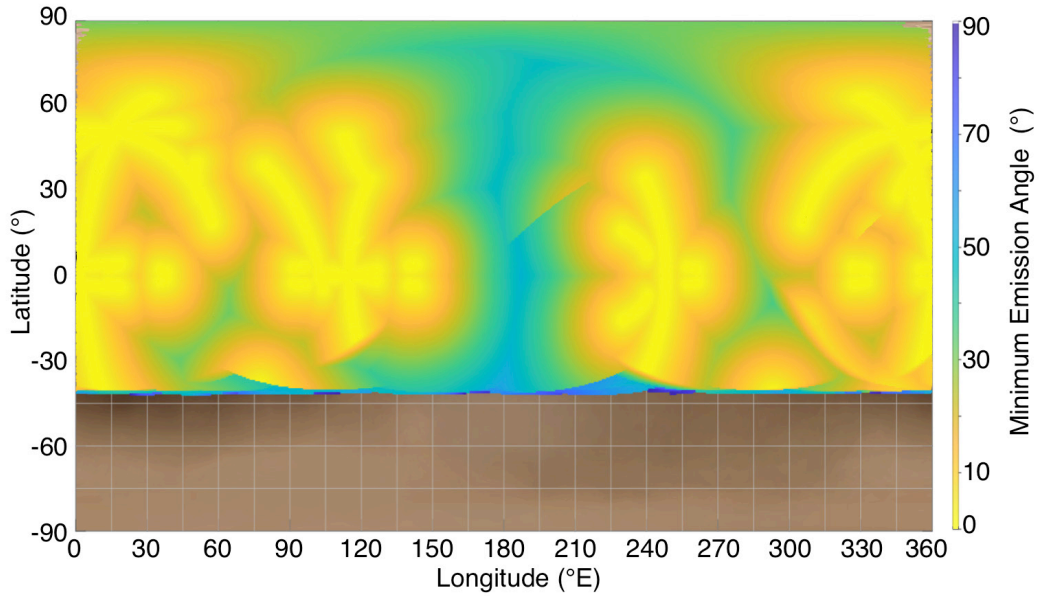


Figure 21. Minimum emission angles taken by the panchromatic and color imager (NAC) of Pluto (black regions indicate where the minimum phase is $<1^\circ$).

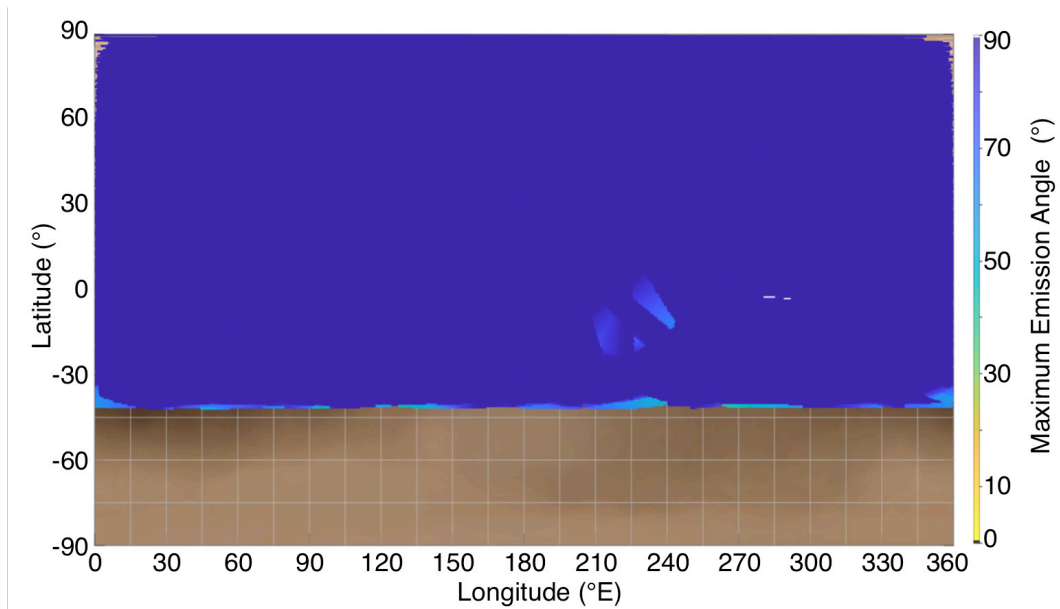


Figure 22. Maximum emission angles taken by the panchromatic and color imager (NAC) of Pluto.

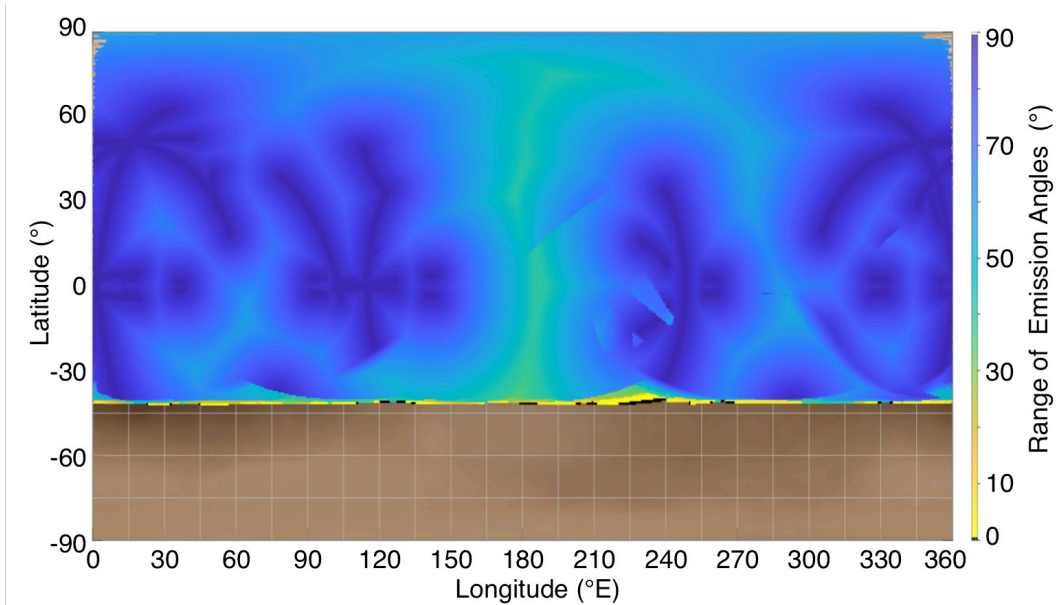


Figure 23. Range of available emission angles taken by the panchromatic and color imager (NAC) of Pluto.

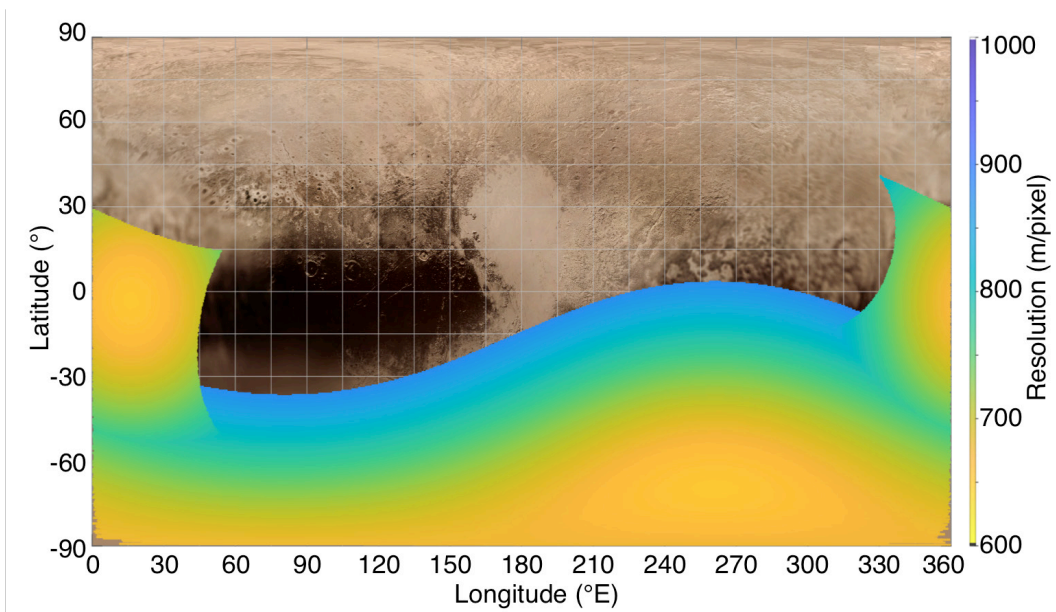


Figure 24. Pluto's surface coverage by the panchromatic (WAC) low-light camera.

Infrared Spectrometer (LEISA)

The Near-IR (NIR) spectrometer will provide surface compositional information on all targets. We model our payload on that of Lucy's Linear Etalon Imaging Spectral Array (LEISA) but with extended wavelength coverage. The requirements, driven by Pluto-observational strategy, are outlined in Table 27. LEISA will dramatically improve on the coverage and spatial resolution of New Horizons (best was 2.7 km/pix) to allow the compositional differences at small scales to be determined (e.g., pits, the convection cells within Sputnik Planitia, and the layered mountain blocks in the chaos region of the al-Idrisi mountains). The surface coverage of Pluto expected by the infrared spectrometer is given in Figure 25.

The wavelength of Lucy’s LEISA is 1–3.6 μm , an extension on New Horizons’ LEISA (1–2.5 μm). However, we require this wavelength range to be extended still further: to 0.8 to 5 μm . The short-wavelength cutoff is lowered to enable overlap between camera and NIR instrument for cross-calibration, and to obtain coverage of the 890-nm CH_4 band. The long-wavelength cutoff is increased to allow the characterization of ice species (H_2O , CH_4 , CO , CO_2 , NH_3) and organic compounds (e.g., tholins, nitriles), which have features located in the 2.5- to 5- μm region. The spectral resolution should be no worse than $350 \text{ \AA}/\text{d}\lambda$, which is driven by compositional investigations, to better constrain the dilution state of N_2 and CH_4 . The detector array should be comparable to Lucy LEISA: 2000×2000 pixels, with a 60- μrad IFOV.

Providing a cold thermal environment for LEISA is important to enable accurate measurement of longer wavelength spectral features, especially on a spacecraft with five RTGs. It is likely its accommodation will have to be optimized, and a radiator may be required. LEISA is data-volume heavy; this would be helped by adding the capability for onboard binning (e.g., some regions of interest should be measured at higher spectral resolution than others).

The absorption coefficient of the 3- μm water-ice feature is a factor of $\sim 10^2$ larger than the water-ice bands at shorter wavelengths (1.5 μm , 1.56 μm , 1.65 μm , and 2.0 μm ; Mastrapa et al., 2008; Warren and Brandt, 2008), enabling the detection of water ice even at low abundances (e.g., Clark et al., 2005; Protopapa et al., 2014). Amorphous ammonia ice presents a spectral feature at 2.96 μm with an absorption coefficient two orders of magnitude larger than the band at 2.23 μm (Zanchet et al., 2013). Nitriles are predicted to precipitate to the surface in photochemical models of Pluto’s atmosphere. Many pure nitriles have been studied in the laboratory, including acetonitrile, propionitrile, acrylonitrile, hydrogen cyanide, cyanogen, cyanoacetylene, dicyanoacetylene, and cyanopropyne, presenting (at 35K) detectable absorption bands between 4.396 μm and 4.843 μm (e.g., Russo and Khanna, 1996). CO ice displays an absorption band around 4.67 μm (Palumbo and Strazzulla, 1993) in laboratory spectra, much stronger than the one at short wavelengths.

Table 27. Observing requirements of the infrared spectrometer.

Observing	Requirement
Composition of geologic units	We require >90% global coverage of illuminated surface at >0.5 km/pix. We prefer incidence angles between 10° and 30° and emission angles between 0° and 60° .
Photometric properties	We require 90% global coverage of illuminated surface at >7 km/pix. We prefer phase angles between 0° and 140° and emission and incidence angles 0 – 80° .

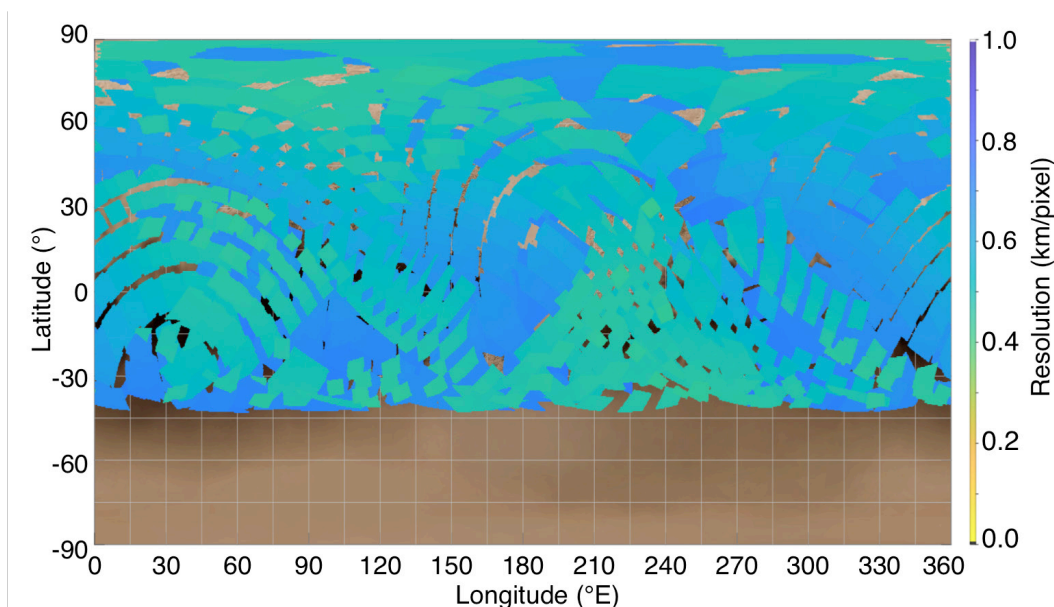


Figure 25. Pluto’s surface coverage by the infrared spectrometer (LEISA).

Thermal Imager (THEMIS)

The thermal imager will enable us determine the heat budget of KBOs and their surface thermal properties, and image the dark side of Pluto. We assume the optics of Mars Odyssey’s Thermal Emission Imaging System (THEMIS) as our baseline instrument but with a different detector to be sensitive to the cold surface temperatures (35–55 K) of the Pluto system and KBOs. This instrument’s Pluto-observational strategy-driven requirements are outlined in Table 28.

We will use the THEMIS optical design but use a thermophile detector and four filters spanning the 20–400 μm —20–50 μm , 50–100 μm , 100–200 μm , 200–400 μm —akin to the Lunar Reconnaissance Orbiter (LRO) Diviner thermal instrument. If possible, we would add an additional filter to extend into the submillimeter to allow cross-comparisons with ground-based observations (e.g., with Atacama Large Millimeter Array [ALMA] at 800 μm). The instrument will have 400- μm pixel pitch (which corresponds to an IFOV of 2 mrad) and 20 cross-track pixels (which produces a cross-track FOV of 4.6°). We expect typical slew rates to be ~1 pix/s (i.e., 4000 $\mu\text{rad/s}$).

As noted in the main report, local time coverage is readily achieved on Pluto and Charon because of this mission’s periodic orbits with varying subsolar longitude. However, this will be difficult during other KBO encounters because of the single rapid flyby, and on the small satellites because their poles precess in a way that makes it hard to predict where they will be when the spacecraft arrives (Showalter and Hamilton, 2015).

Table 28. Requirements on the thermal spectrometer observing strategy.

Observing	Requirement
Global surface coverage	We require the instrument to resolve 95% of both the illuminated and unilluminated surface at >20 km/pixel.
Local time coverage	Thermal emission is required to be measured between 9 a.m. and 3 p.m. and between 6 p.m. and 6 a.m. local time, at 10 geologically and compositionally diverse surface locations, at >10 km/pixel.

The thermal instrument will measure a target’s thermal emission regardless of whether it is sunlit or not. The surface coverage and spatial resolutions it will obtain of Pluto are shown in Figure 26. To derive thermal inertia and albedo from the measurements, the surface’s thermal emission has to be derived at a broad range of local times. Figure 27 shows this local time coverage in two ways (mapped and by longitude); the results show that Pluto’s surface will be mapped at sufficient local time coverage (i.e., at day and night) to derive its thermophysical parameters.

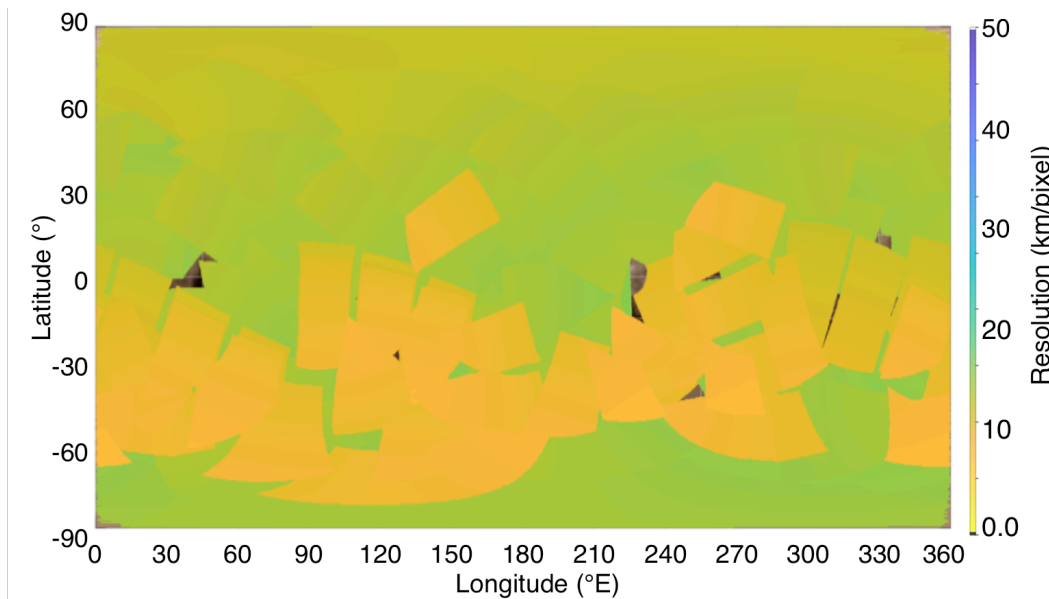
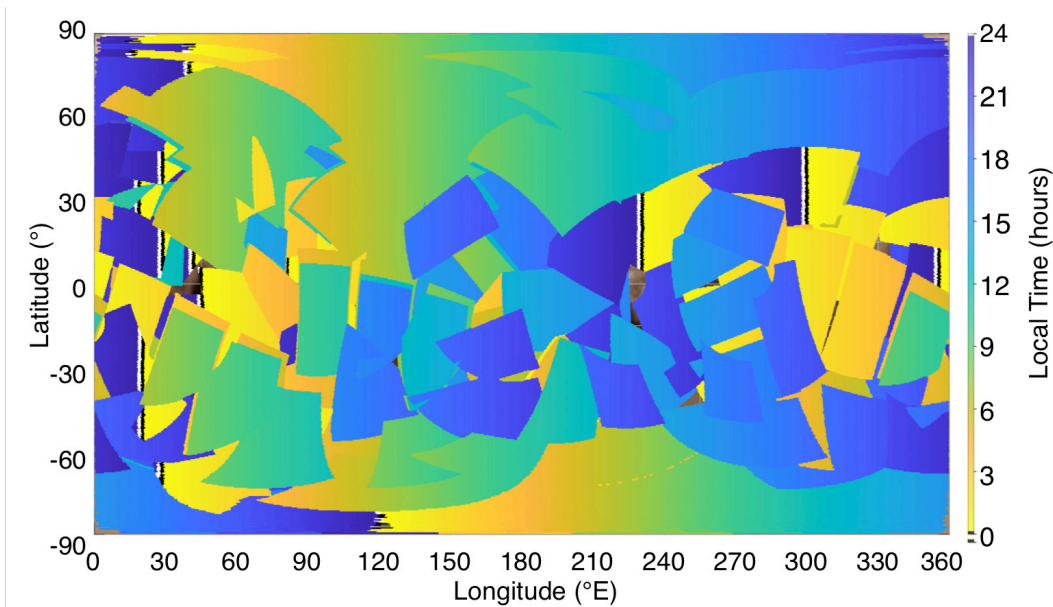
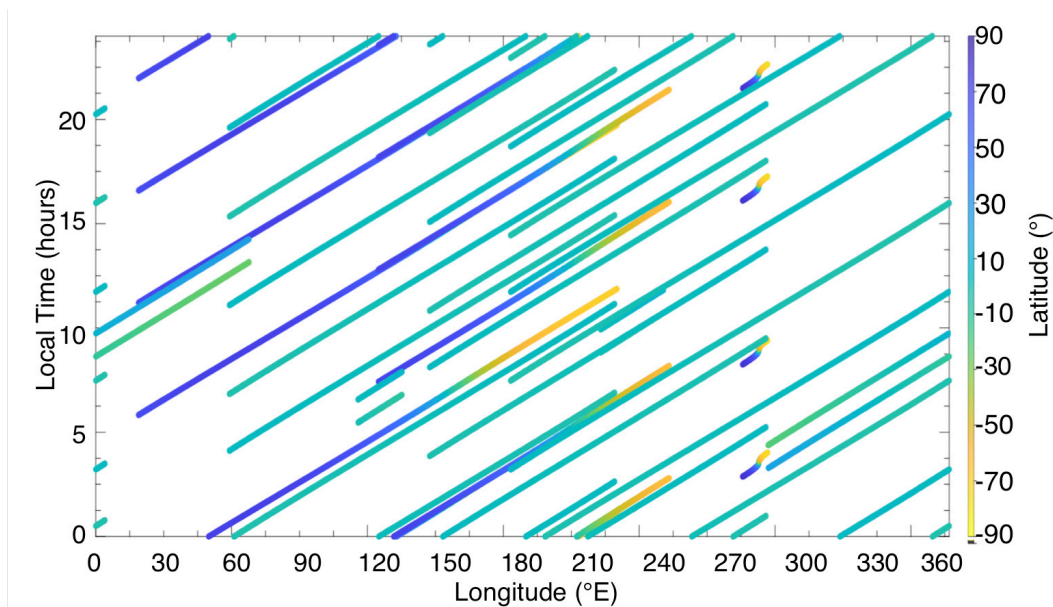


Figure 26. The surface coverage of Pluto by the thermal infrared instrument (THEMIS).



(a) Mapped local time of Pluto



(b) Local time coverage plotted as a function of longitude of Pluto

Figure 27. The local time coverage of Pluto that the infrared spectrometer (THEMIS) will obtain.

Mass Spectrometer

The purpose of this instrument is to measure in situ the composition and density of Pluto's—and any other body's—atmosphere and exosphere (including escape) and set new upper limits on the ionosphere. We require a large range of altitudes to be sampled, with a preference that the instrument is operational for most/all of the orbital period. The most critical operational period of this instrument is at altitudes below 2000 km down to 500 km. We require the instrument to measure the atmosphere at multiple local times.

We baseline the Europa Clipper MAss SPectrometer for Planetary EXploration/Europa (MASPEX) instrument, and the key instrument parameters are outlined in Table 29. We have selected specifications to

maximize the science return. A reduced range or sensitivity degrades the utility of the instrument, but it will still detect everything in its mass range, regardless of species/ionization, etc. With a slightly reduced capability, this instrument would continue to detect molecules other instruments cannot see. The MASPEX sensitivity $m/\Delta m > 8000$ can distinguish N_2 from CO, which Cassini INMS was unable to resolve (Brockwell et al., 2016).

A complication for this instrument operation is outgassing from the spacecraft, which may contaminate measurements in the tenuous region of the atmosphere. Therefore, the instrument requires a clear FOV. To this end, the most demanding measurements will be of Pluto's exosphere. The minimum altitude is chosen to be 500 km, consistent with the predicted density peaks of photochemical products and ions produced from the absorption of solar UV/EUV (Krasnopolsky, 2020). However, like Cassini INMS, this altitude can be adjusted during the mission after initial measurements (Waite et al., 2004).

Table 29. Mass spectrometer key parameters.

Observing	Requirement
Mass range	> 300 amu
Minimum sensitivity	> $\sim 10^4$ molecules/cm ³
Mass resolution	$m/\Delta m > 8000$ (i.e., to distinguish N_2 from CO) selectable up to 25,000
Altitude range	500 km (10^{10} molecules/cm ³) to 2000 km ($\sim 10^4$ molecules/cm ³)
Altitude resolution	< 20 km
Modifications to MASPEX	Addition: open ion source (to measure ionosphere) Removal: Radiation Shielding and Cryotrap

Radio Science

The radio science experiment has two distinct aims: One is radio science, specifically to measure the degree-2 spherical harmonics of Pluto's mass distribution for studies of internal structure and planet formation. The second is to work as a radio frequency (RF) spectrometer, to sound Pluto's atmosphere to derive its structure and composition. The requirements on the instrument operations are outlined in Table 30.

No changes from the New Horizons Radio Science Experiment (REX) are required. We note that this instrument requires an ultra-stable oscillator (USO) to provide a stable source (i.e., one with temperature control).

Because of the high power required for RF transmission, there will be little power available for the instruments. The global shape of a target is also required along with radio science to derive gravity. Altimetry measurements provide accurate shape information but because of their small FOV cannot provide global coverage. Imaging can also be used to determine shape information, which can be done globally but is less accurate than altimetry. Thus, to provide global accurate shape information, simultaneous altimetry and imaging should be taken, to allow the imaging to be corrected for uncertainties such as spacecraft position.

New Horizons showed that the REX instrument can be used to provide crude resolved measurements of the radio brightness temperature at 4.17 cm (7.18 GHz) across a planetary disk (Tyler et al., 2008; Bird et al., 2019). This is achieved by continually pointing the spacecraft antenna at Earth while scanning across the target, and dubbed therm-scans.

Table 30. Observing requirements for radio science.

Observing	Requirement
Radio frequency spectrometer – atmosphere	Earth-pointed with DSN contact over a minimum of two different locations (Sputnik Planitia has to be one), and two different local times for each location (dawn and dusk). (USO is required for REX to operate in this mode.)
Radio frequency spectrometer – surface	At least one therm-scan of the surface, which must intersect with the region scanned by New Horizons (on Pluto and Charon). The therm-scan region should also be covered by the thermal instrument to allow cross-calibration.

Observing	Requirement
Radio science	Seven passes with periapsis <1000 km; best if apoapsis is low and no maneuvers during series of five passes. <ul style="list-style-type: none"> One of these passes must cover latitudes > 70° at < 1000 km (closer is better, but > 500 km to avoid atmospheric drag). Five high-latitude passes are required. These passes should be distributed in longitude. Two of these five passes should be over Sputnik Planitia at least at 500-km altitude and not more than 700-km altitude.
	DSN contact is required for altitudes <3000 km. Requires the high-gain antenna (HGA) to be pointed at Earth during the periapsis pass. This may preclude useful pointing for most instruments.
	Measurements will be made via two-wave Doppler tracking during low-altitude (<10,000 km) periapses (no USO requirement). The uncertainty of Doppler has to be >0.1 mm/s over 1 minute.
	To use these data for constraining a target's interior structure, we also require accurate information on global shape to an accuracy of >100 m.
	We also requires accurate regional topography of areas of interest, particularly Sputnik Planitia, to >100 m.

UV Spectrometer

The purpose of a UV spectrometer is to provide pressure or number density, and composition profiles, of an atmosphere and exosphere, as well as to aid in characterizing the surface composition of airless bodies. The UV spectrometer's observing requirements are given in Table 31. The instrument should be boresighted with the camera and infrared spectrometer for its main telescope. The slit scan direction should be consistent with any scanning direction of a camera and IR spectrometer (if they are scanning devices); they should not be orthogonal or backward. For solar occultations, have a second optical path pointed in some other direction, like the HGA.

The baseline instrument is New Horizons' Alice. The instrument specs are driven by Pluto and are outlined in Table 32. However, we note that this instrument will be used at all visited bodies. More on the occultation opportunities is given in the following section.

Table 31. UV spectrometer observing strategy.

Observing	Requirement
Occultations	100 limb and disk, solar and stellar occultation profiles
	These profiles should be distributed in time, longitude, and latitude
Ring search occultations	3
Surface scans	Pluto: 50
	Charon: 10; Small satellites: 5 (disk integrated); Encountered KBOs: >5
Airglow spectra	50

Table 32. Requirements on the UV spectrometer.

Instrument Parameter	Requirement
Wavelength range	570–2000 Å
Spectral resolution	10 Å
Vertical resolution	10 km for ranges ≤5000 km

Occultation Opportunities

Examples of the ground position of the limb for Earth and solar occultations available (for all remote sensing instruments) and the UV-bright stellar occultations (for the UV spectrometer specifically) available are shown in Figure 28 and Figure 29, respectively.

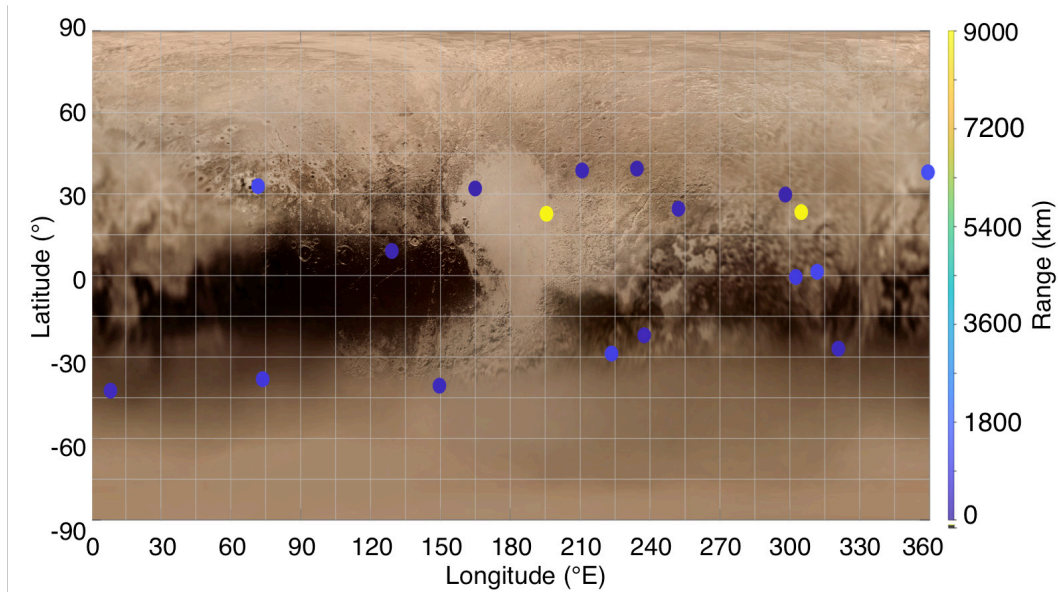


Figure 28. Earth and solar occultation opportunities of Pluto. The points show the sub-spacecraft position at the time of the occultation, and the distance to the limb (which defines the resolution) is given by the color of the points.

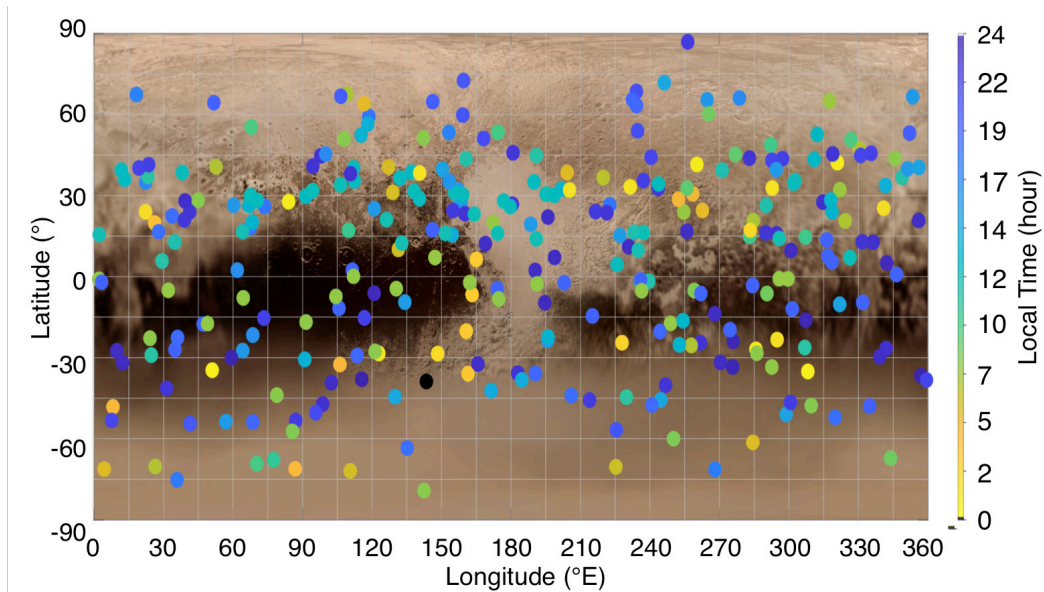


Figure 29. An example of stellar occultation opportunities. Only ten of the hundreds of possible UV-bright stars were used to make this plot.

Magnetometer

Models predict Pluto to have an asymmetric bowshock, and the standoff distance can move based on various factors (including a variable solar wind) (see Figure 30). Thus, being able to have multiple samples will significantly help map the solar wind's interaction with Pluto. At least one set of observations should be during dawn, and at least one set during dusk, to look for asymmetries predicted in some models (Delamere, 2019).

Simulations of the Pluto environment (e.g., Figure 30) suggest asymmetric features such as a bow shock extending far down the tail on one side, but quickly turning to bands of density waves on the other, with intricate time-varying plasma interactions between. Figure 31 show how the spacecraft would sample these regions from many different local times and distances, allowing us study Pluto's varied interactions with the solar wind.

During close object passes, high-rate data will be collected to understand and map boundary layers/interaction distances. Based on the data and model results from New Horizons, at least five periapses with high-rate data should be below 1000 km, and at least one should be below 500 km for this sampling. Additionally, there should be at least one equatorial orbit ($<20^\circ$ relative to the equator) and one polar orbit ($>70^\circ$ relative to the equator) to get a better 3D model of Pluto's interaction with the solar wind.

Calibration can be done farther from the planetary body and must be done away from such boundaries as the bow shock or Plutopause. Data gathered soon after launch, while still in the inner solar system, would allow cross-calibration with other plasma science instruments currently on flight hardware. The magnetometer should be operated during cruise, in order to gather data about the solar wind. It should also be operated while near Jupiter assuming a Jupiter gravity assist.

The most demanding observation is not a consequence of the instrument but whether its high data rate and desire to operate during periapsis would conflict with other instruments that might be deemed higher priority. Otherwise, this is a passive instrument that just needs to be "on" and does not have specific pointing requirements.

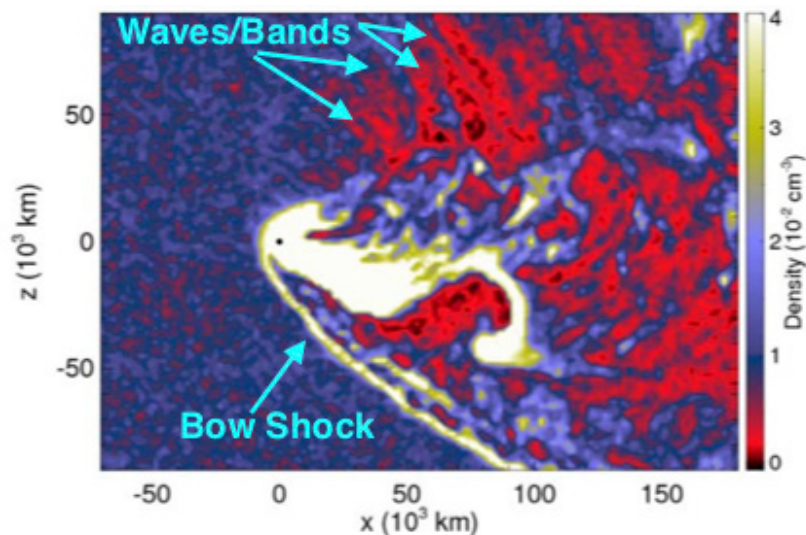
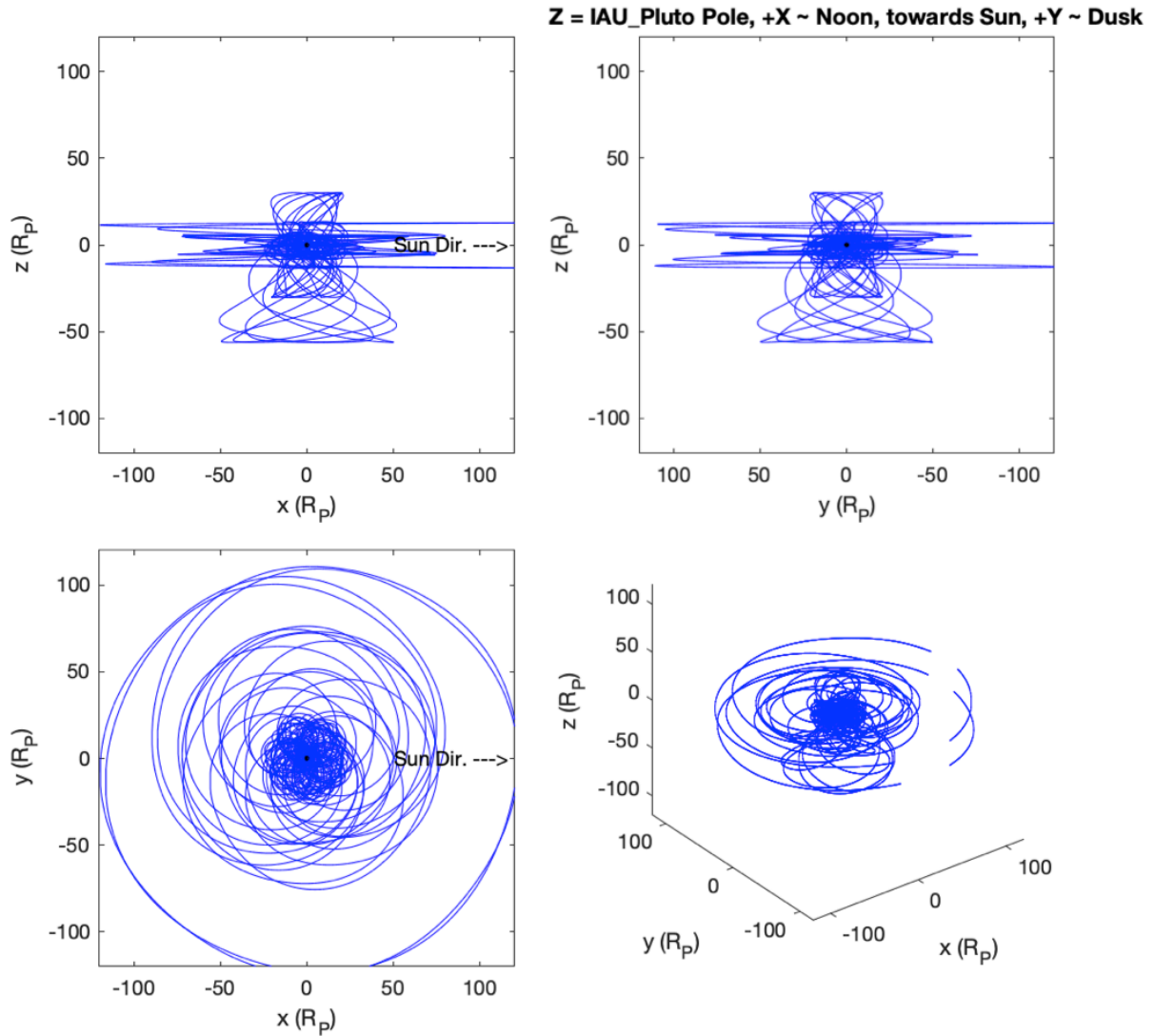
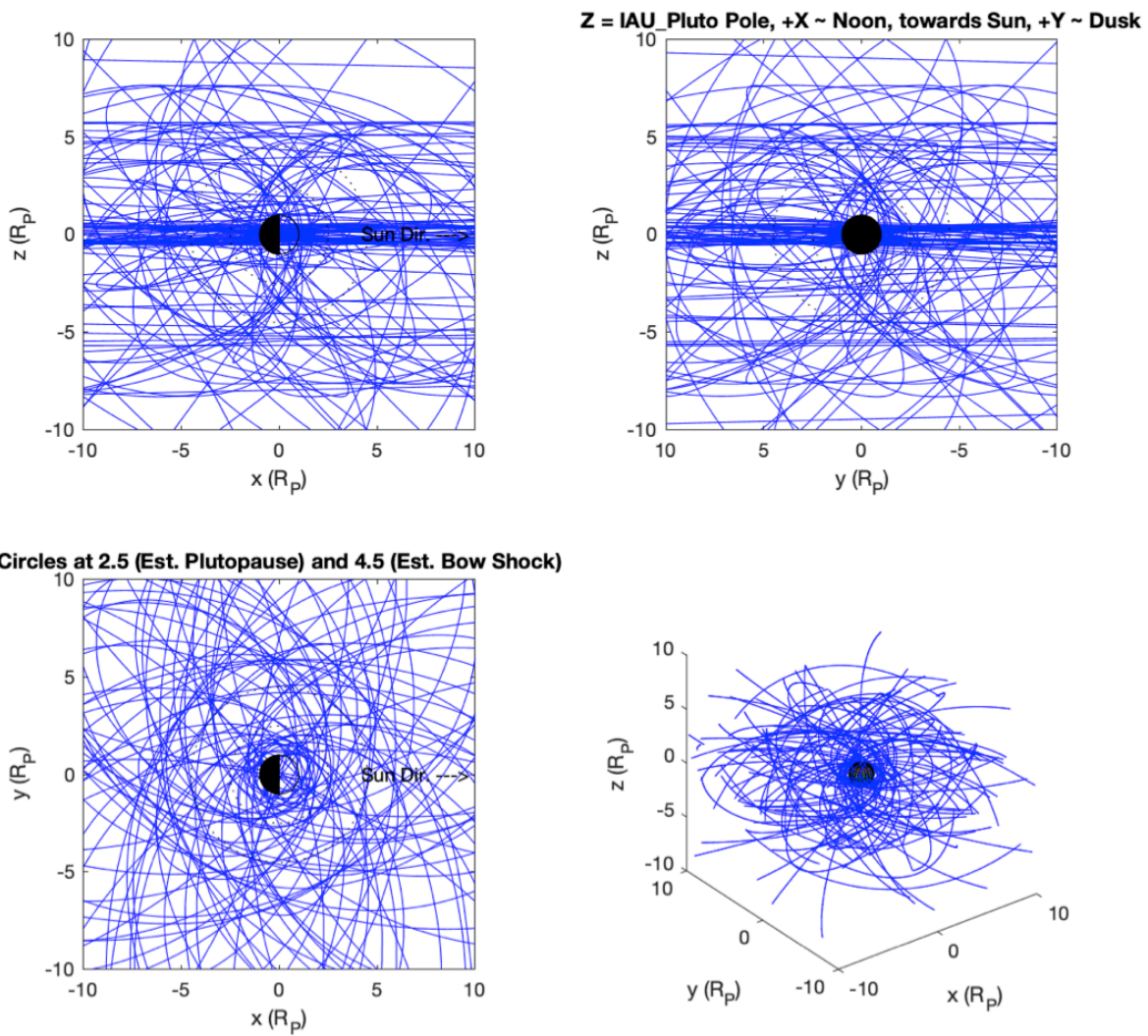
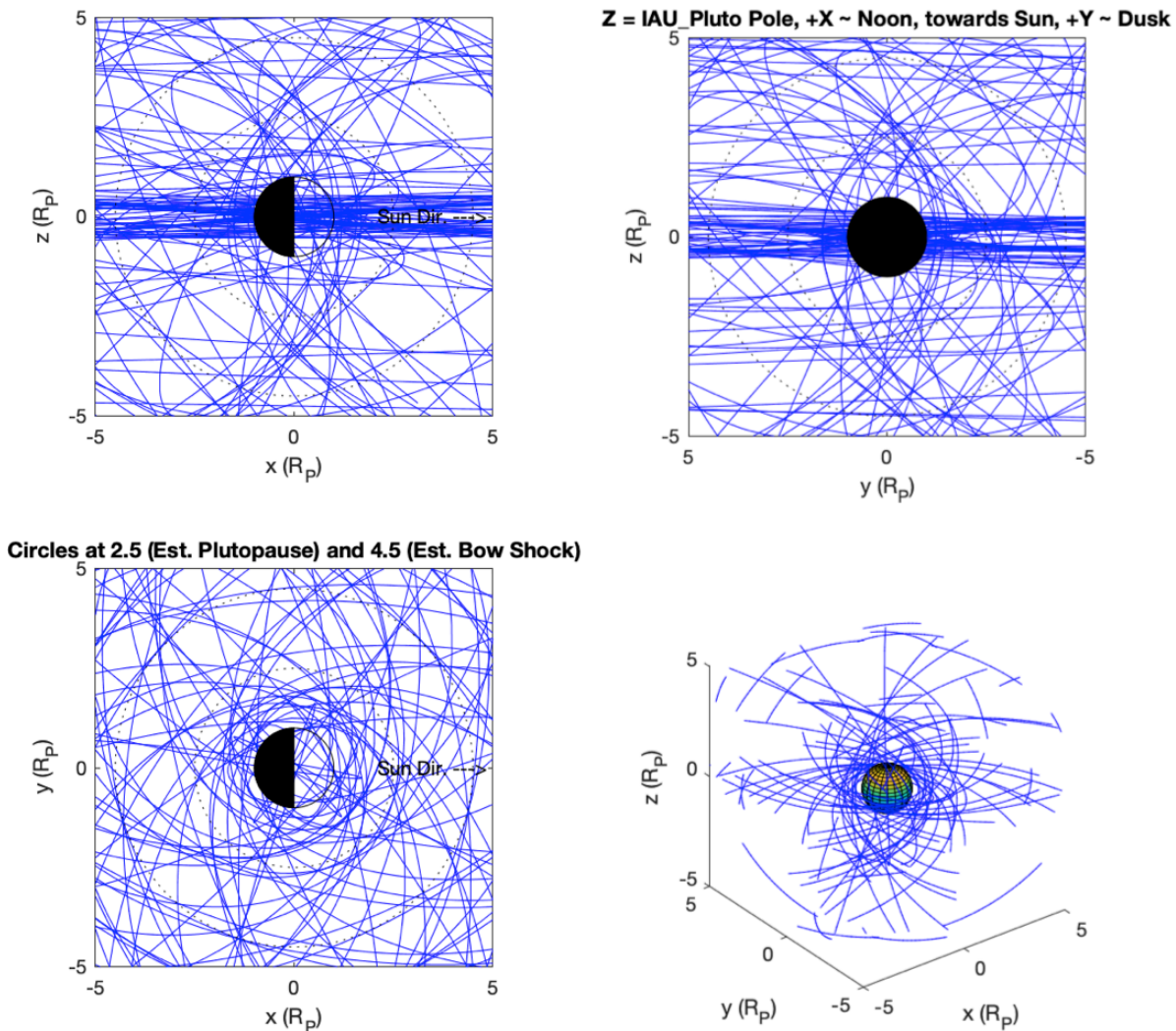


Figure 30. Simulations of Pluto's interaction with the solar wind. The Sun is on the left. There is a distinct bow shock on one side and a broader wave or banded region on the other side (Figure adapted from Figure 2 of Delamere, 2009).



(a) Geometry of the full tour, shown out to 120 R_p





(c) Geometry of the full tour, shown out to 5 Rp

Figure 31. Orbital tour shown from different perspectives, and different distances from Pluto.

Plasma Spectrometer

In the inner heliosphere from 1 to 5 AU, the solar wind typically ranges between 250 and 830 km/s and, similarly, the densities typically range between 0.1 and 50 cm⁻³ (McComas et al., 1999; Richardson et al., 1996). This means the number fluxes from 1 to 5 AU typically range from 2.5E+06 to 4.15E+09 cm⁻² s⁻¹. The higher number fluxes are closer to 1 AU because the solar wind number flux decreases with increasing radial distance from the Sun ($\propto r^{-2}$) for the solar wind owing to the nearly spherical expansion (Elliott et al., 2012, 2016, 2018, 2019; Richardson et al., 1996). The number flux will likely be too high at 1 AU if the instrument is optimized for the solar wind in the outer heliosphere. We recommend focusing on mass > 2 amu in the inner heliosphere and adding the ability to reduce the geometric factor in the inner heliosphere (<5 AU). Beyond 5 AU, even a design like CoDICE can measure protons in the solar wind without reducing the geometric factor. As a safety precaution, CoDICE already is implementing sweeping from high to low energy and stopping when the number flux of low mass solar wind ions exceeds a safety limit on a sweep-by-sweep basis. CoDICE also is implementing the ability to reduce the geometric factor for high number flux events by a factor of 100 such that extreme space weather events of great interest can

also be studied. These safety measures are triggered on a sweep-by-sweep basis as high fluxes are encountered. Implementing such features would allow a plasma ion instrument on Persephone to operate in the inner heliosphere, near Jupiter, and in Pluto's lower ionosphere at lower altitudes where the number fluxes could approach fluxes comparable to solar wind fluxes in the inner heliosphere. With a mass resolution of $M/\Delta M \sim 2\text{--}10$, CoDICE would be able to separate some isotopes, which is important for understanding Pluto's extended atmosphere (Figure 32; McComas et al., 2018).

New Horizons measured heavy Plutogenic ions from 10.5 Rp (12,487 km) at closest approach to ~ 105 Rp (124,772 km) in the tail and found the density ranged from 0.08 to 10^{-4} cm^{-3} and the speeds ranged from 60 to 140 km/s. The peak total ionospheric ion density at Pluto estimated using the Krasnopolsky (2020) model is 800 cm^{-3} . If we estimate number fluxes using McComas et al. (2016) or using the peak density from Krasnopolsky (2020), we need to make assumptions. For estimates using McComas et al., a logical assumption is to increase the fluxes by r^2 , which is assuming a hydrostatic density profile for Pluto's ionosphere. We also need to assume values for the speeds to estimate the number flux. Most likely the speed in the ionosphere will be lower than that observed far from Pluto by New Horizons. A worse case would be to assume the speed in the ionosphere is similar to the speeds observed at New Horizons ranging from 60 to 140 km/s at distances ranging from 10.5 to 105 Rp. However, that speed range is much higher than typical ionospheric speeds at Earth, which are typically tens of meters per second. Estimating a worse-case high flux would be to assume 140 km/s and 0.08 cm^{-3} , and that produces a flux of $6.97\text{E}+10 \text{ cm}^{-2}\text{s}^{-1}$ scaling from 105 Rp to 500 km from the surface. This is probably an overestimate, and a more reasonable estimate might be to take the 800 cm^{-3} and assume 50 m/s, which produces a flux of $4.00\text{E}+06 \text{ cm}^{-2}\text{s}^{-1}$. To measure ions in the ionosphere, the same safety precautions necessary to measure the solar wind ions in the inner heliosphere are still needed, or alternatively, the operations could be limited to ~ 2 Rp (2376.6 km) above the surface.

Electrons were considered for removal from the main detection because they are unlikely to add significantly to the science, and New Horizons did not see energetic electrons near Pluto. A separate electron instrument was *not* considered in this design run for this PMCS. There is no good, existing instrument that includes both a field of view (FOV) and sensitivity that is desired. The SWAP instrument had optimal sensitivity but does not measure mass and has limited angular coverage. The CoDICE-Lo instrument FOV would need to have deflectors added. FIPS has a larger instantaneous FOV but will not be sensitive enough at Pluto. Therefore, the recommendation should be for a generic plasma instrument that meets the above requirements.

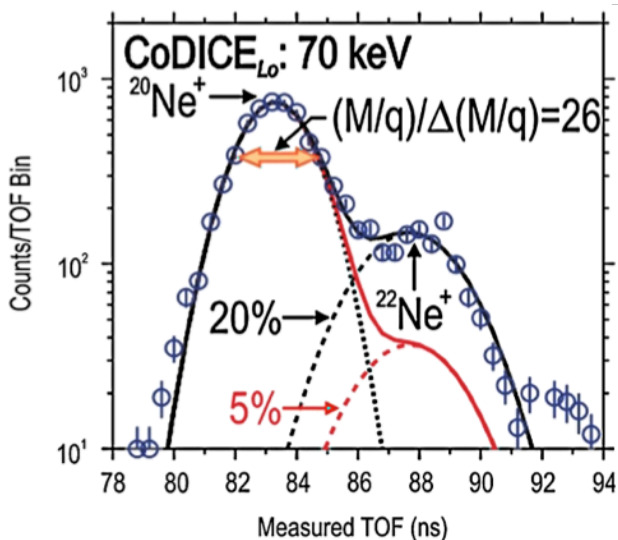


Figure 32. Example of mass resolutions for the CoDICE time of flight (TOF).